EFFECT OF SURFACE CONDITIONING OF PLATINUM ALUMINIDE BOND COATS ON THERMAL BARRIER COATING LIFE

by

Scot J. Laney

BS, University of Pittsburgh, 2001

Submitted to the Graduate Faculty of

The School of Engineering in partial fulfillment

of the requirements for the degree of

Masters of Science

University of Pittsburgh

2004

UNIVERSITY OF PITTSBURGH

SCHOOL OF ENGINEERING

This thesis was presented

by

Scot J. Laney

It was defended on

June 3, 2004

and approved by

Dr. I. Nettleship, Associate Professor, Department of Materials Science and Engineering

Dr. J.A. Barnard, Professor and Chairman, Department of Materials Science and Engineering

Dr. G. H. Meier, Professor, Department of Materials Science and Engineering
Thesis Advisor

Dr. F. S. Pettit Professor, Department of Materials Science and Engineering
Thesis Advisor

EFFECT OF SURFACE CONDITIONING OF PLATIUNUM ALUMINIDE BOND COATS ON THERMAL BARRIER COATING LIFE

Scot Laney, MS

University of Pittsburgh, 2004

Thermal Barrier Coatings (TBC) have been used for a number of years on components for use in aircraft gas turbine engines. The standard for processing these components includes grit blasting the bond coat prior to TBC deposition by Electron Beam Physical Vapor Deposition (EBPVD). While grit blasting has worked well for industry, it is argued that EBPVD TBC's are able to form strong bonds on smoother surface finishes. This would theoretically improve the component lifetime. This study involved the examination of the performance and failure of several industrially and economically viable alternative surface finishes as well as the effect of pre-oxidation treatments on the lifetime of the TBC. The system used consisted of a substrate of CMSX4 (Ni based superalloy), a platinum modified diffusional aluminide coating, and yttrium stabilized zirconia (YSZ) deposited by EBPVD as the TBC. Surface finishes applied prior to TBC deposition include 120 and 40 minute media finishes, barrel finish, and 3 μm hand polish. The various atmospheres were chosen for the pre-oxidation treatments in order to grow metastable and stable alumina scales. Exposure was done cyclically (1 hour cycles) at 1121^{o}C in laboratory air until failure. Samples with the combination of media finish and mostly α alumina scales had lifetimes up to 1040 cycles. This is well beyond the expected value (~750 cycles) of a grit blasted sample in the same exposure conditions.

TABLE OF CONTENTS

LIST OF TABLES

LIST OF FIGURES

ACKNOWLEDGMENTS

I would like to first and foremost thank Dr. Pettit and Dr. Meier for their patience, support, and seemingly infinite knowledge. Very rarely was there ever a question dealing with this research that was not met by at least an educated guess. My colleagues in the high temperature group also provided different ideas and perspectives that made this work enjoyable.

I would also like to acknowledge financial support from a subcontract with the University of Connecticut, which was in turn supported by the DOE. Some of the data presented here was generated at UCONN by Dr. Eric Jordan and Dr. Maurice Gell and their students, for which I am grateful.

Finally, I would like to thank my family. They have provided unwavering supported to me through every choice I've made in my life, good or bad. They also think more of me and want more for me than I could ever dream of for myself.

1.0 INTRODUCTION

Humans have long been fascinated by the idea of flight, as evidenced by the myths and legends of our ancient cultures. One popular Greek story tells of Daedalus and Icarus making wings out of wax and feathers. The father/son duo was able to fly like birds until Icarus flew too close to the sun and the wax on his wings melted. He fell from the great height into the ocean. All that Daedalus found of his son were a few feathers floating on the water[1]. The barrier between our imagination and reality is frequently due to the limitations of materials. Even today, we travel further, higher and faster than the Greeks ever dared to imagine, but we are still limited by properties of materials.

In today's world, we fly regularly in planes powered by gas turbine engines. The environment that a material in one of these engines is exposed to is much worse than a little heat from the sun. It is one of the harshest environments we have devised. The chosen system must have high strength and toughness at high temperatures and resistance to thermal shock, thermal cycling, fatigue, creep, oxidation/corrosion, etc.

Currently there is not a single material that fits the bill. Ceramics have the common problem of cost and their inherent brittleness. The high melting point, refractory metals also have a cost issue and brittleness. They also have the additional problems of usually forming volatile, non protective oxides. There is some work with alloys of these materials to reduce this problem, but a viable material is likely far down the road. There is also a need to use materials with good strength to weight ratios, and the refractory metals are very dense and heavy. The

next step is transition metals and their alloys. Most of the properties and the cost are favorable for usage, with the exception of the melting point. For the gas turbine engine to run efficiently, the operating temperature must be at or above the melting points of these materials. The current solution is a composite structure. This composite utilizes the good properties and cost of a transition metal alloy and its oxide, and protects it using a coating of a thermally insulating ceramic or thermal barrier coating (TBC).

The TBC system is gaining popularity for usage in gas turbine engines. Much work has been done on the system through the years. It has almost reached a point where further improvement through material choice is no longer possible. It is now necessary to refine the processing and gain what improvements are possible by that route. This work will look at what effects modifications to the bond coat surface, prior to TBC deposition, have on the lifetime of the TBC system.

2.0 BACKGROUND

The TBC system will be discussed in more detail. Items that directly relate to this project will be emphasized. Starting with the substrate and building up to the TBC, each major component will be touched upon. Next, the current state of the art TBC system and its inherent problems will be discussed briefly. Finally, the modifications and their proposed effects will be introduced.

2.1 SUBSTRATE

The substrate makes up the bulk of the TBC system. Due to the high temperatures encountered, only alloys able to maintain mechanical properties at or near their respective melting points can be used. These are generally called superalloys. The most common superalloys are nickel, cobalt, or iron based, with nickel being the most popular for the higher temperature components.

2.1.1 Superalloy Strengthening Scheme

Given the high temperatures, only certain methods of strengthening will be effective. For example, work hardening effects will essentially be annealed out at the service temperatures. Since diffusive creep is a major concern at these temperatures, most of the components are manufactured as single crystals or are directionally solidified and have large grains. This eliminates grain size strengthening as a possible mechanism. The two methods that are effective are solid solution strengthening and precipitate or particle strengthening. There are several elements that are added to a superalloy that accomplish solid solution strengthening, but the most abundant is chromium. Molybdenum and tungsten are also common additives to improve the

solid solution strengthening. Nickel is also known to form a precipitate phase, γ', with elements such as aluminum (Ni_3Al) and titanium (Ni_3Ti). Figure 2-1 shows the Ni – Al binary phase diagram. Aluminum is the most commonly seen additive for this purpose. A nickel based superalloy, in the most simple form, is an array of coherent γ' precipitates (usually cubic in morphology) in a matrix of γ nickel that is solid solution strengthened by chromium additions[2] (Figure 2-2). Once again the NiCrAl alloys are essentially model alloys. There are several other elements present in the current superalloys for strengthening and other purposes.

2.1.2 Stand Alone Oxidation Resistance

Superalloys must also maintain oxidation resistance. While this is not a major concern in the TBC system, it is important in other applications. Most high temperature oxidation resistance is accomplished by selectively oxidizing one of the elements in the alloy. Selective oxidation means simply that an alloying element in the alloy is preferentially oxidized due to the fact that the oxide is the most stable (most negative free energy of formation) that the alloy can form. The effectiveness of the oxide as a protective layer depends on the ability to form and then maintain a continuous scale. This depends on the concentration of the element and how fast the element can diffuse to the scale. If the concentration is low, the most stable oxide will form in discontinuous islands (internal oxidation) and the next stable oxide will try to form a continuous layer. If the diffusion rate is slow, the metal cations cannot get to the interface fast enough. The local concentration at the interface drops. When the conditions are met for the next most stable oxide to form, it will oxidize. When the conditions are favorable for the initial oxide to form, it will once again be preferentially oxidized, leaving a layered oxide. If the concentration and diffusion rate are both high enough, the protective oxide will form and be maintained until the

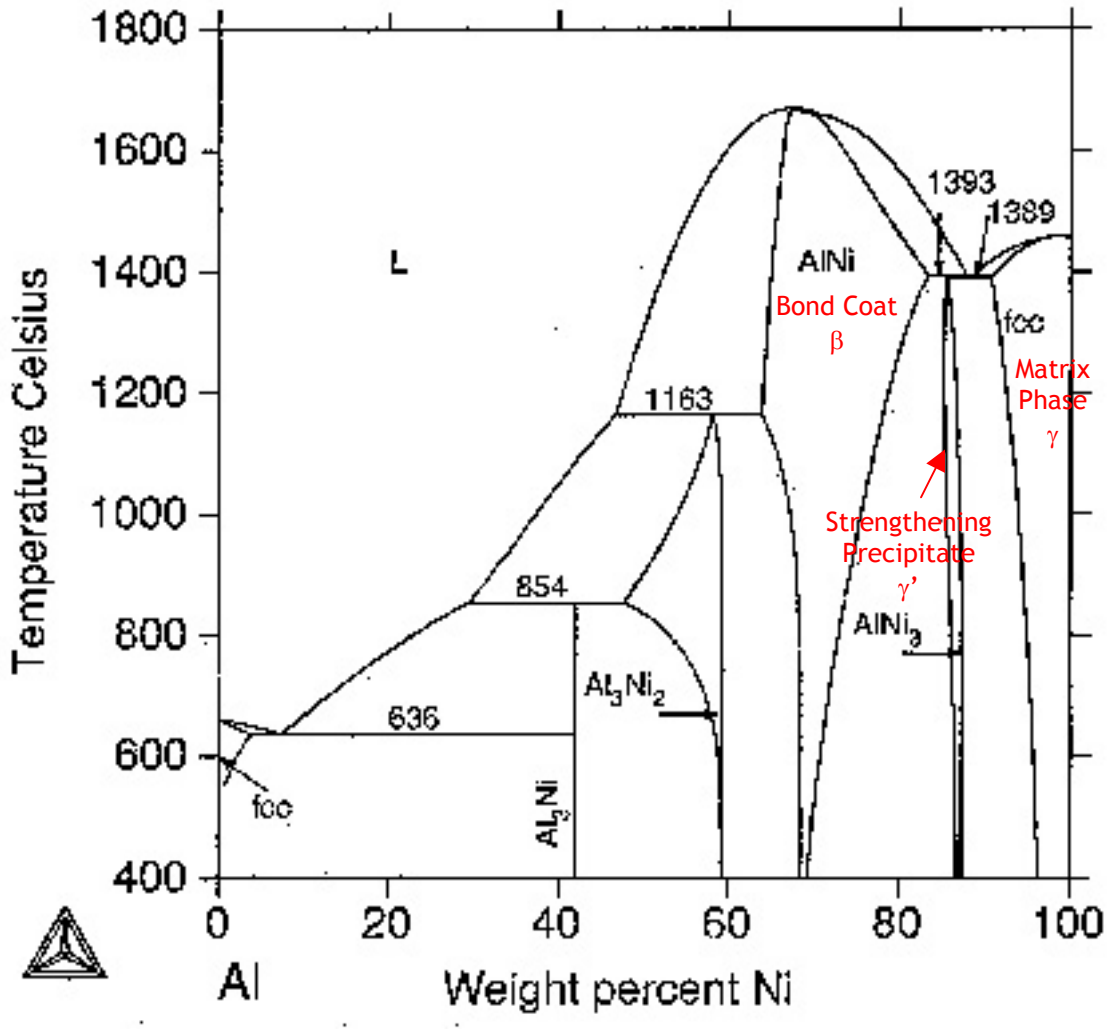

Figure 2-1. The binary phase diagram for the Ni – Al system.

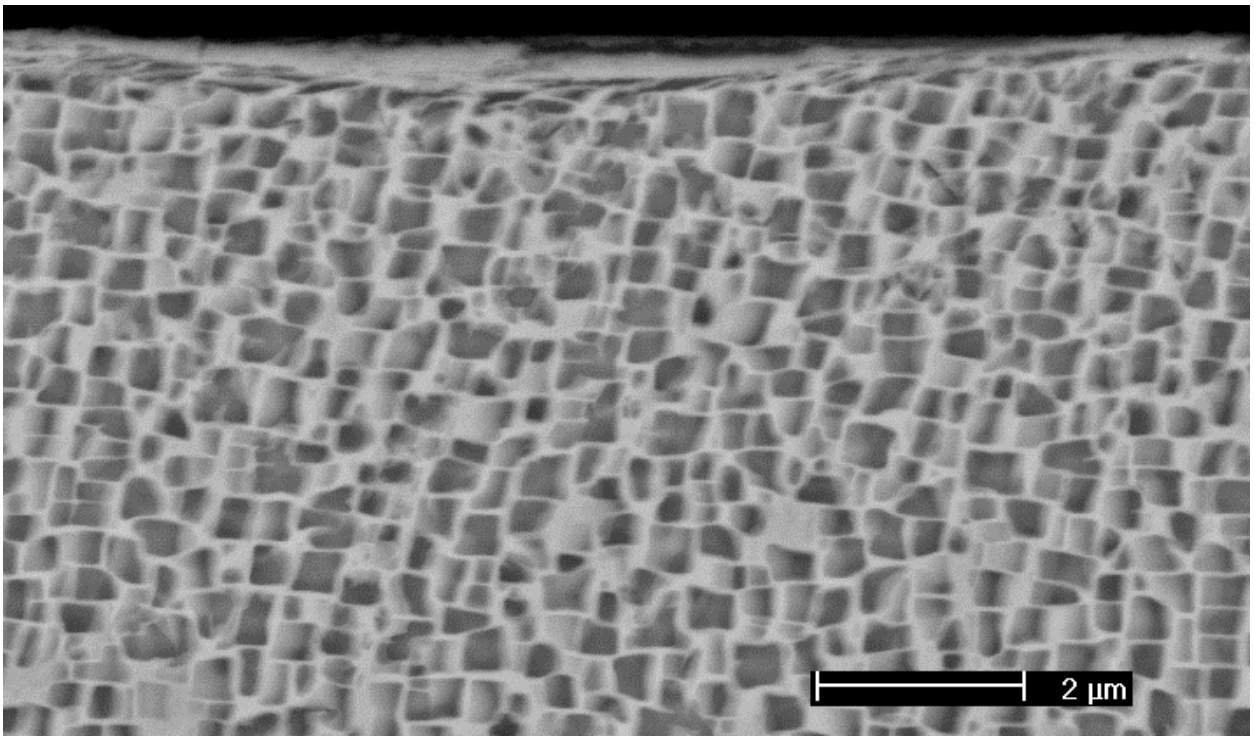

Figure 2-2. Typical microstructure of a Ni based superalloy (Low Sulfur PWA 1484, etched). The γ' phase (Ni3Al) tends to form as a cubic precipitate in the γ matrix.

alloy is significantly depleted of that element. It is also important to note that other less stable oxides may form first due to kinetics (transient oxidation), but the most stable oxide will eventually form the continuous layer. The transient oxides are then cut off from the substrate and stop growing when the stable oxide becomes continuous[3,4]. Examples of other properties of the scale that are desirable are chemical stability (inertness), good adherence to the alloy, slow growth rate, high density (fewer short circuit diffusion paths), resistance to thermal shock, and strain tolerance.

The best choices of oxide that offer high temperature protection are alumina, chromia, and silica as shown by Figure 2-3. Chromia and silica are useful at lower temperatures (700 – 900 ^{o}C), but have a plethora of problems that are mostly amplified at elevated temperatures (>1000 ^{o}C). Alumina, on the other hand, is the slowest growing (Figure 2-3b) and most stable (Figure 2-3a) of the group. It does not form a volatile phase in any conditions as Cr_2O_3 and SiO_2 are known to do. It is also a decent thermal insulator. Alumina is the best choice for oxidation protection at these temperatures.

Aluminum has a dual purpose in the superalloy. First it forms the precipitate □' and second it must form a protective alumina layer. The "rules" of selective oxidation must now be applied to the superalloy. Using the basic model of NiCrAl, aluminum forms the most stable oxide (Figure 2-3a). The aluminum must be in a sufficient amount to be able to form a continuous layer on the outer surface of the alloy. If this threshold value is not met, the alumina will form internal oxide particles that offer no oxidation protection. Chromia, being much more stable than nickel oxide (Figure 2-3a), will then be selectively formed and attempt to form the protective layer. As mentioned before, chromia is not effective at higher temperatures, so it is imperative that the aluminum content is sufficient for alumina to form a continuous layer for

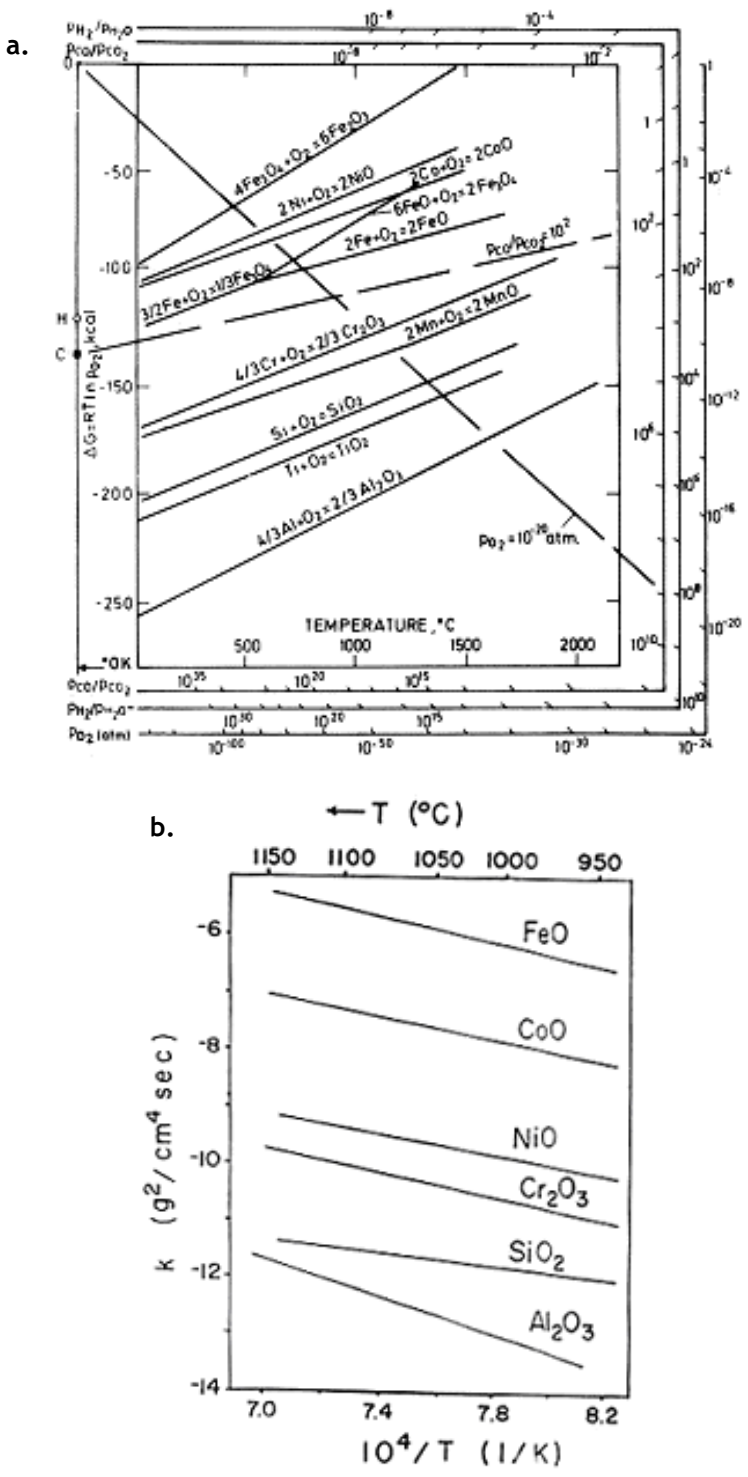

Figure 2-3. Ellingham diagram (a.) showing the stability of common oxides and plot of parabolic rate constants (b.) of oxides that can form on alloys used in high temperature applications.

maximum protection. By some unknown mechanism, additions of chromium have been shown to reduce the amount of aluminum required to form the initial layer[3]. There must also be even more aluminum in the alloy to maintain the oxide layer and it must be able to diffuse to the oxide fast enough. Forming alumina on the surface locally depletes the alloy of aluminum. To keep the layer intact, the alloy must be able to supply aluminum to the depleted areas.

This is a problem in nickel-based superalloys, because aluminum is part of the strengthening scheme. Aluminum in the alloy, not tied up in forming γ', can make the alloy too hard and brittle. A balance between the amount of aluminum needed for a continuous TGO and the mechanical properties must be met. Another important problem is that to supply the TGO with aluminum, the γ' particles are dissolved, leading to a localized weakening of the alloy. This leads to the need for a coating.

2.1.3 Processing

The superalloy parts for this application demand special processing. As mentioned above, the superalloy part must consist of a single crystal or large directional grains to improve the creep resistance. This means that a method of selecting the growth direction, the number of grains, and in some cases the orientation or texture of the grains must be developed. The cooling channels are usually not machined, but rather are part of the mold. The part is also usually not a shape that lends itself to machining, so the part must be near net shape.

The company that did much of the processing for this work, Howmet, uses investment casting (also known as the lost wax process). In this process, a replica of the part is fashioned from wax. The cooling channels are also included in the replica as ceramic cores. The replica is then alternately dipped into a slurry or dusted with stucco to build up a wall thickness of about half an inch. Between each step the mold is allowed to dry and harden. After about 15 dips, the

mold is put into a high temperature, high pressure furnace to remove the wax. A strong ceramic mold remains after the dewaxing. The liquid alloy is then poured into the mold. For directionally solidified and single crystals, the mold is heated to a temperature higher than the melting point of the alloy, and has a chill plate on the bottom. This ensures that solidification will start from the chill plate and grow out and away from it. In the case of single crystals, there is a "pig tail" shaped grain selector between the chill plate and the main body of the mold that allows only one of the solidifying grains to continue to grow. When the mold is completely solidified and cooled, any sprues or gating is cut off and the ceramic mold is hammered, water jet blasted, and chemically etched away from the part. The part is then submitted for several nondestructive tests and is then ready for further processing[5].

2.2. BOND COAT

As mentioned above, superalloys can have difficulty maintaining a balance between oxidation resistance and mechanical properties if used alone. The aluminum that is used to form and maintain the TGO is the same aluminum that forms the γ' phase that gives the alloy its strength. Also mentioned is that adding more aluminum to the alloy increases the brittleness of the alloy and is not a viable option.

The solution is to place an aluminum rich layer over the superalloy to act as the reservoir. Since this is a thin layer and not the bulk material, most of the mechanical properties are not as vital. This allows for coatings of brittle, high aluminum alloys to be of use. The two most common choices are the intermetallic NiAl and the multi phase MCrAlY (usually M = Ni and/or Co). Only NiAl is relevant to this study and will be discussed in further detail.

2.2.1 Aluminide Bond Coat

NiAl (β) has been known to offer remarkable oxidation resistance[6]. The coating rapidly forms a continuous alumina layer due to the large amount of aluminum present. Nickel is the only element present that can form transient oxides. This means that the protective alumina is relatively pure, dense, adherent, and slow growing. The lifetime of this coating is long in the case for isothermal or nearly isothermal exposures.

During more rapid cycling, the performance is greatly diminished. Thermal stresses are generated due to the incompatibilities of the expansions and contractions that occur during thermal cycling between the metal and the ceramic oxide (thermal stresses). The TGO is growing at the same time, repairing itself (i.e. filling in micro cracks) and gaining thickness. These actions cause growth stresses to be generated. The TGO can react to alleviate these stresses by several mechanisms. The oxide can detach from the bond coat and then buckle. Larger scale cracking and spalling of the oxide can also occur. These stresses have also been attributed to causing large scale deformation of the bond coat surface (TGO is still adhered), called rumpling[7]. The lost oxide due to spallation must be reformed to maintain protection. Reforming the scale causes depletion of Al. Aluminum is also lost due to interdiffusion with the substrate. As the aluminum content drops, phase changes occur ($\beta - \gamma' - \gamma$). Figure 2-4shows phase changes at both bond coat interfaces due to aluminum depletion. These phase changes have also been linked to rumpling[8]. Eventually the coating is unable to maintain the alumina layer. Another problem is the propensity of the coating to form large voids, by various mechanisms, which can shorten the life of the material (Figure 2-5). NiAl is also brittle and has been known to crack under forces as small as those generated during cross sectional sample preparation (Figure 2-6).

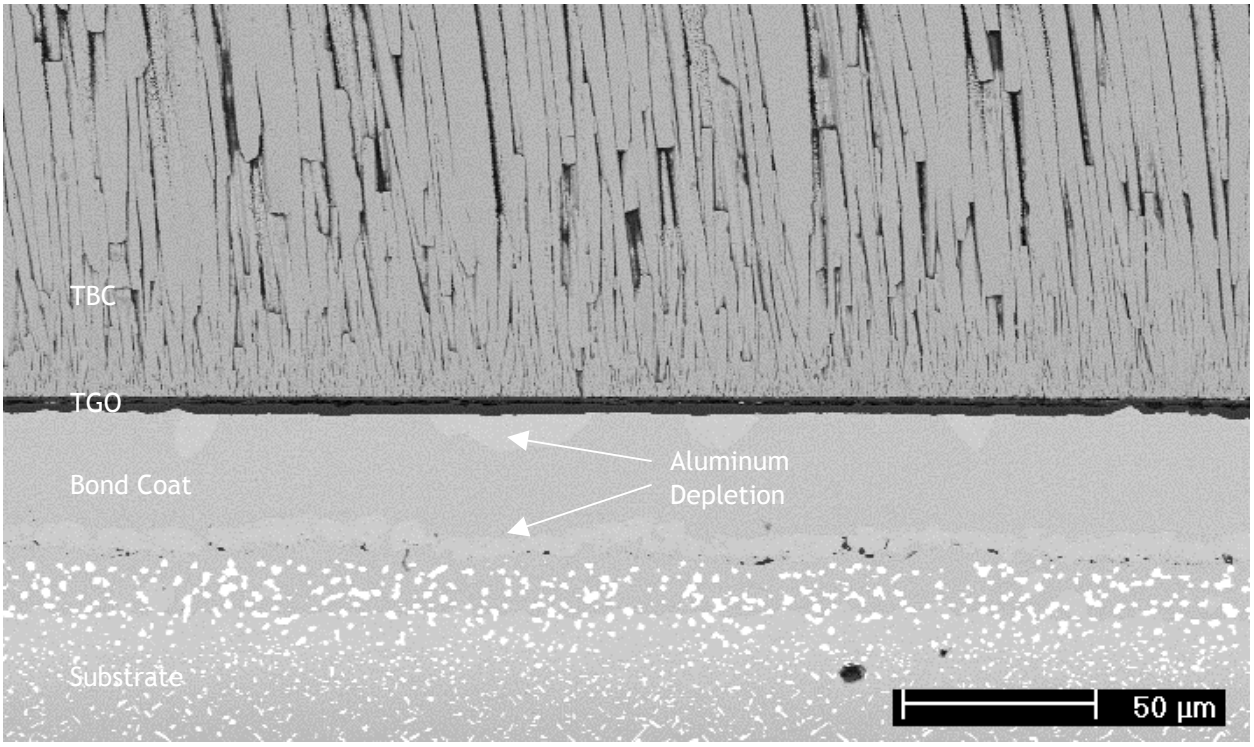

Figure 2-4. Micrograph showing phase changes (β => γ')at both bond coat interfaces due to aluminum depletion.

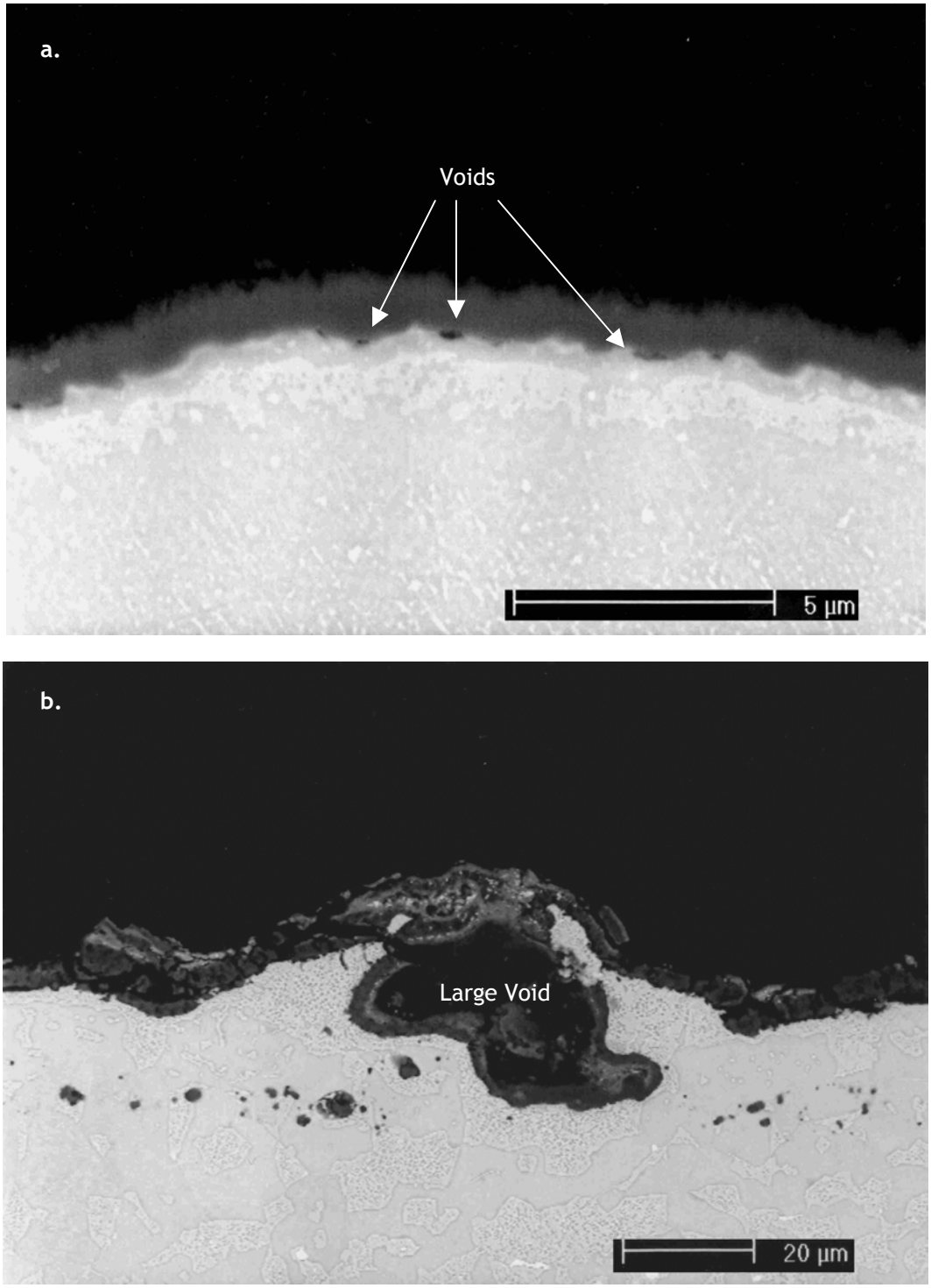

Figure 2-5. Micrographs showing voids that formed in NiAl bond coat after 50 (a) and 650 (b) cycles

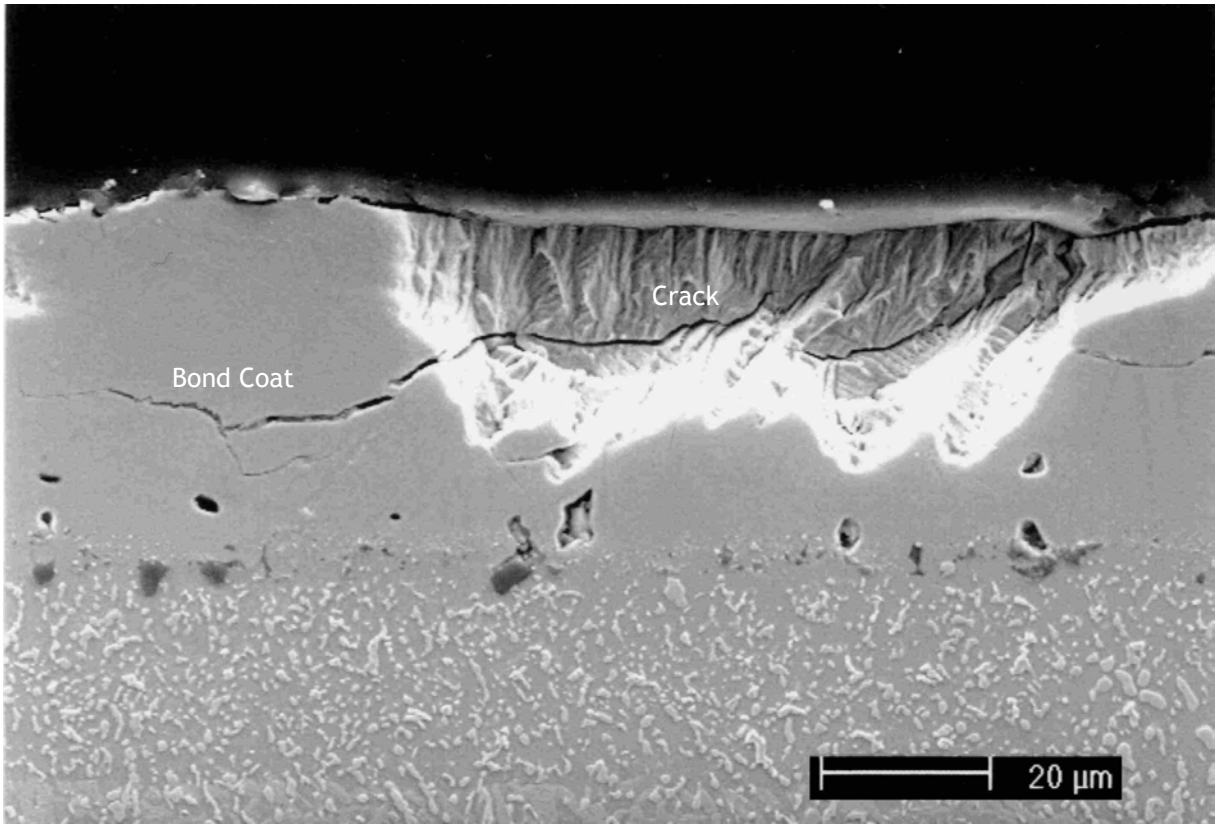

Figure 2-6. Section of Pt modified aluminide bond coat that cracked during sample preparation

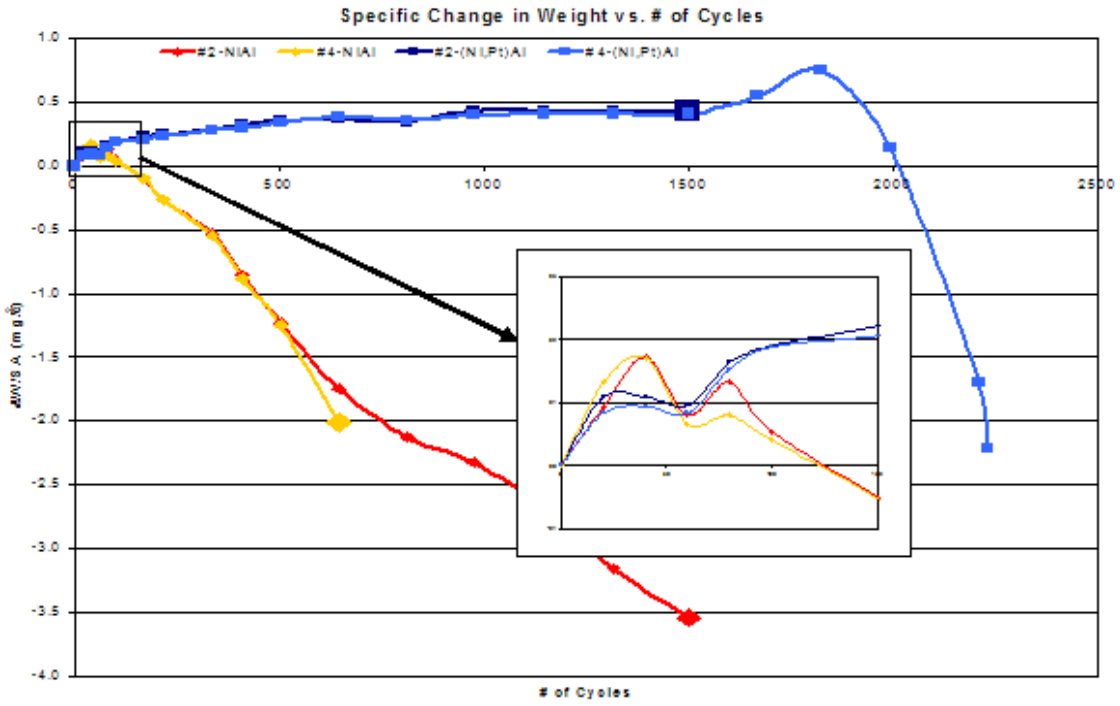

Figure 2-7. Cyclic oxidation data for PtAl and NiAl (1 hour cycles at 1100°C). The plain aluminide curve crosses zero (indication of failure) at 150 cycles, while the platinum modified aluminide crosses at 2233 cycles.

2.2.2 Platinum Modified Bond Coat

With all the problems that NiAl has, all is not lost. It is known, but not entirely understood, that platinum additions to NiAl significantly increase the useful life of this type of coating[9]. It is not unheard of to obtain an order of magnitude or more increase in usable lifetime for "platinum aluminide" bond coats during cyclic exposure. For example, a previous study by the author demonstrated an increase from 150 cycles for the plain nickel aluminide to 2233 cycles for the platinum modified aluminide[10] (Figure 2-7). Below is a list of some proposed effects of platinum that was compiled by Zhang[11, 12].

- Reduction of Growth Stresses in oxide
- Enhanced Al diffusion in the coating
- Mechanical keying by alloy protrusions into the scale
- Suppression of void formation beneath the TGO
- Slows diffusion of substrate elements
- Reduces detrimental effects of sulfur

2.2.3 Processing

Applying a platinum modified bond coat involves combination of processes and the exact method is usually proprietary. The substrate is first given a certain surface finish. The next process is to electroplate the part with 5-6 μm of platinum[13]. Electroplating is a rather straight forward process and will not be discussed further, with the exception of noting that the process is a possible source of sulfur to the system. The part is then aluminized using either pack cementation or chemical vapor deposition (CVD). Both of these methods use a chemical reaction between aluminum –halide (ex. Cl and F) vapor and the solid metal surface to deposit

aluminum on the part which is then dissolved into the alloy or reacts with the nickel and platinum. The part must then be heated to allow the aluminum rich surface layer to form the proper phase, β (Ni, Pt)Al. There are two exposure routes that can be taken, high temperature low activity (HTLA) and low temperature high activity (LTHA). The difference between the two are obviously the exposure temperature and which element, Ni or Al that diffuses first. Activity refers to the Al activity in the aluminizing vapor. The microstructures are also slightly different. The HTLA process yields a single phase (Ni, Pt) Al coating[14], while the LTHA shows multiple Pt rich phases, substrate element and carbides in the coating. Judging from the microstructures of the samples that were used in this work (Figure 2-8), it is assumed the HTLA process was used and it will be discussed in more detail.

In the case of HTLA, the substrate is heated above 1000^{o}C. The temperature and Al activity are such that the Ni diffuses outward from the substrate into the coating. A NiAl layer continues to grow outward. The nickel concentration near the substrate surface is reduced. This allows the alloying elements to come out of solution in the form of precipitates. The region that this occurs in is called the interdiffusion zone. The resulting microstructure is the same as that shown in Figure 2-8.

2.3 THERMAL BARRIER COATING

The system described thus far meets all of the mechanical and chemical requirements of materials to withstand the gas turbine engine environment. The temperature requirements for higher engine efficiency must now be considered. Unfortunately, the substrate and bond coat can only withstand temperatures around 1300^{o}C before melting. The surrounding temperature can be slightly higher if cooling channels are used in the substrate to lower the temperature of the

component. To increase the temperature further, some other method must be used to lower the temperature the metal "sees". This is accomplished by adding a layer of an insulating material called a thermal barrier coating. With the addition of the TBC, the system is complete. Figure 2-9 shows a schematic of the full TBC system.

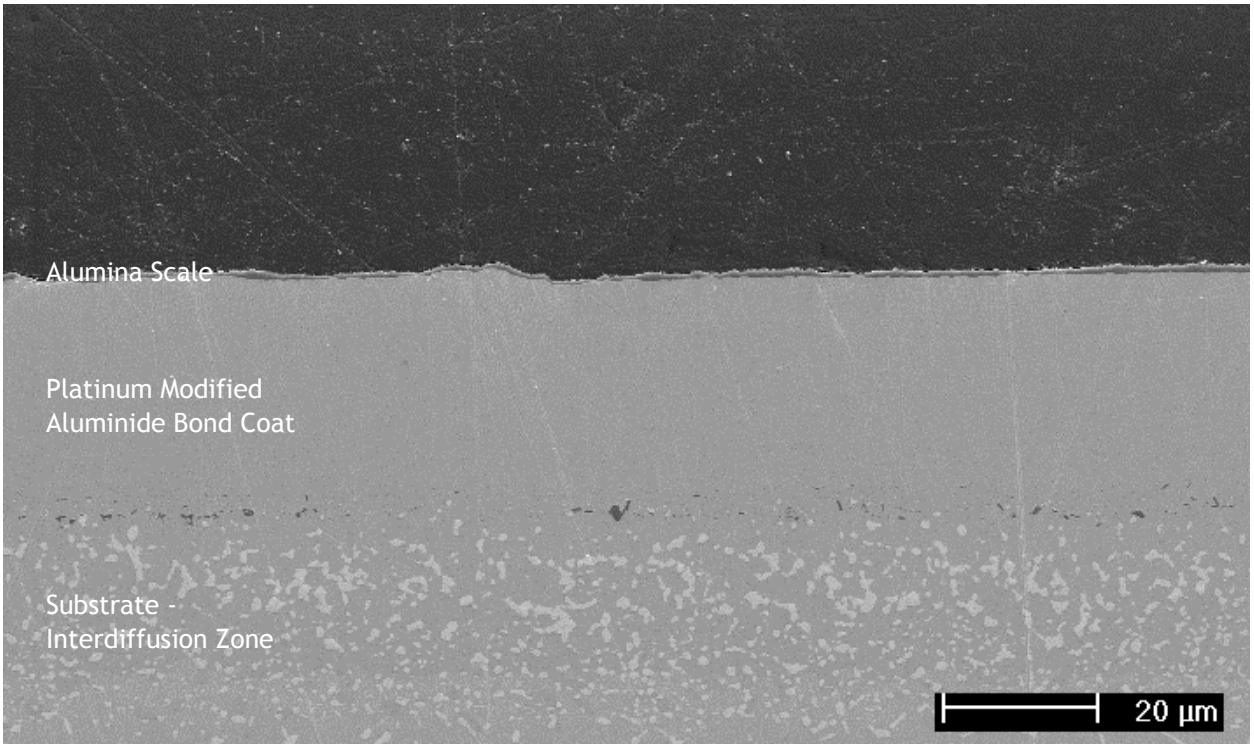

Figure 2-8. Typical microstructure of the substrate and bond coat of the samples used in this project.

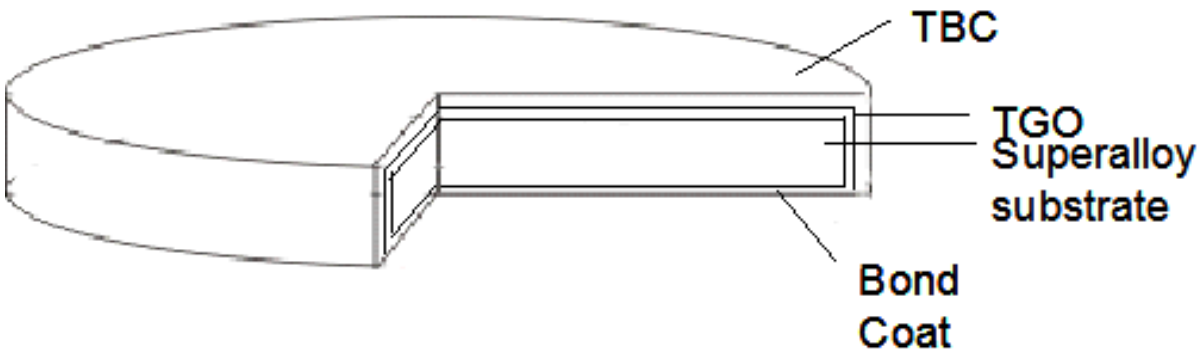

Figure 2-9. Schematic drawing of the full TBC system

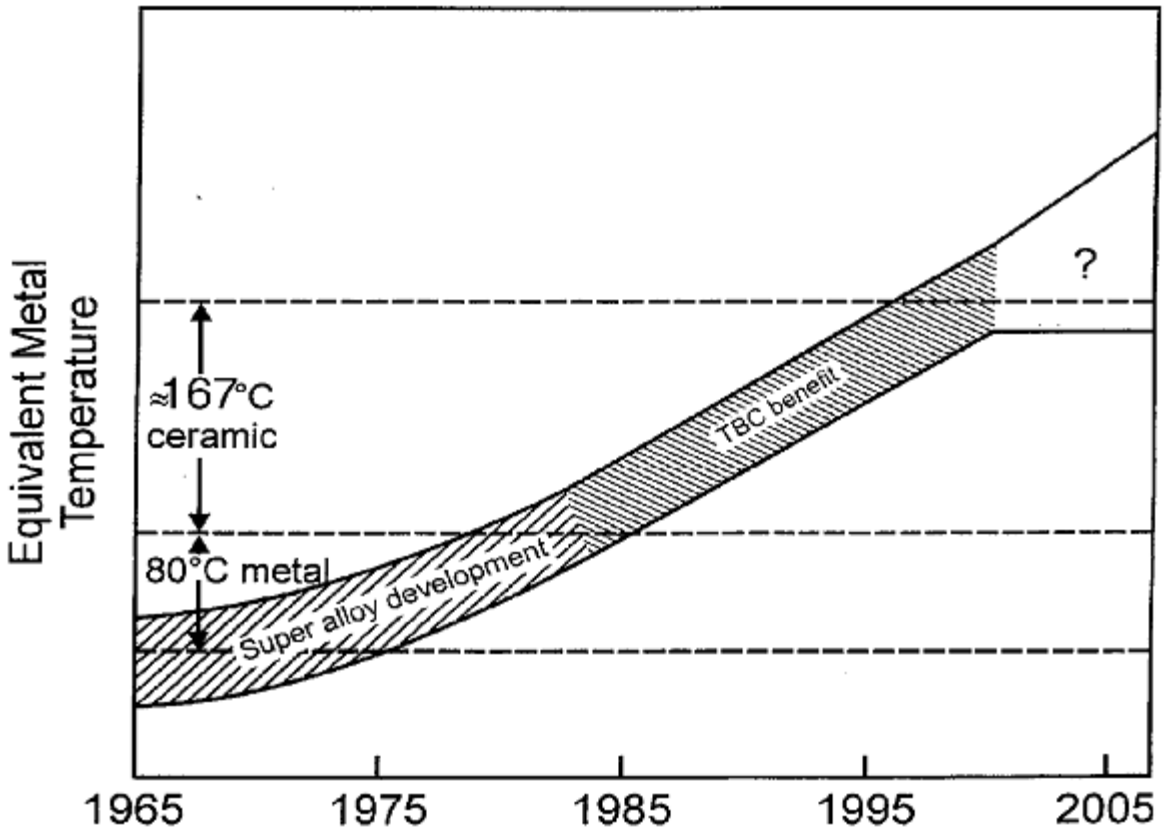

Figure 2-10. Plot showing the benefits gained by using a TBC to protect metallic components.

2.3.1 Yttrium Stabilized Zirconia

Most thermal barrier coatings are made of zirconia (ZrO_2). Zirconia goes through three allotropic phase changes when cooled from high temperatures. The structures are cubic, tetragonal, and monoclinic. For use as a TBC, ~8% yttria is added to maintain a structure of cubic and tetragonal phases. The yttria prevents the tetragonal phase from transforming to the monoclinic phase of zirconia at 1170^{o}C. This transformation includes a volume increase that adds stress to the TBC, and should therefore be avoided. The TBC has good thermal shock resistance, which is vital in a high cycle application. Fully stabilized cubic zirconia does not have the thermal shock resistance of the two phase partially stabilized zirconia[15]. This yttria stabilized zirconia (YSZ) is an excellent thermal insulator and causes a temperature differential between its interfaces of over 150^{o}C (Figure 2-10)[16]. Being a ceramic material, it is relatively resistant to chemical attack. YSZ is an ionic conductor with high diffusion coefficients for oxygen, and therefore is essentially transparent to the oxygen in the environment, reinforcing the need for an alumina forming bond coat to protect the metallic components.

2.3.2 Processing

There are two common methods for TBC deposition, plasma spraying and electron beam physical vapor deposition (EBPVD). These two methods have vastly different structures so that each has their pros and cons. The structure of the EBPVD TBC's is the most practical for application in aircraft gas turbines, and therefore will be the only method discussed in further detail.

EBPVD is a method similar to the CVD processing of the bond coat. They differ in the method that the vapor is produced. In the former case, the vapor is created by the evaporation of the target (an ingot of the TBC material) by a high energy electron beam. The vapor moves

along a line of sight to the substrate. The vapor then condenses on the preheated substrate[17]. The zirconia becomes oxygen deficient during vaporization and therefore deposition is done in a low P_{O2} environment to maintain the ZrO_2 stoichiometry (recombination occurs at low P_{O2})[18]. Chemical bonding provides the adhesion of the coating to the substrate. High deposition temperatures and post coating heat treatments must be done to achieve this[19].

EBPVD can produce several microstructures depending on the coating conditions. These parameters include deposition temperature, deposition rate, angle of incidence, gas pressure, etc[20]. The aim structure for use as a TBC is a columnar structure, where the columns are loosely bonded. This adds significant strain tolerance to the TBC. The substrate and bond coat are metals that have very different coefficients of thermal expansion than the ceramic TGO and TBC. The columns allow the TBC to expand and contract to a certain degree with the metal, while being strongly bonded to it. This slows down the stress build up in the TBC, prolonging the lifetime of the system.

2.4 CURRENT STATE OF THE ART TBC

2.4.1 Processing

A typical TBC component is manufactured with the process described below. The substrate is made of the current generation nickel based superalloy. This surface is grit blasted with alumina grit before the bond coat is applied. The bond coat is either platinum modified aluminide or MCrAlY. The platinum aluminide is applied in the manner described above. MCrAlY bond coats are applied by several different methods, including detonation gun and low pressure plasma spraying. After the bond coat is applied, the part is then grit blasted again or shot peened and subsequently grit blasted (in the case of some MCrAlY's). Frequently, the sample is then

preoxidized until α alumina forms (X-ray Diffraction is used to determine this). Then the TBC is applied by EBPVD[21].

2.4.2 Problems

There are some problems with this method of manufacture. Occasionally, some of the grit remains in the system after both grit blasting steps. It is common to see these particles near the interdiffusion zone in cross sections (Figure 2-11a). It is also common to form voids near these particles after long cyclic exposures (Figure 2-11b), since they act similarly to the markers in diffusion couples (Kirkendall – Smigelskas effect). Alumina grit has also been seen on the surface of bond coats in the as coated condition (Figure 2-12). These grit blast particles can occasionally be seen remaining in the sample after the TBC has been applied (Figure 2-13). Another major problem with the grit blasting of the bond coat, is that the rough surface can cause defects to form in the TBC during the deposition (Figure 2-14).

2.5 PREOXIDATION

It is essential to the performance of the system that the TGO be as pure and defect free as possible. This promotes the best adherence and slowest growth. It is also essential to achieve the strongest possible bond between the TBC and the surface it is deposited on. For these reasons, it is common to expose the bond coat in a controlled manner in order to produce the equilibrium alumina phase, α, prior to TBC deposition. There is also the interesting situation that occurs when the TBC is deposited directly on the bond coat. The TGO is being formed

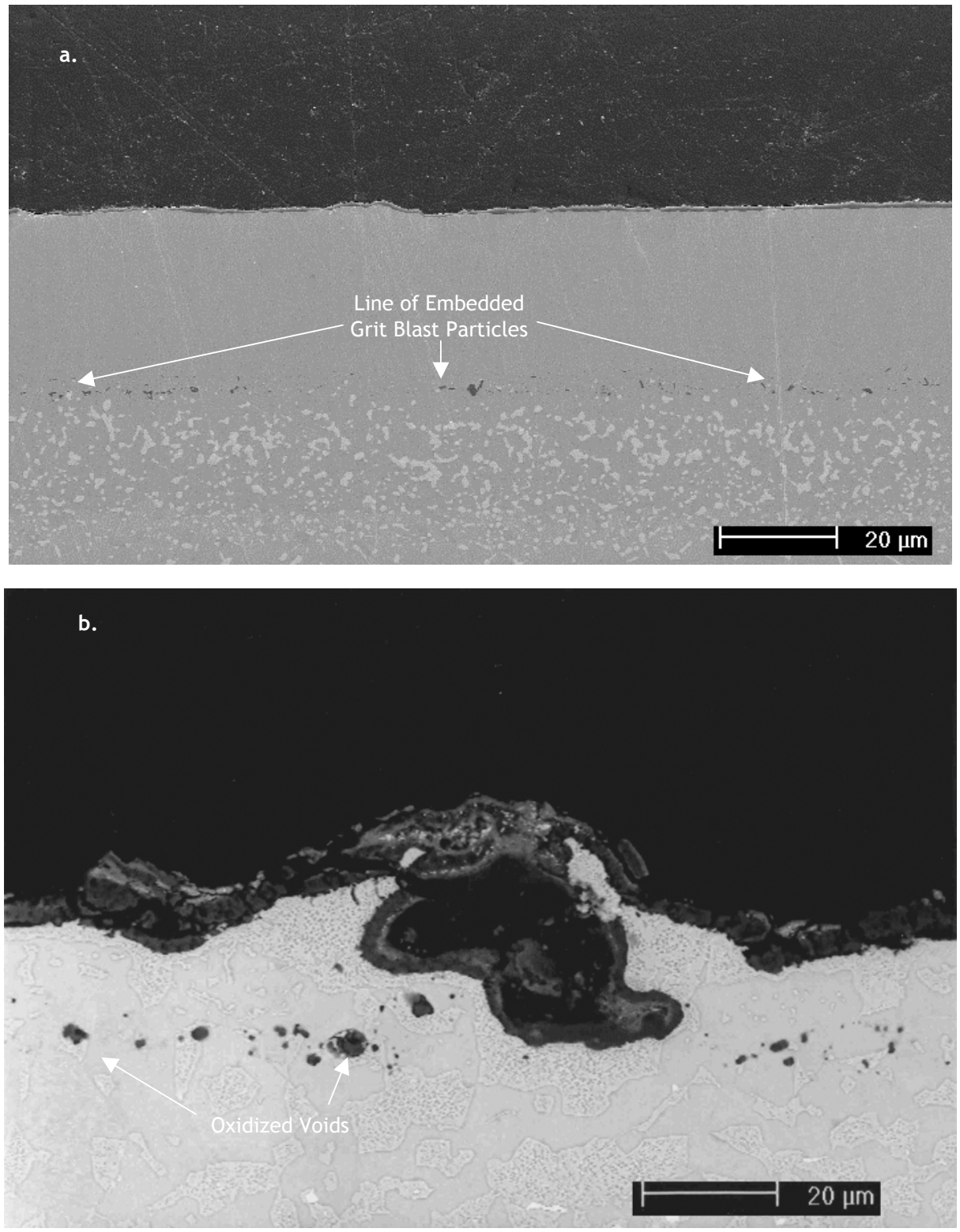

Figure 2-11. Alumina particles from grit blasting at substrate bond coat in an as processed sample (a.). After 650 cycles, voids have formed near these particles (b.).

Figure 2-12. Alumina grit embedded in the surface of a platinum aluminide bond coat in the as coated condition.

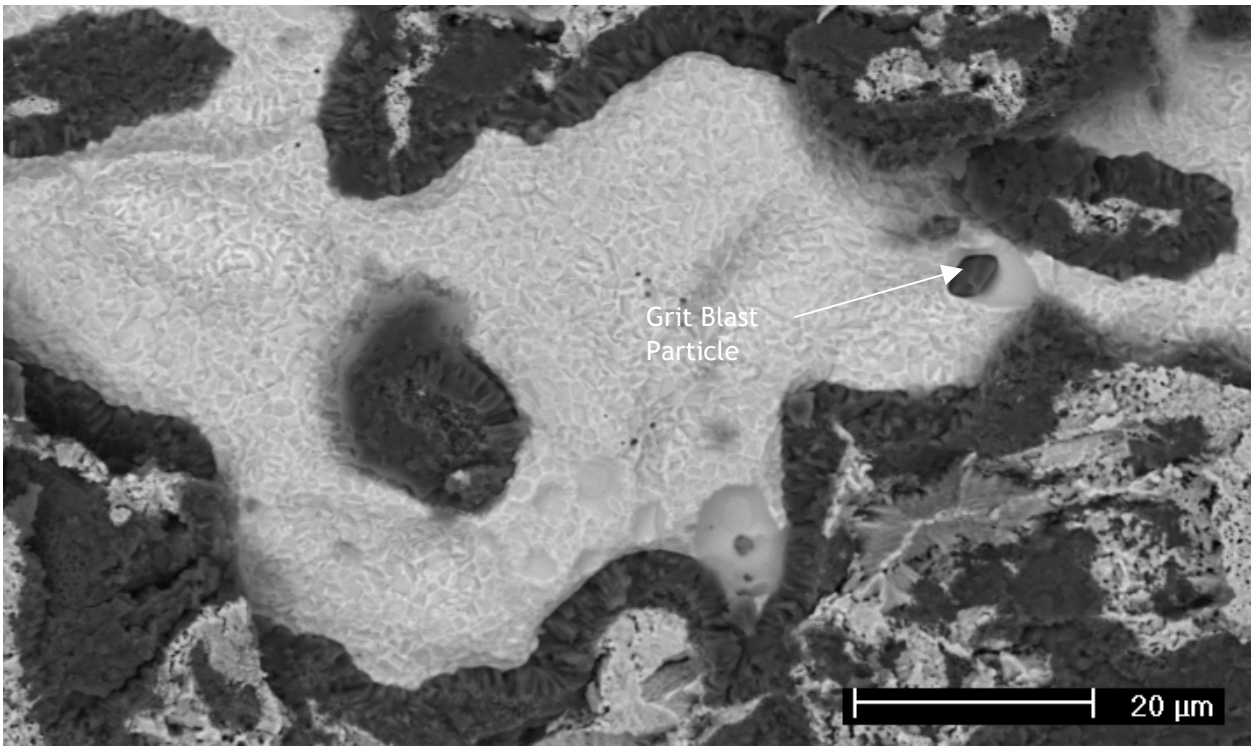

Figure 2-13. Alumina grit blast particles initially at the bond coat (grit blasted) surface remaining after application of the TBC.

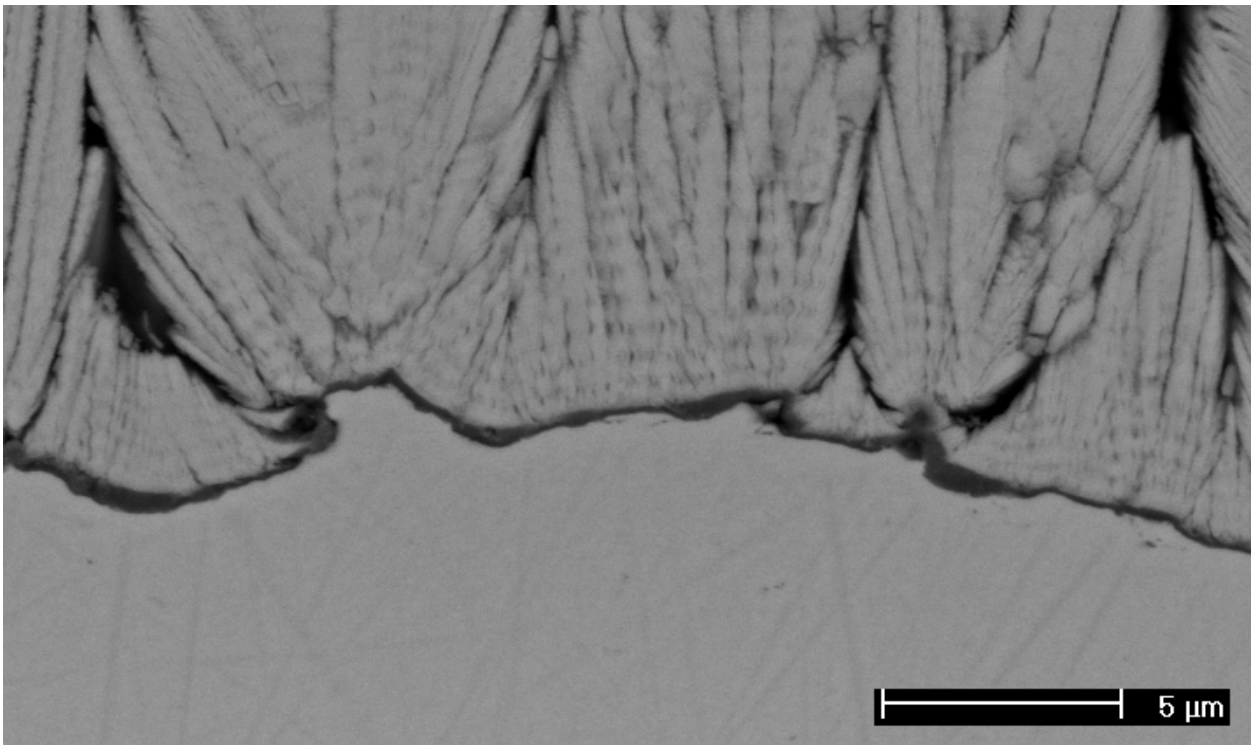

Figure 2-14. Defects in the TBC on grit blasted bond coats

between these two layers. It is hard to imagine what might be happening to the bonding of the TBC when the TGO is forming.

During the TBC deposition process, the preformed oxide will grow further. This inevitable growth of the oxide prior to any service exposure may be a cause of a shortened lifetime. A possible solution to this is to preoxidize in a manner that the TGO is as thin as possible. Controlling the temperature and oxygen partial pressure are ways to ensure a thinner alumina. At relatively low temperatures (~900^{o}C) alumina forms metastable phases such as θ and γ instead of the equilibrium phase α. Reducing the oxygen partial pressure can also form thin, metastable alumina. Lowering the oxygen partial pressure below 10^{-8} atm will eliminate any impurities or defects created by nickel oxidation. Combining low temperatures and low oxygen pressure, very thin (~0.5 μm or less) and pure alumina scales are achieved.

The lifetime of the TBC may be improved by starting with the thinner scale that develops. There are some concerns that arise by starting with the metastable TGO. The oxide will most likely transform to the stable a phase during the coating process. As a matter of fact, there may be several phase transitions between the various metastable phases (ex. γ, δ, and θ – aluminas) before transforming to the stable α alumina phase, depending on temperature and kinetics[22]. These phase transitions occur topotactically, in that the oxygen remains in an fcc-close packed lattice while the aluminum cations move[23]. The final transition to α alumina is different, due to the fact that it is a nucleation and growth process that occurs at the metal/oxide interface. It is known that there is a significant volume reduction that occurs during the θ to α alumina phase transformation and that failure can occur if the transformation occurs after deposition[24, 25]. In all cases the metastable phases show faster growth rates than the stable phase[y]. It is known that certain additions (ex. La, Ba, Si, Li, K, Ce, and Y) can retard the

transformation to the stable phase for bulk alumina[26]. Grabke argues that additions to NiAl, such as Y and Ce, end up enhancing the nucleation rate of α alumina and suppressing θ alumina formation. The adverse retardation effect is not at play in this case because only very small amounts of these are incorporated in to the scale[22]. It is also possible that Pt additions may actually allow for a more persistent θ alumina scale[27]. It is not clear what effect these phase changes can have on the TGO/TBC interface if the transformation occurs just before or during the deposition.

2.6 SMOOTHER SURFACES

There is some disagreement between the research community and industry regarding the surface roughness requirements for an EBPVD-TBC to adhere to the bond coat. As mentioned previously, the industry trend is to roughen the surface by grit blasting. Researchers claim that the EBPVD TBC's do not require a rough surface. In fact, highly polished single crystal aluminide systems have been said to "break records" in terms of lifetime[28].

The platinum aluminide bond coat surface as processed has ~50μm grain size. There are 3-5 μm high ridges at grain boundaries and very smooth faces between the ridges. The work of Yanar[29] as well as some earlier work by Gell, etal.[30] demonstrates that TBC's on bond coats in this condition tend to crack above the grain boundary ridges, while the TBC above the grain face remain well adhered. The ridges create some interesting problems. The TBC can be different in morphology (i.e. the columns are not perfectly vertical) due to the convex surface on which it is deposited. This can alter the local strain tolerance of the TBC and lead to cracking in the TBC. The area above the ridge also creates a situation of out of plane stresses in the TGO. When stresses due to thermal expansion and oxide growth are applied to the TGO, cracks can develop

and eventually spallation occurs. Both of these lead to a loss of the TBC above the ridge area. The question now becomes; by eliminating the ridges/out of plane stresses of the bond coat, will the system last longer?

Deformation of some sort is the easiest way to remove the ridges. The ideal situation would be to polish the surface flat to a similar roughness as the grain face. A flat surface will reduce or eliminate the out of plane stresses in the TGO and the defects in the TBC. Another bonus of a smoother surface is the reduction of surface area. The less surface the alumina needs to cover leads to less aluminum needed to initially form the oxide. This leaves more aluminum to maintain the oxide later on and a longer lifetime. The smooth surface can also eliminate any effect of differing diffusion distances in the rougher surface. This is more important for outward diffusion of cations than the expected inward diffusion of oxygen.

As with most "ideal" situations, there are always problems. It is also not possible to polish the complex shapes and sizes in an economical way to the traditional idea of polishing. Aluminide bond coats can occasionally reform ridges or show grooving at the grain boundaries on a polished sample[31]. Either can jeopardize the improvement gained by polishing. As mentioned above, industry has utilized grit blasting to remove the ridges. But as also mentioned above, the grit blasted surface is very rough and can cause problems. Figure 2-15 shows a schematic of the difference in the stress states in an oxide layer on grit blasted and polished surfaces. The vertical stress in the case of the grit blasted surface can lead to cracking of the oxide layer. An alternative solution to polishing or grit blasting is a method such as a milling process that uses hard ceramic media to erode the ridges away. Two methods similar to this will be discussed later.

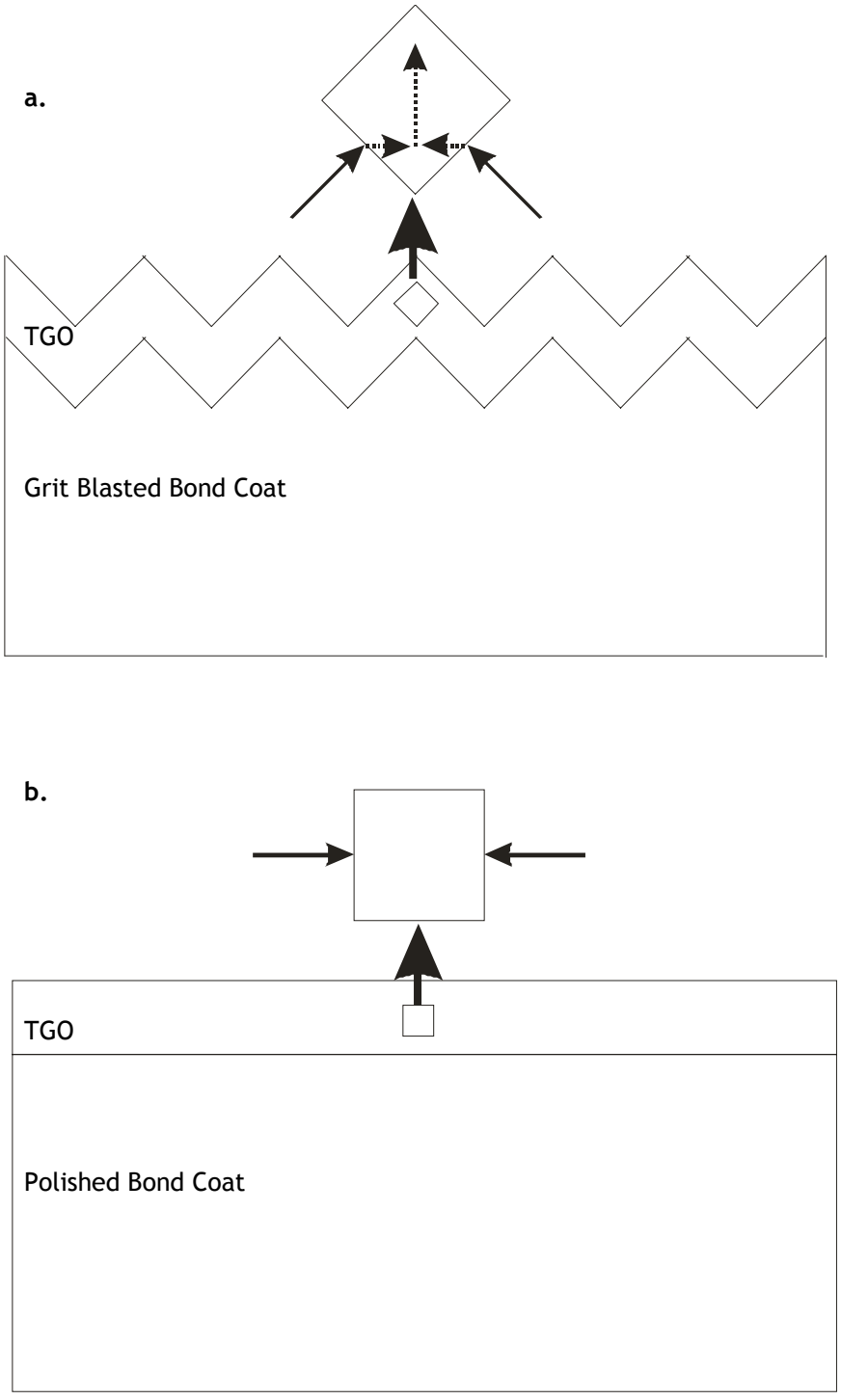

Figure 2-15. Schematic of the forces at work during thermal cycling in an oxide layer on grit blasted (a.) and polished (b.) surfaces.

3.0 EXPERMINETAL PROCEDURE

This study was done in conjunction with similar studies at the University of Connecticut (UCONN) on NiCoCrAlY + Si and Hf bond coats and University of Central Florida (UCF) on NiCoCrAlY bond coats, with UCONN being the primary contractor. UCONN and Howmet were responsible for preparing the initial samples, so the exact method used is not known. The substrate for all samples was the nickel based superalloy CMSX4 (composition shown in Table 1). The bond coat used was a platinum modified nickel aluminide that was ~50 μm thick on all sides. The samples were discs with a ~25.4 mm diameter and ~3.2 mm thick in the as aluminized condition. The samples were received in this as aluminized condition.

Table 1. Composition of Ni based superalloy CMSX4

Element	Ni	Co	Cr	Al	Ti	Ta	Mo	W	Re	Hf
wt %	61.7	9.0	6.5	5.6	1.0	6.5	0.6	6.0	3.0	0.1
at %	63.7	9.3	7.6	12.6	1.3	2.2	0.4	2.0	1.0	0.03

The research was conducted in three stages. The first is a preoxidation study done on as aluminized samples. The second is to apply the chosen surface and preoxidation treatments. The final stage was to apply TBCs to the samples from the second stage and expose until failure.

3.1 PREOXIDATION STUDY

Preoxidation treatments are believed to improve the performance of the TBC system. The goal of this stage was to determine what pretreatments would produce entirely α alumina, as much θ alumina as possible, and an even mixture of both. To accomplish this, a matrix for exposures was created for atmospheres of pure O_2 (P_{O2} = 1 atm), dry air (P_{O2} ~ 0.2 atm), and Ar-H_2 (P_{O2} ~ 10^{-8} atm) and temperatures of 900, 1000, and 1100 ^{o}C. As mentioned above, the samples were in the as aluminized condition. To conserve samples, they were cut into quarters using an abrasive cut off wheel. It was assumed that the uncoated surfaces created by cutting the samples would have no effect due to the short exposure time.

3.1.1 Exposure Techniques

The furnace used for the exposures was a horizontal tube furnace with quartz tubes (Figure 3-1). A flow meter and several valves control the input gases. The exiting gases are passed through an oil bubbler and are then run into a fume hood. A mechanical vacuum pump was attached to evacuate the furnace for low P_{O2} exposures and can be taken on or off line by valves. The samples were supported in the furnace by a basket constructed of platinum wire. The temperature was controlled by the furnace control thermocouple and manually checked by an external thermocouple placed into the quartz tube as needed.

The exposures were essentially the same for each sample. The sample was placed in the basket and the furnace was sealed. The gas was allowed to flow through the furnace and the flow rate was set at ~ 1 cm/s, or 1 bubble (out of the oil bubbler) per second. Once the flow was set, the temperature was set and the furnace was turned on. If the Ar-H_2 gas was to be used, the furnace was evacuated using the vacuum pump and then back filled with the Ar-H_2 gas prior to

heating the furnace. When the temperature was reached, the sample basket was slid into the hot zone using a magnet. After 2 hours, the sample was removed from the hot zone and the furnace turned off. The apparatus was allowed to cool overnight with the gas flowing. The gas was turned off and the sample was then removed.

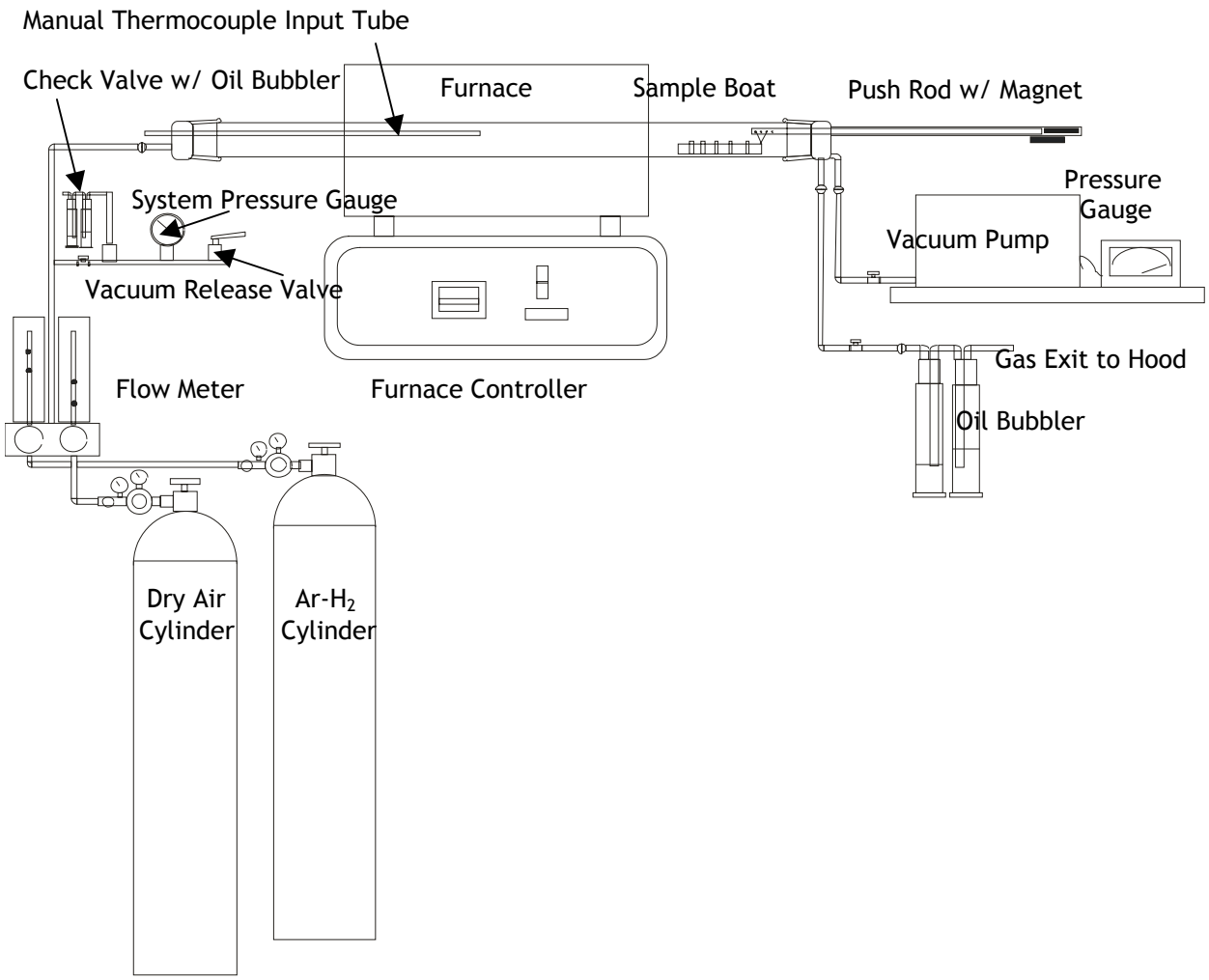

Figure 3-1. Schematic of the horizontal furnace used for preoxidation treatments

3.1.2 Analysis Techniques

Samples were examined using Scanning Electron Microscopy (SEM), X-Ray Diffraction (XRD), and Laser Photoluminescence (LP, done at UCONN). The SEM was used to observe the surface morphology of the samples and to determine the amount of transient oxides, if any, that formed on the surface. The other two analyses were used to determine the phase or phases of the alumina scale. Two scans were done using XRD. The first was a $\theta - 2\theta$ scan to determine the peaks that are from the substrate. The second was a low angle, fixed incidence scan to attempt to maximize the amount of the oxide the X-rays sampled in order to determine the oxide phase. As mentioned above, the laser photoluminescence work was done at UCONN, and therefore the exact method for gaining the returned data is not known. From this pool of data, the preoxidation treatments to be used in the remainder of the research were chosen.

3.2 PRE-DEPOSITION SAMPLE PREPARATIONS

The procedure for this phase of the work was to have commercially available surface finishes applied to the samples, apply the preoxidation treatments, and then examine again before coating. The chosen finishes were Howmet's media finish and barrel finish applied by USF Surface Preparation Group. These finishes are smoother than the grit blast and (depending on size of test area) the as aluminized samples. Therefore, some samples were hand polished to attain the smoothest surface possible. A brief description of the method of applying each finish will be discussed below.

3.2.1 Description of Surface Finishing Methods

The commercial finishes are proprietary, therefore very little is known about the specifics of each method. The media finish by Howmet uses abrasive stones in a vibrating bowl to erode the surface. The barrel finish apparatus is a centrifugal ball mill. The barrel is rotated in a way that creates a 20g or 20 times the force of gravity force on the media and sample. The media can be of any material and any combination of shapes and sizes to create customized finishes. It is even theoretically possible to create a nearly polished finish[32]. There is a concern with both of these finishes for use with platinum aluminide bond coats due to the tendency for the platinum in the sample to remain near the surface. Removing large amounts of material to arrive at a given finish could possibly also remove some of the platinum. In the case of this work the barrel finish is even further at risk because the samples already had a media finish applied to them. They also may have been batched with the MCrAlY samples from UCONN and UCF, which are thicker and do not have the same concern with material removal.

Hand polishing is not currently a viable surface preparation for commercial usage, so the finish had to be applied "in house". Due to the relatively thin bond coat and the tendency for much of the platinum to be located near the surface, care had to be taken during preparation. The sample was placed on top of a thin glass slide cover and then on top of a larger piece of glass that was assumed to be flat. A jig (Figure 3-2), consisting of a large steel hexagon (with set screws) and a brass cylinder, was placed on top. The cylinder was pushed snuggly against the sample and the set screws were tightened to hold it in place. The jig was removed and the glass slide cover was taken from underneath the sample. The jig was then heated on a hot plate and a small amount of crystalbond wax was melted on the brass cylinder. The jig was then placed back over the sample and allowed to cool. The wax takes the place of the slide cover and is assumed to

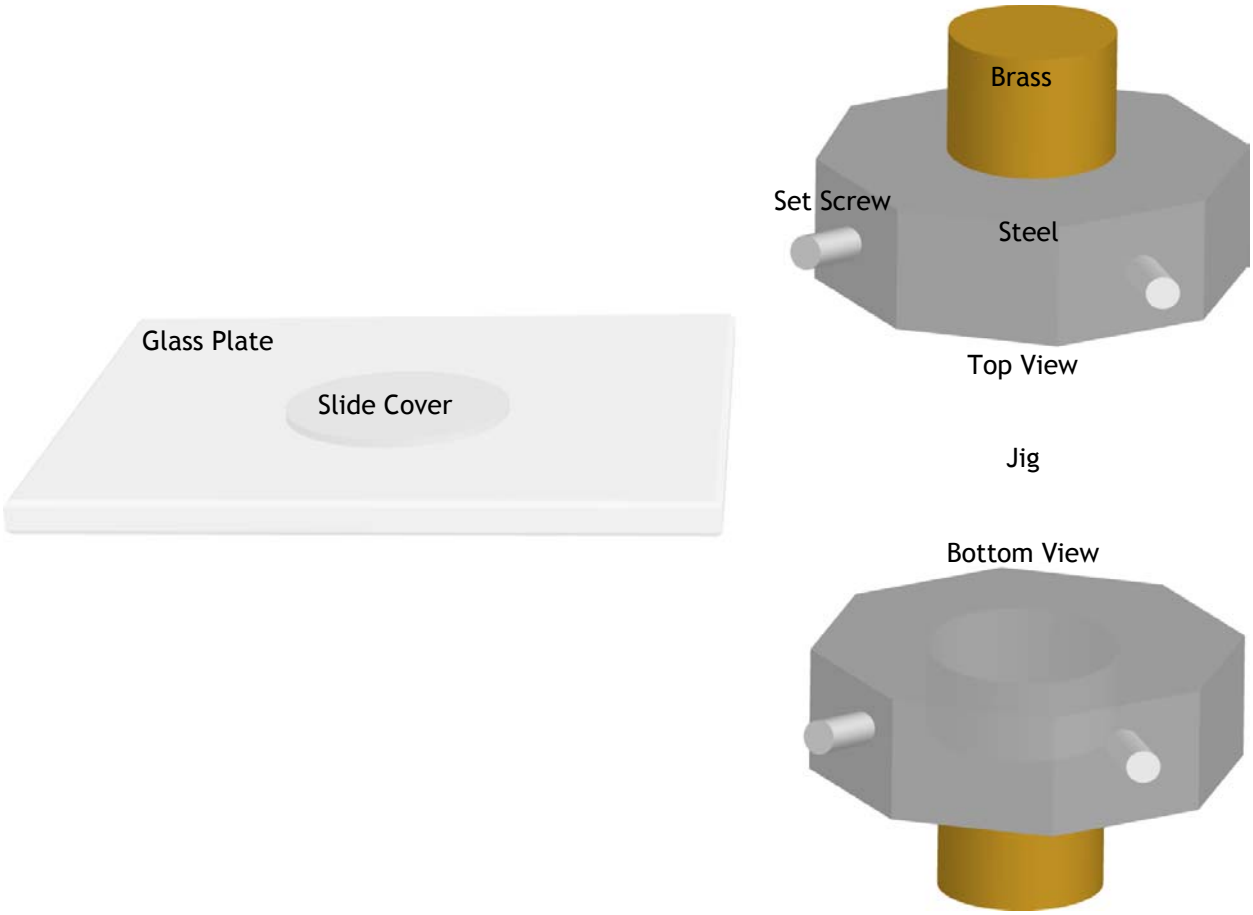

Figure 3-2. Schematic drawing of the tools used to ensure a planar sample surface during polishing to remove the grain boundary ridges.

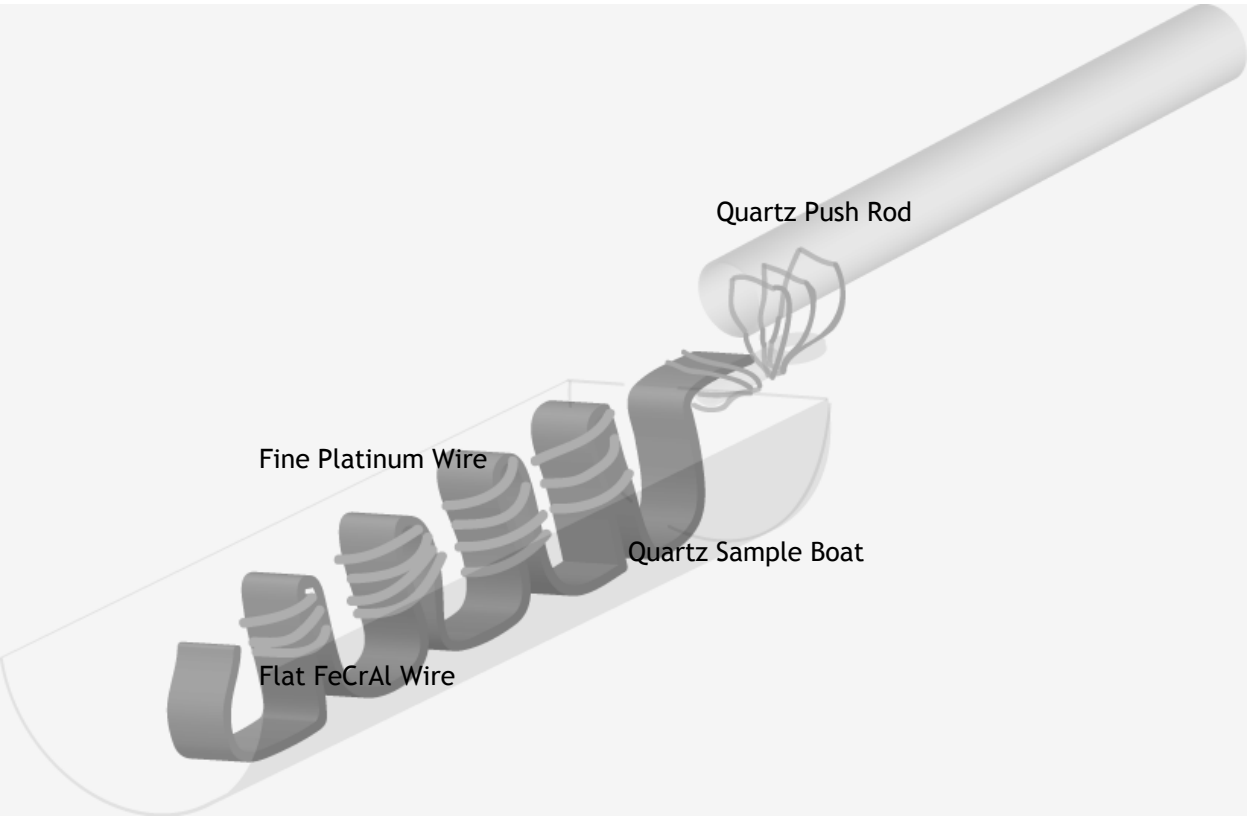

Figure 3.3. Schematic drawing of the sample boat created to accommodate larger samples in the preoxidation furnace.

shrink uniformly; therefore, the sample remains flat and affixed to the jig. This entire structure was then polished with 600 grit, SiC paper. The bond coat appeared to be thicker near the edges, so the samples were polished until the ridges were removed to the half radius of the sample, leaving some ridges in the center. From this point, the sample and the brass cylinder were removed to prevent damage to the polishing wheel and then further polished to 3 μm diamond. The sample was removed from the cylinder by heating and the remaining wax was removed by ultrasonic cleaning in acetone.

3.2.2 Exposure Technique

The preoxidation treatments were performed using the same procedure as the previous stage. The sample boat (Figure 3-3) was modified to accommodate larger specimens. The chosen treatments were: Ar-H_2 at 900 ^{o}C (max θ alumina), Ar-H_2 at 1100 ^{o}C (mixture of α and θ alumina), and dry air at 1100 ^{o}C (all α alumina). As a baseline, a few samples were not given a preoxidation treatment. It was attempted to have at least duplicate specimens for each treatment. Table 2 shows the treatments and the sample distribution in each, as well as other data.

Table 2. Summary of results from samples coated with TBC's

Pre-ox/Finish	Sample	RA(μm)	θ	failure time
1100°C Dry Air 2hr 40 min Media	LI9	0.737	14617	0
	LI10	0.960	14612	900
	LI11	0.414	14613	0
	LI12	0.713	14617	1020
1100°C Ar-H 2hr 40 min Media	LI14	0.636	14611	---
	LI16	0.704	14613	0
	LI17	0.871	14612	*260
	LI18	0.583	14617	*260
1100°C Dry Air 2hr 120 min Media	LH92	0.601	0	---
	LH94	0.438	0	1020
	LH95	0.502	0	960
	LH96	0.425	0	1040
1100°C Ar-H 2hr 120 min Media	LH97	0.434	14546	0
	LH98	0.351	14543	260
	LH99	0.343	14542	120
	LH100	0.485	14543	100
NONE 120 min Media	LI4	---	---	0
	LH93	---	---	0

Pre-ox/Finish	Sample	RA(μm)	θ	failure time
900°C Ar-H 2hr 120 min Media	LI5	0.350	14543	0
	LI6	0.407	14543	0
	LI7	0.410	14547	0
	LI8	0.429	14547	0
1100°C Ar-H 2hr 3μm Polish	LG94	0.073	0	---
	LG99	0.057	0	640
	LG00	0.048	0	200
	LH01	0.104	0	240
NONE 3μm Polish	LG89	---	---	0
	LG90	---	---	0
	LG91	---	---	0
1000°C Dry Air 4hr 3μm Polish	LG93	---	---	300
NONE Barrel	LG95	---	---	40
1100°C Ar-H 2hr Barrel	LI13	---	---	---
	LI15	---	---	200

*examined prior to failure (samples from Jentek)
--- in failure time means analyzed as coated
0 in failure time means failed at the coater

3.2.3 Analysis Techniques

The samples were examined using the same methods above. They were additionally examined using surface interferometry (done at UCONN). This technique compares interference in a light beam on the sample to a reference beam to quantify surface roughness and other parameters. The more common "mechanical" surface roughness equipment in the Mechanical Engineering Department was also used, but the stylus size was too large to get precise measurements on these smoother surfaces.

3.3 TBC EXPOSURES

The samples were returned to Howmet for TBC deposition after all examinations were complete. The TBC consisted of YSZ deposited by EBPVD. The exposures were done in a bottom loading furnace. Since the work was part of a larger project, the furnace was slightly modified to match the furnaces at UCONN and UCF. The furnace uses a control thermocouple in the hot zone to control the temperature. Another thermocouple runs through the sample tray as a check on the sample temperature. In the case of this study, the control thermocouple was switched to the sample tray and the other thermocouple was placed in the hot zone. A dummy specimen was then placed on the control thermocouple to better simulate the specimen temperature. This set up is shown schematically in Figure 3-4. The exposures were cyclic and done at 1121 ^{o}C (2050 ^{o}F). One cycle consisted of a 10 minute ramp up to 1121 ^{o}C, a 45 minute hold, and then a 5 minute cool to ~160 ^{o}C (this depends on external conditions in the lab). Figure 3-5 shows a typical cycle. After every 20 cycles, the samples were removed from the furnace and placed in a desiccator for 4 hours where they could be observed visually. The samples were removed from testing when they displayed large scale buckling or TBC loss.

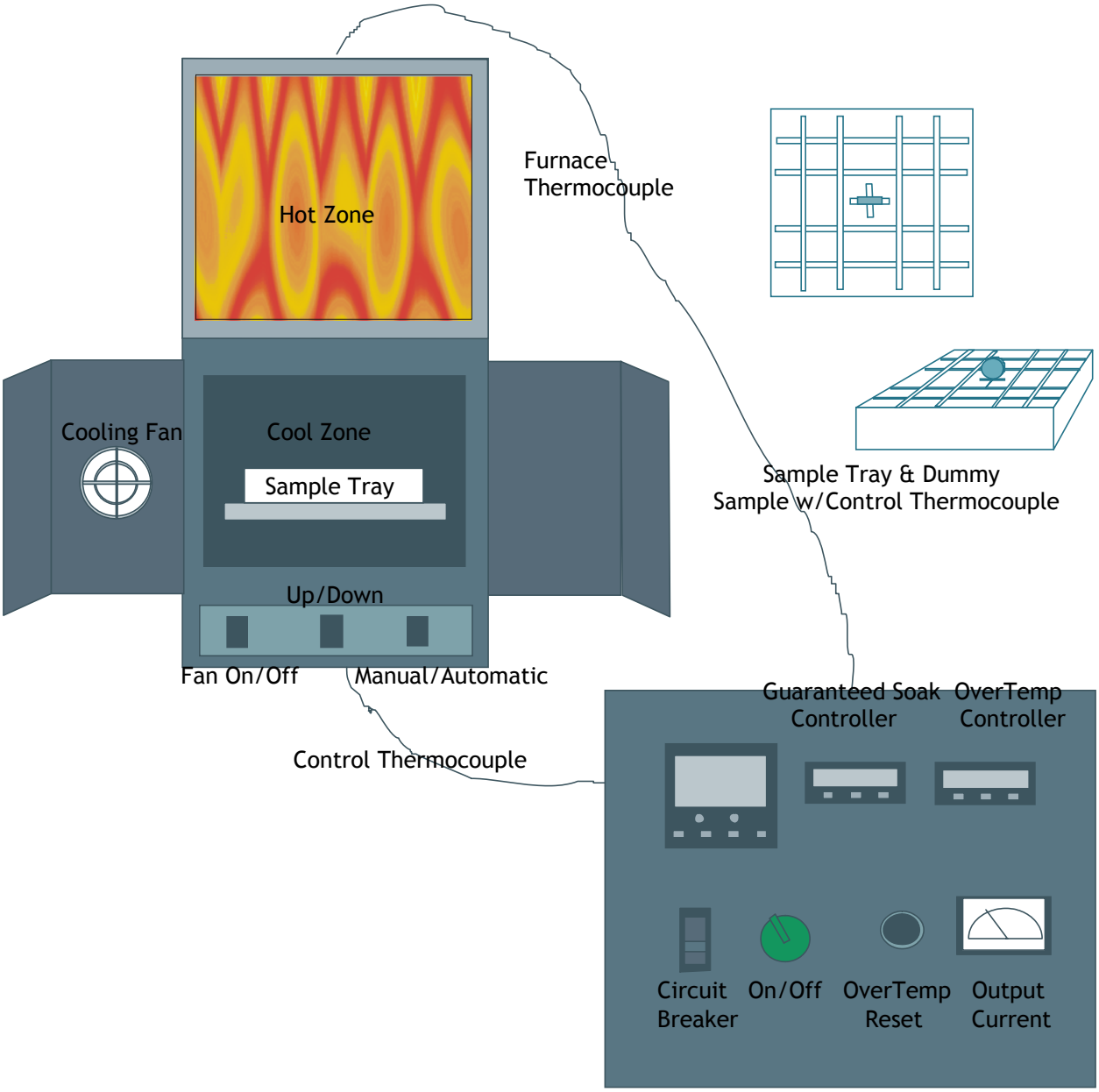

Figure 3-4. Schematic drawing of the bottom loading furnace and modifications to the sample tray.

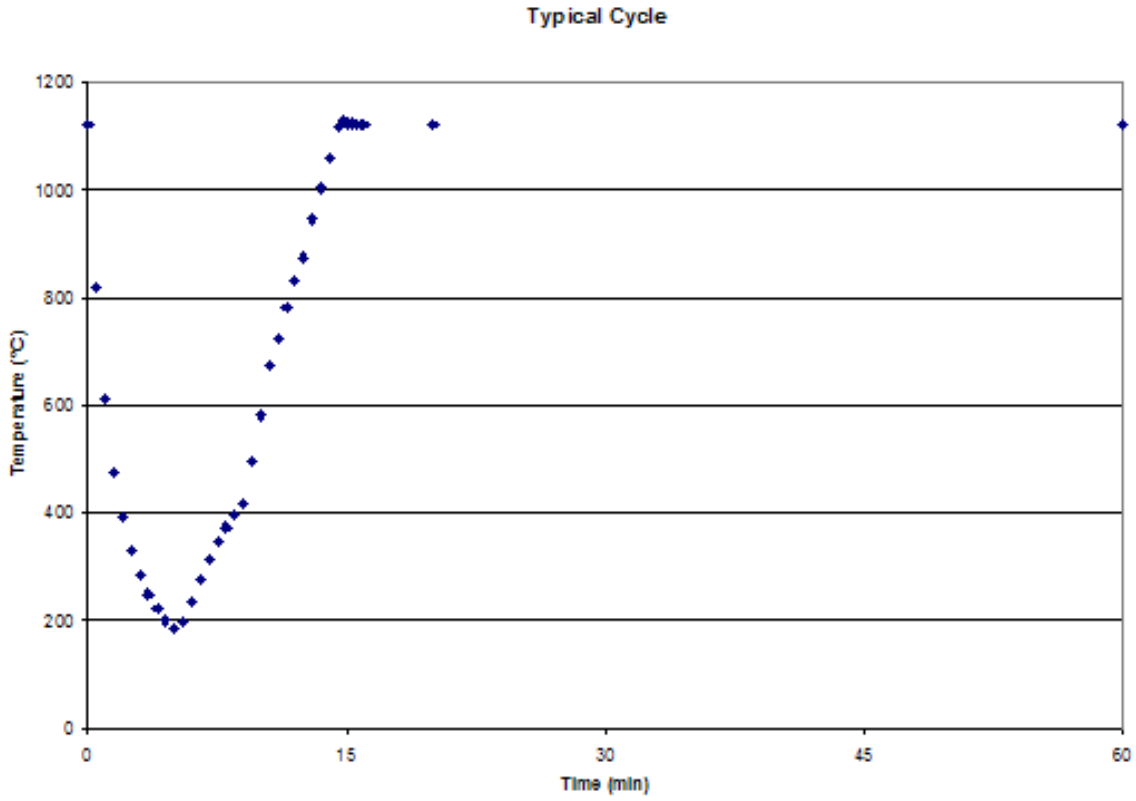

Figure 3-5. Plot of the temperature profile for a typical cycle (10 min. heat up, 45 min. hold at 1121°C, 5 min. cool down) in the bottom loading furnace. Due to the modifications to the furnace, this profile is that of the dummy sample, not the hot zone of the furnace.

After failure, the fracture surface and cross-sections were examined using the SEM. The fracture surface was observed first. This includes viewing both sides of the fracture (substrate/bond coat side and underside of the TBC) and occasionally the top of the TBC. Despite the TBC being a ceramic, it is not necessary to apply a conductive coating to the sample prior to observation of the surface. The spalled TBC pieces were attached to a non vital (ex. on top of areas of TBC still intact) area of the sample by carbon tape. The cross section samples were mounted in Struers Triofix cold mount and held upright by metallic clips. Dipping the cured mount in acetone removes any sticky residue from the mounting process. The mold was shorter than the samples, so the excess sample and some of the mount was cut off prior to polishing. The samples were positioned in a manner that this cut would include areas of failed and intact TBC in the cross section, if possible. Polishing was done by an automatic polishing machine through 3 μm diamond and finished with 0.05 μm SiO_2. The cross sections were sputter coated with palladium before SEM analysis.

4.0 RESULTS AND DISCUSSION

As with the procedure section, it is convenient to break the results and discussion into three major groups. Several of the results in each group were similar, allowing the larger groups to be broken into smaller sub groups.

4.1 RESULTS OF PREOXIDATION STUDY

The results of the preoxidation study were very intriguing. The first three sections will discuss various morphological features as observed with the SEM. The final section will discuss the results of the XRD and luminescence work.

4.1.1 Void Formation

Platinum aluminide bond coats usually show very long lives in cyclic oxidation studies. NiAl based materials are also prone to void formation after prolonged exposure. This is a long known and well documented problem. Due to the long lifetime of the coating, not much work has been done on oxidation exposures similar to the 2 hours exposures in this study. Several of the samples formed voids just below the alumina scale, giving the samples a leopard print appearance (Figure 4-1). The voids appeared to be small (~ 1 μm) and somewhat faceted. The volume of voids varied by grain and appeared to line up in some cases on what could be crystallographically significant directions (Figure 4-2). This suggests a relation to grain orientation. Some grains also showed linking of the small voids into larger irregular shapes. Figure 4-3 shows this in an area where the oxide scale has spalled. The voids appear to have

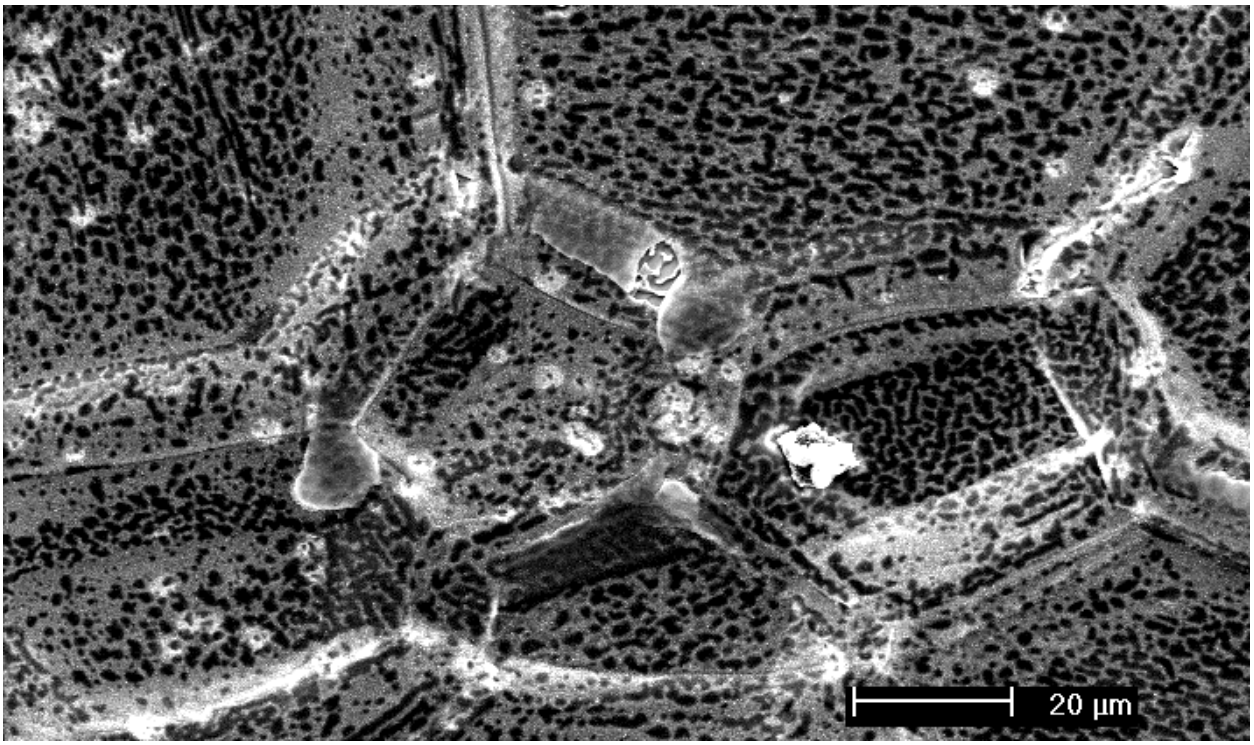

Figure 4-1. Micrograph of a platinum aluminide bond coat exposed in Ar - H2 at 1100^{o}C for 2 hrs. The surface has a leopard print appearance due to the formation of small voids (appear black) between the bond coat and the alumina scale.

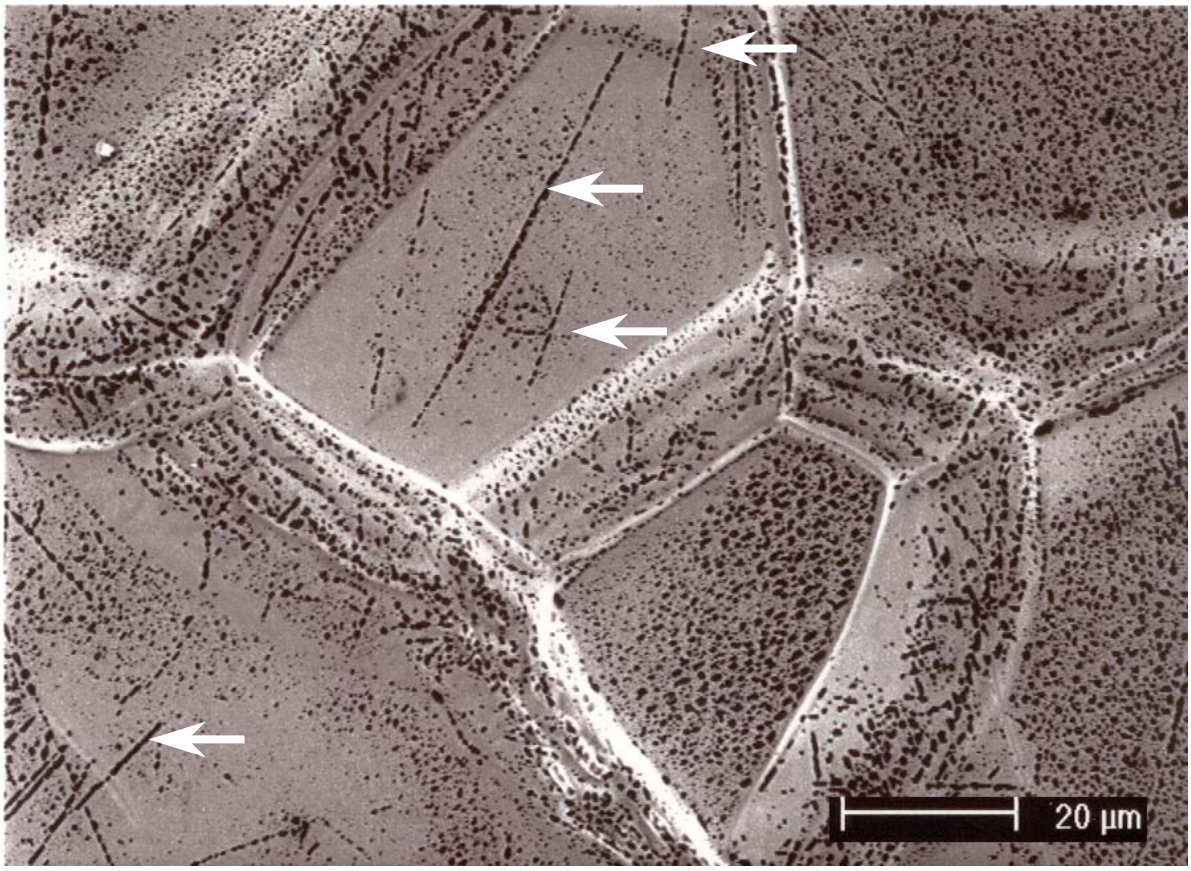

Figure 4-2. Surface of as processed platinum aluminide bond coat after 2 hr exposure at 900°C in an Ar – H2 gas mixture. The arrows indicate voids in lines that could be crystallographically significant.

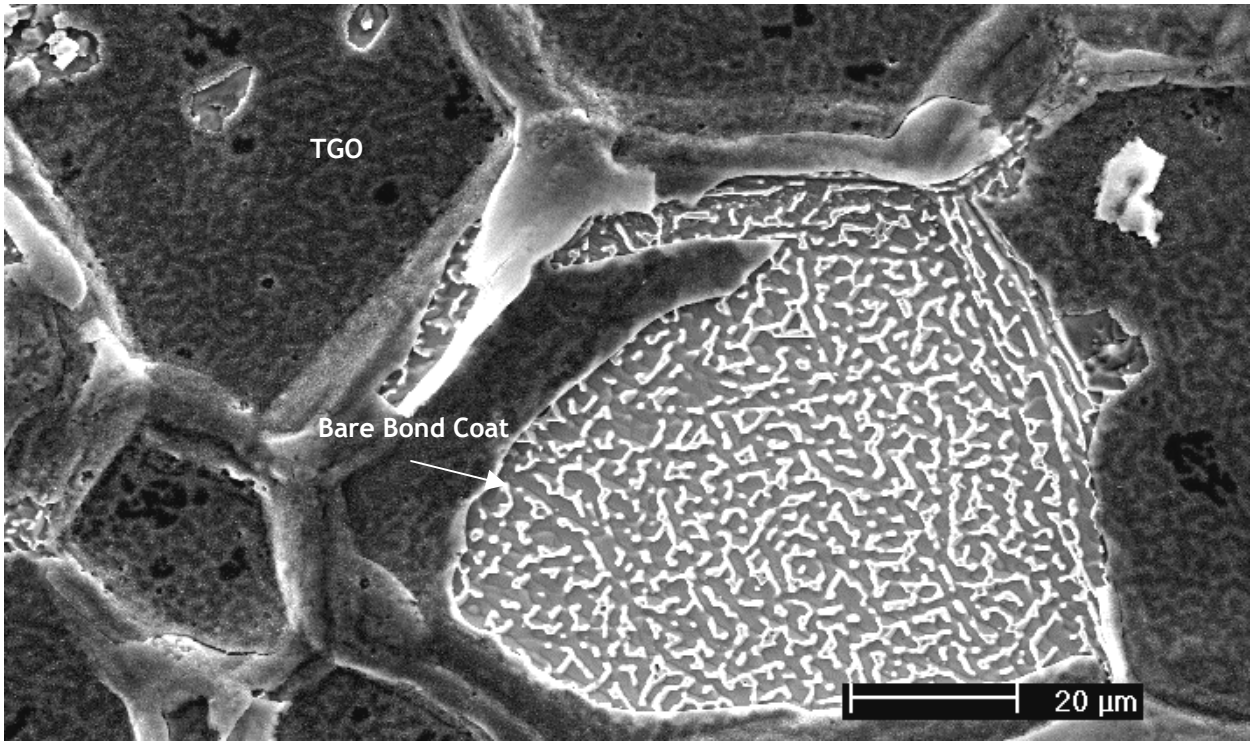

Figure 4-3. Micrograph of sample LF27-L (exposed for 2 hrs. in dry air at 1000°C) showing the intricate void structure that develops under the oxide scale.

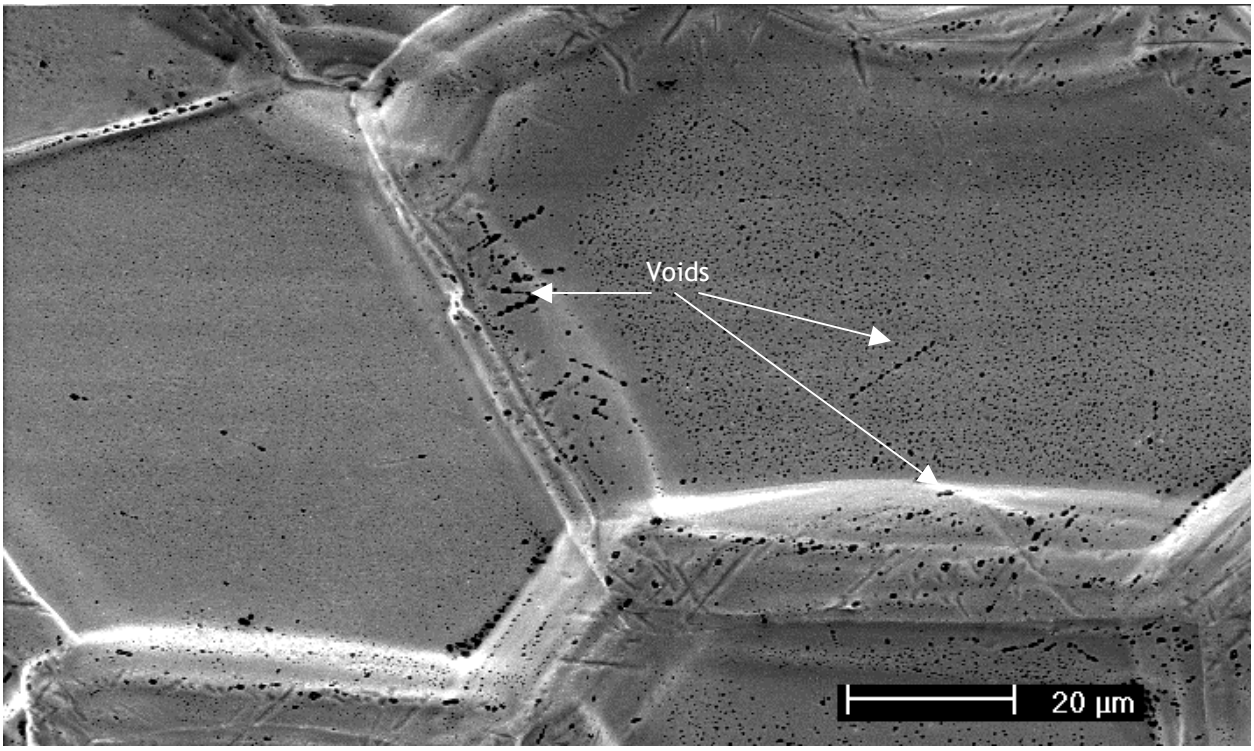

Figure 4-4. Sample LF28-2 displays beginnings of void formation after a 15 minute exposure in Ar-H_2 at 1000^{o}C.

coalesced into a network of void space under the scale. A sample was exposed at 1000 ^{o}C in the Ar-H_2 gas for 15 minutes and showed several sub micron voids (Figure 4-4). Another sample was preoxidized in an environment that was known to form voids and then reexposed for 45 hours in dry air at 1100 ^{o}C. The voids remained after the exposure, but were harder to observe due to the increased oxide thickness (Figure 4-5a). The voids on this sample were not visible in cross section (Figure 4-5b). They did however appear on other cross section samples as shown in Figure 4-6. These voids form very early during exposure and appear to remain after prolonged exposures. Restrictions in the number of specimens available did not allow further work to understand this phenomenon.

Others have observed voids similar to these. Smialek[6] observed them on polished NiAl and Oquab and Monceau[33] on β-(Ni, Pd)Al. Haynes[34] has seen voids on as coated TBC samples. Tolpygo[35] has observed larger faceted voids after ~300 hours of exposure.

4.1.2 Rosette Morphology

Another interesting observation was the formation of a rosette-like morphology. It was found that exposures at 1100 ^{o}C in the Ar-H_2 environment reproducibly formed the morphology shown in Figure 4-7. The bond coat forms light colored circles or rosettes of oxide in a dark oxide matrix, where light and dark refer to the shade (SEM backscatter images) in Figure 4-7. Both areas are alumina, with the rosettes showing slightly more nickel. This most likely means that the oxide is thinner in those regions. The centers of the rosettes appeared more plate-like in morphology, similar to what is frequently seen on a fully α alumina scale (Figure 4-8). The "matrix" area appears to be grainy in appearance. It is possible that the exposure conditions catch the θ to α alumina transition as it is occurring, with the "dark" areas being the θ alumina

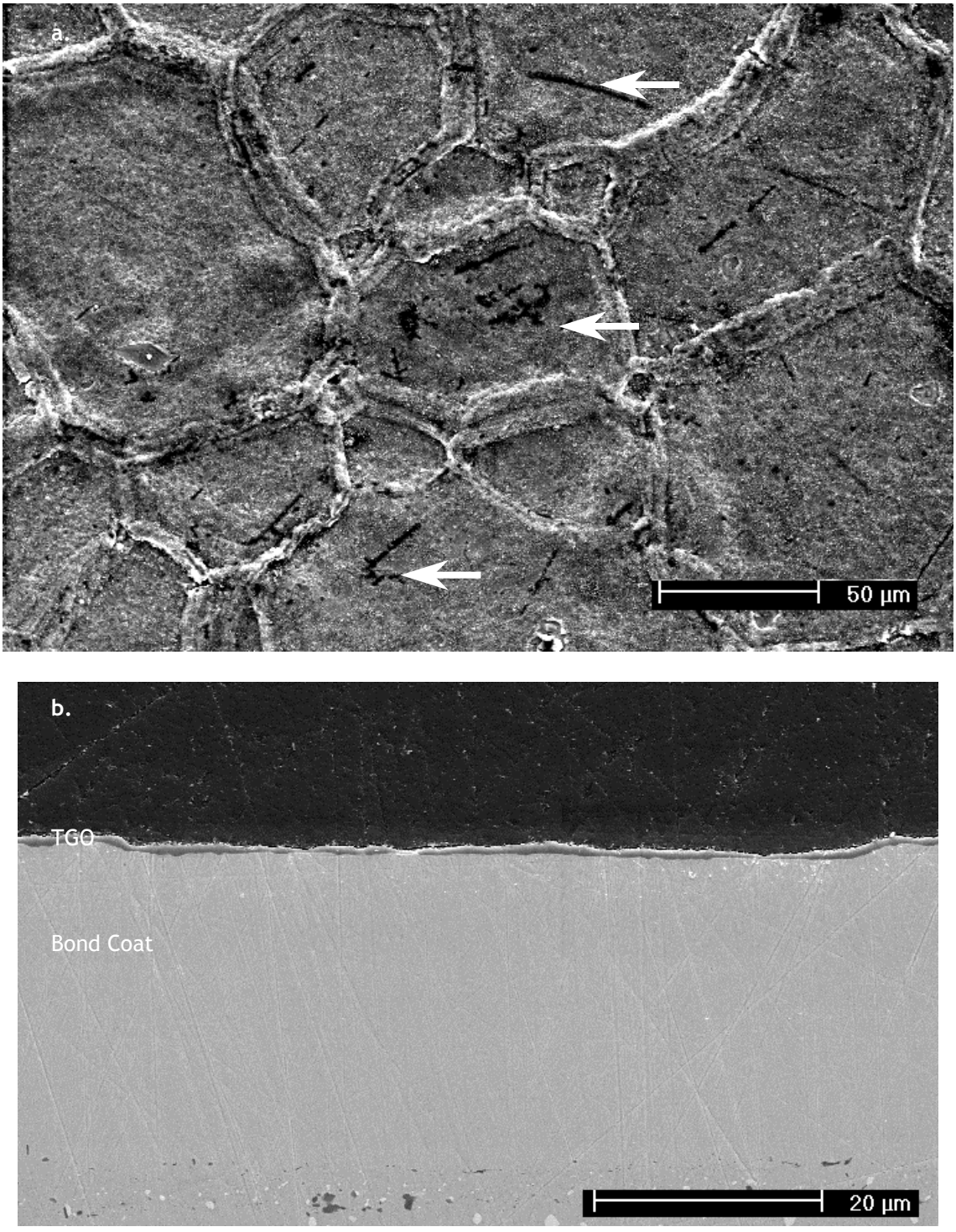

Figure 4-5. LF27-F exposed for an additional 45 hr in dry air at 1100°C still shows lines of voids still visible through the scale, (a.). The voids are not present in the cross section micrograph, (b.).

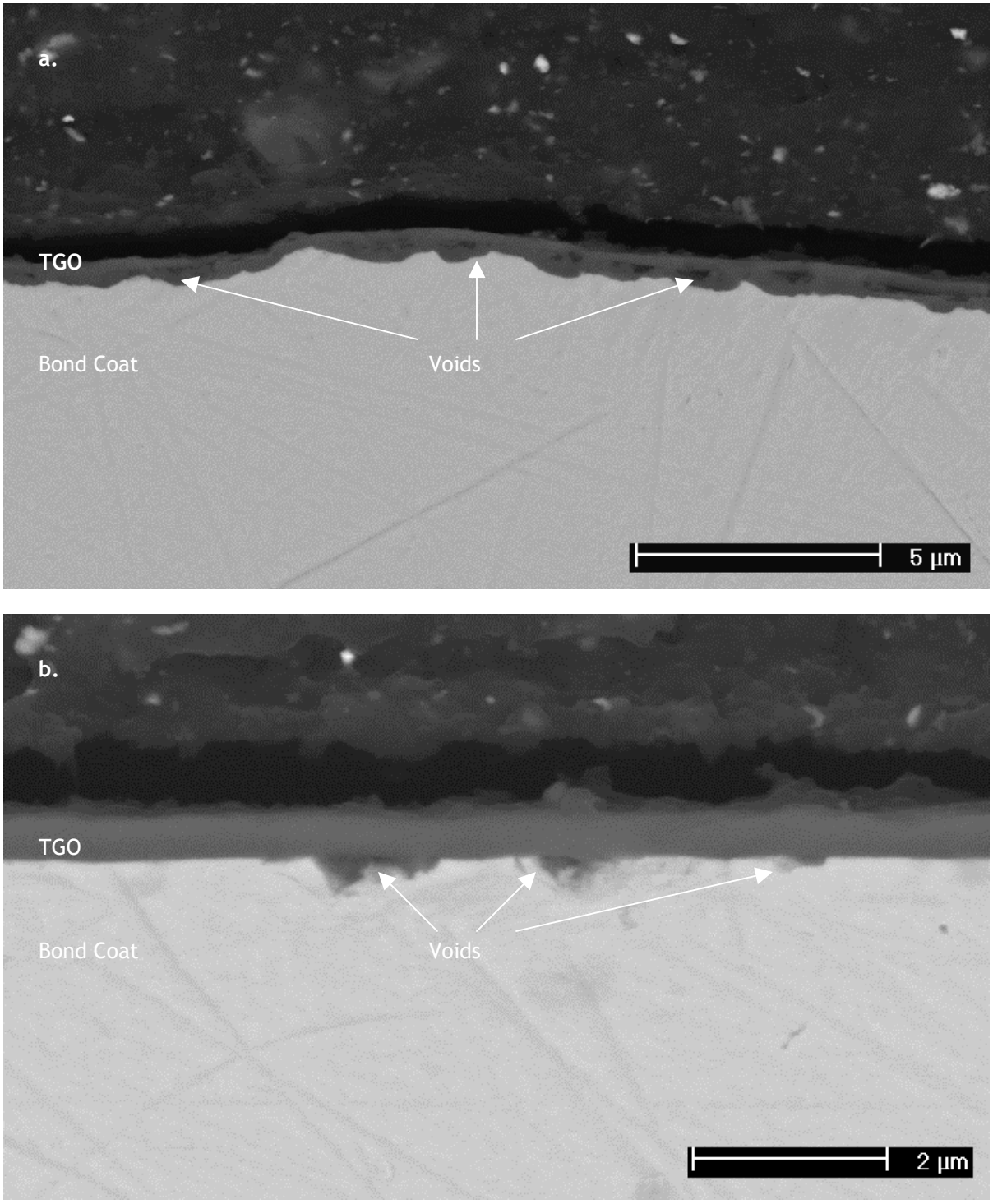

Figure 4-6. Cross sectional micrographs of specimens showing voids in the TGO (a.) after exposure in dry air at 1100^{o}C for 2 hrs and at the bond coat/TGO interface (b.) after exposure in Ar-H2 at 1100^{o}C for 2 hrs.

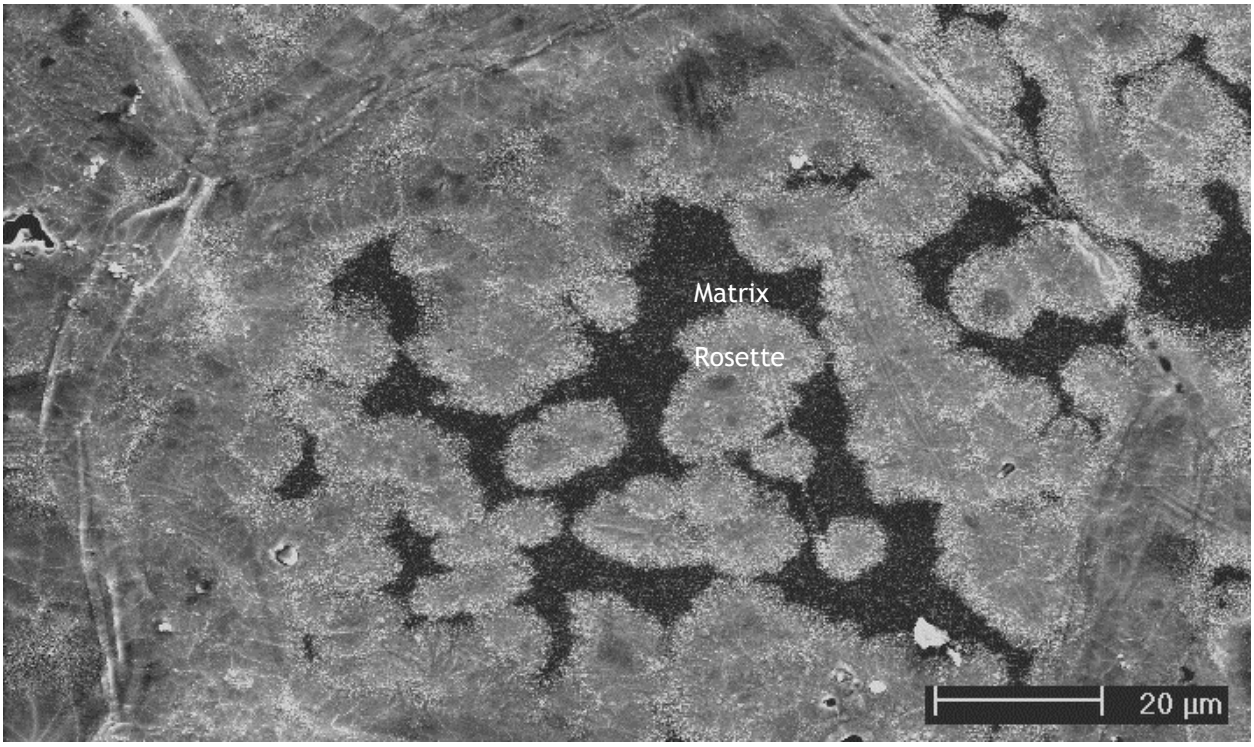

Figure 4-7. Micrograph of sample exposed in Ar – H2 for 2 hrs at 1100^{o}C showing circular shaped, light regions (rosettes) in a matrix of dark regions.

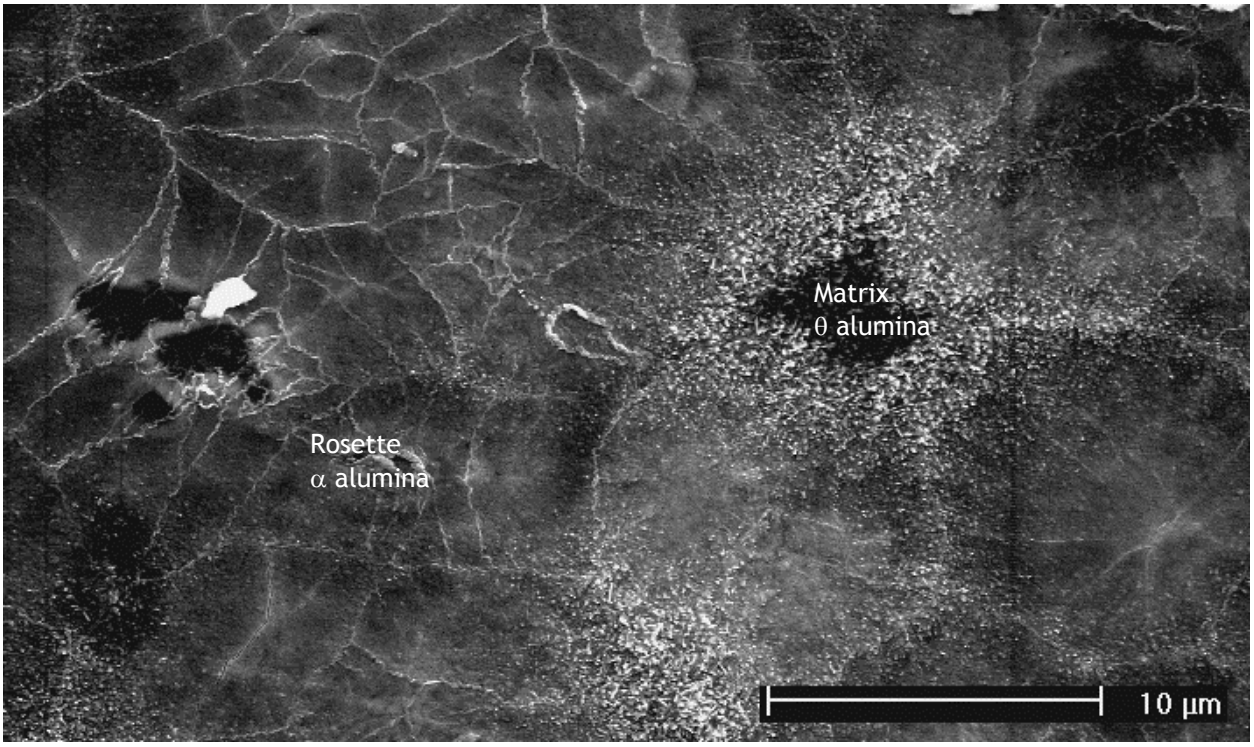

Figure 4-8. Higher magnification image of the rosette morphology. The lighter, more plate-like regions are believed to be α alumina and the darker, grainier regions are believed to be metastable alumina.

and the thinner (due to the volume reduction during transformation), "lighter" areas being the transformed α alumina[36].

4.1.3 Other Samples

With the observation of the voids, there was a concern that they could have a detrimental effect on the TBC specimens. Howmet supplied media finished and grit blasted specimens as well as specimens in the as aluminized state that were prepared differently than the previous specimens in an attempt to eliminate void formation by more careful processing. The grit blasted sample (Figure 4-9) showed no obvious void formation after exposure. The media finish (Figure 4-10) did show voids, but the volume was greatly reduced compared to the as aluminized state. The alternately processed samples (Figure 4-11) formed a large number of voids. As a result of this, Howmet supplied another sample which was given longer exposure times. Very few voids were seen. Another sample was given a 600 grit polish (using SiC paper, in house). This sample also did not show any voids after exposure (Figure 4-12).

With this information, a few comments/speculations as to the cause of these voids can be made. A possible mechanism of void formation involves the oxidation of the sample and is shown schematically in Figure 4-13. The transitional alumina phase θ grows via outward diffusion of aluminum towards the surface. Since there is a net flux of atoms towards the surface, a flux of vacancies must exist in the opposite direction. These vacancies condense out at the bond coat/TGO interface, forming voids and would appear similar to Figure 4-6b. When the alumina transforms to the stable α phase, it changes to an inward growth mechanism (i.e. oxygen diffusion to the bond coat/TGO interface). The metal oxide interface now moves inward and incorporates any artifacts, such as voids, into the oxide as seen in Figure 4-6a. Unfortunately,

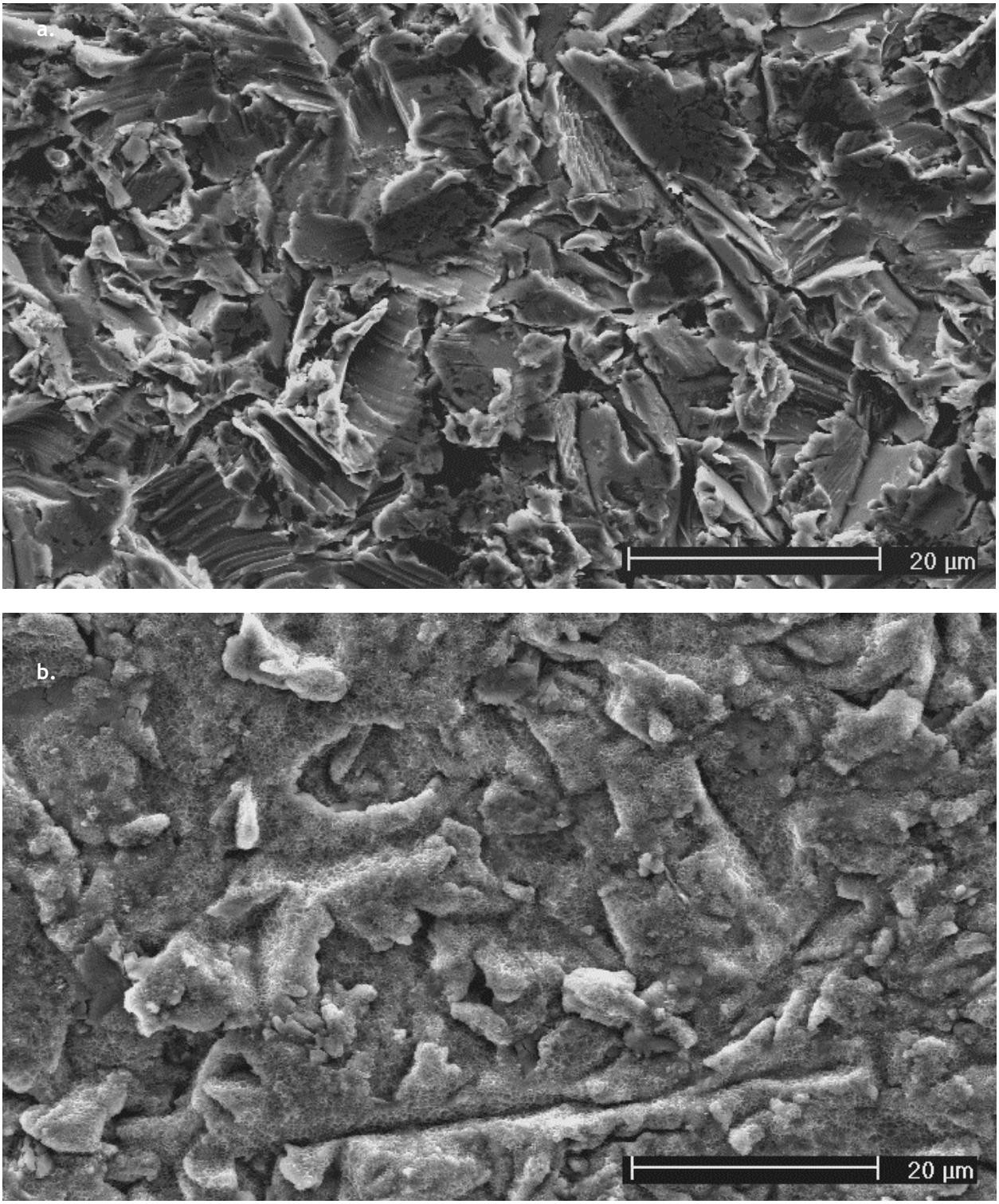

Figure 4-9. Surface micrographs of grit blasted bond coats as finished (a.) and after exposure at 1100^{o}C in dry air for 2 hrs (b.). There are no voids visible in the exposed specimen.

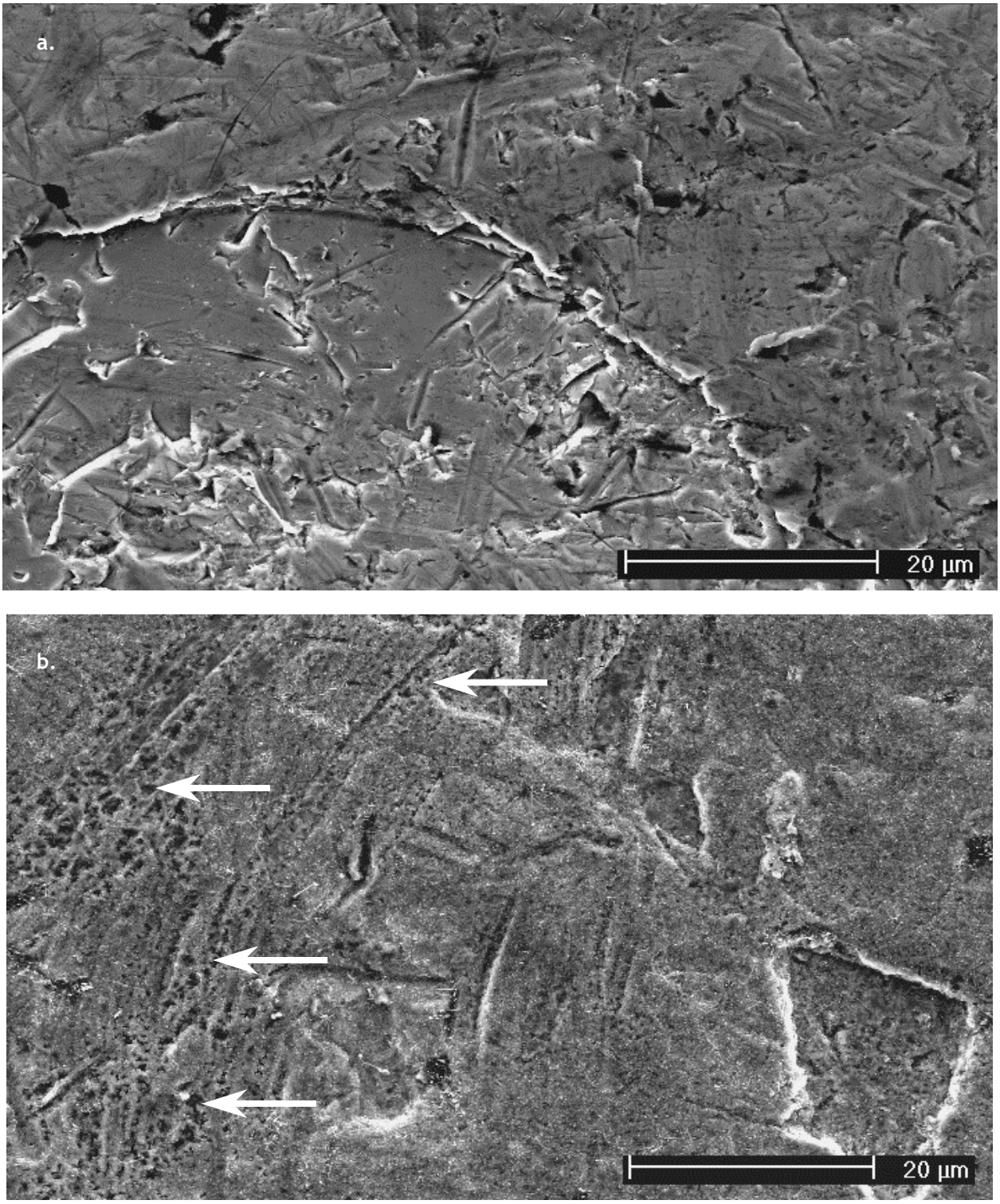

Figure 4-10. Micrographs of media finished samples in the as finished (a. 120 minute media finished and c. 40 minute media finished) and exposed ($Ar - H_2$ at 1100°C for 2 hrs) conditions (b. 120 minute media finished and d. 40 minute media finished). Voids (indicated by arrows) can be seen in b.

Figure 10 (continued)

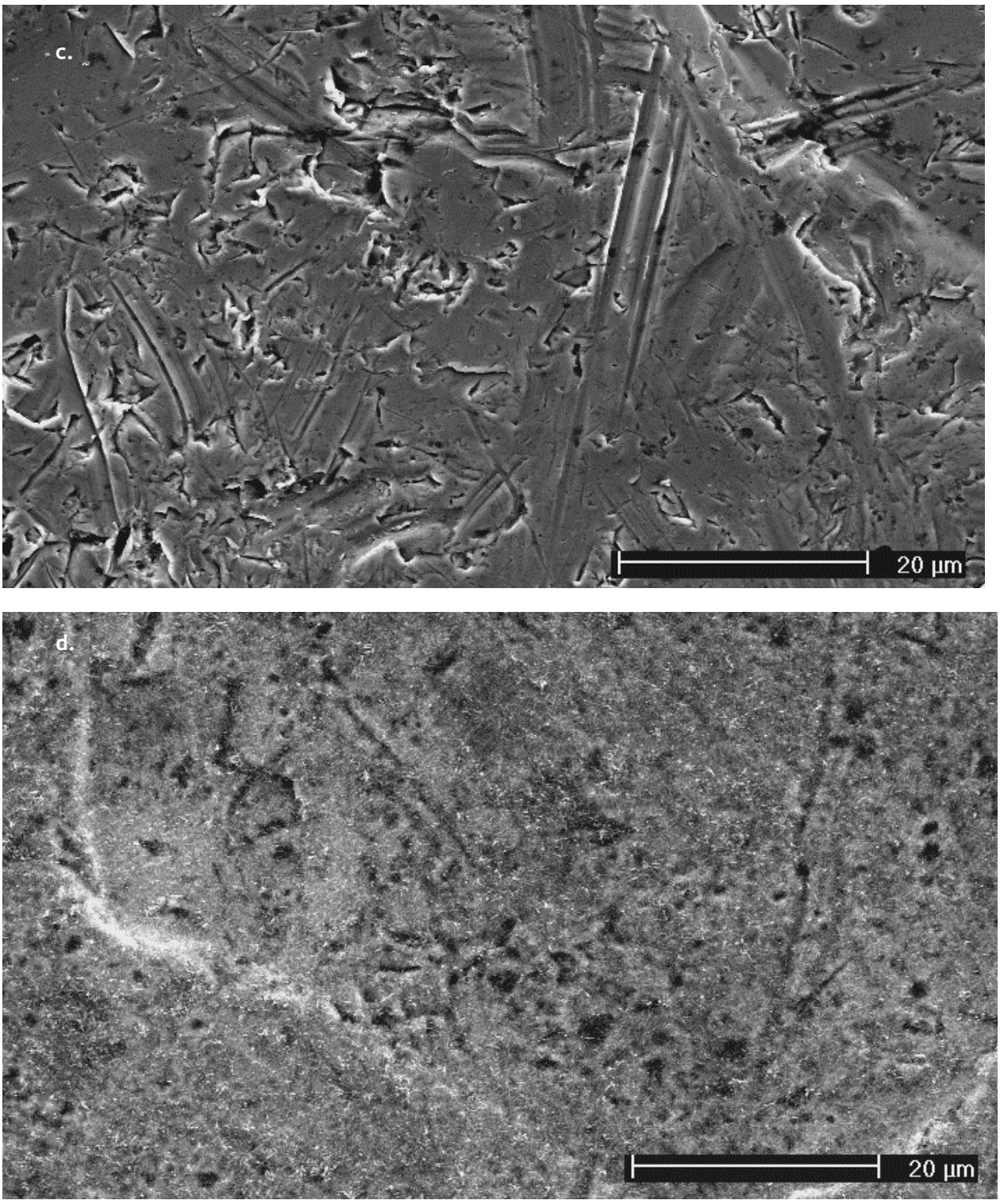

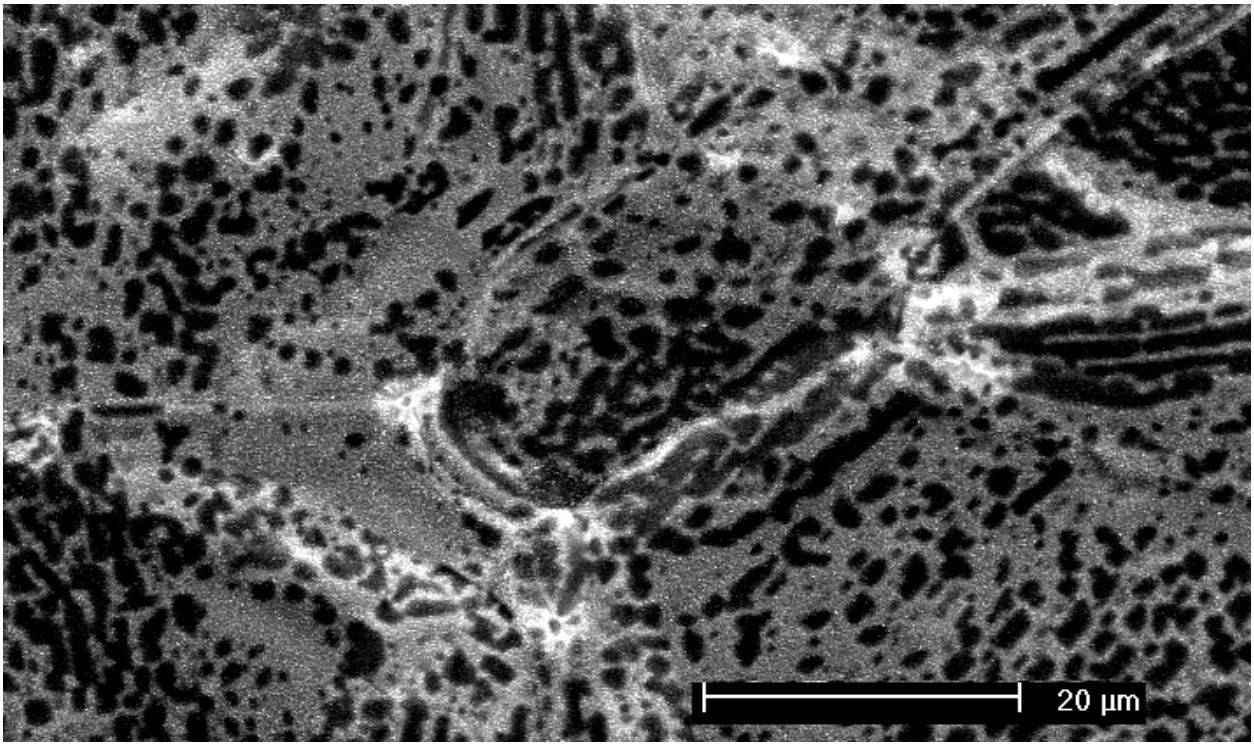

Figure 4-11. Voids (black) appearing in a sample from Howmet that was given alternate processing.

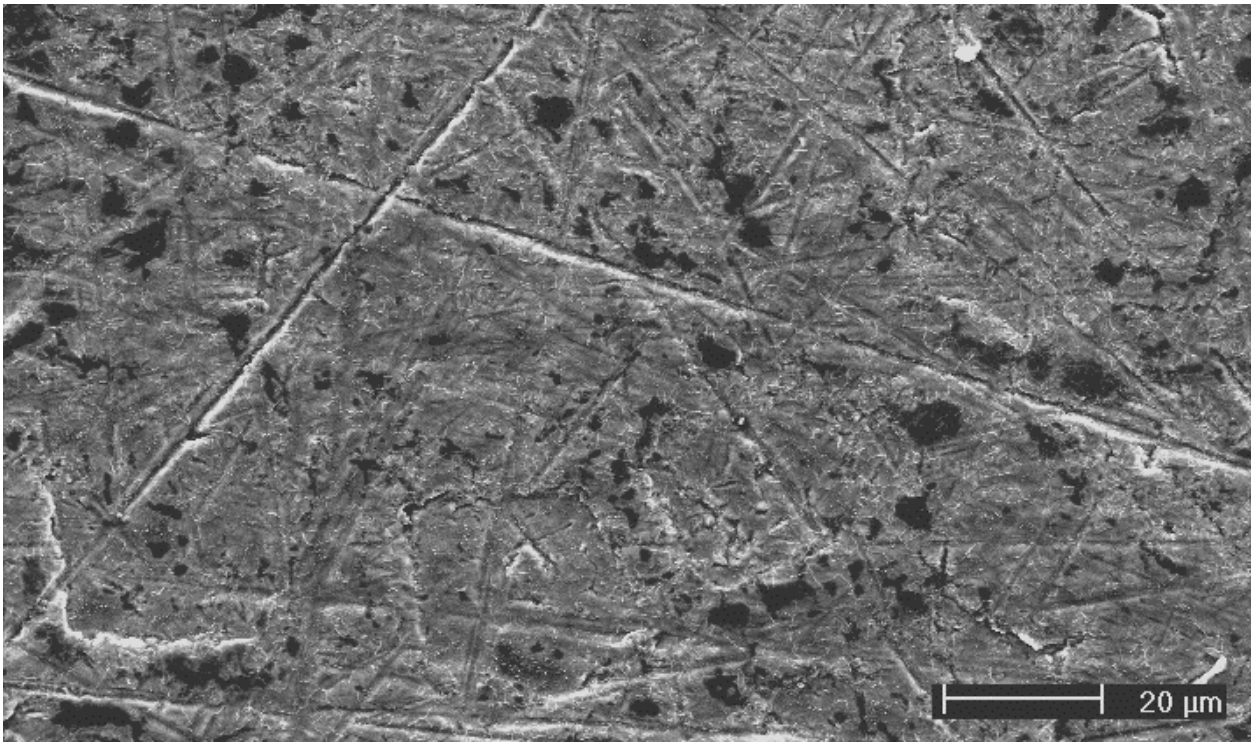

Figure 4-12. Micrograph of a sample that was given a 600 grit polish (SiC paper) prior to exposure at 1100^{o}C in dry air for 2 hrs. The dark areas are artifacts from the polishing. No voids appear on this sample.

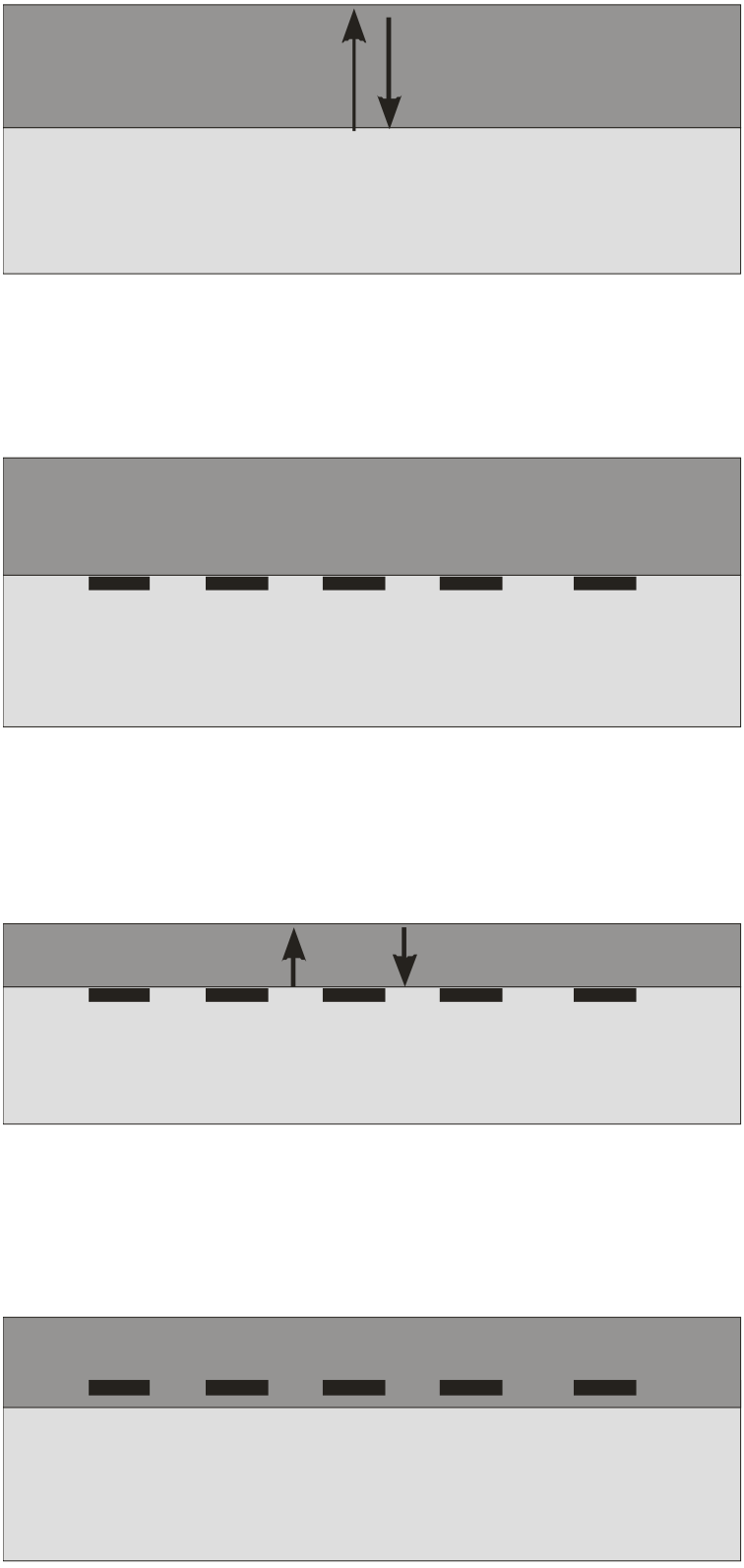

Figure 4-13. Schematic of a mechanism for void formation related to the oxidation behavior of the different alumina phases

samples that were preoxidized in conditions that α alumina would be expected to form quickly, such as pure O_2 at 1100°C, also formed voids. Other candidates are high vacancy concentrations in the bond coat. Since the preoxidation exposure can also be thought of as a high temperature anneal, the bond coat may try to reduce the vacancy concentration by nucleating voids at the interface. This mechanism is supported by the fact that Howmet was able to produce a sample that formed virtually no voids. Careful processing can eliminate vacancies by annealing and slow cooling. Surface deformation can do the same by increasing the dislocation density and the vacancies can be annihilated by dislocation climb. Once again the media finish and grit blasted samples exhibited significantly fewer voids than the undeformed samples. The voids could also be a result of some impurity effects, which would also be reduced by better processing and surface deformation of the bond coat. Once again, there were insufficient samples available to determine exactly what caused the void phenomenon.

4.1.4 XRD and Photoluminescence Measurements

The photoluminescence work showed more understandable results than the SEM. Table 3 shows some of the results. A ratio was taken of the θ alumina and the α alumina peak intensities to get an idea of the amount of θ alumina present. Numbers close to 1 represent more θ alumina on the sample, whereas those close to 0 represent more α alumina. Media finished samples showed less θ than the as aluminized sample for the same sample exposure. The longer time media finish also showed less θ alumina that the shorter finish time sample. Grit blasted samples have been shown to form α alumina faster than as coated samples[37], and the same appears to be true here. The larger the amount of deformation, the less θ alumina was detected.

Table 3. Summary of the ratios of peak intensities from the laser photoluminescence measurements for the metastable and stable alumina phases. Ratios close to 1 indicate presence of θ alumina, while those near 0 indicate more α alumina.

Pretreatment	Ratio
900°C Ar-H_2 120 media finish	0.45
900°C Ar-H_2 40 media finish	0.57
1080°C dry air as aluminized	0.18
900°C dry air as aluminized	0.89
900°C Ar-H_2 as aluminized	0.88
900°C O_2 as aluminized	0.05
1100°C Ar-H_2 as aluminized	0.12

From this data, the preoxidation treatments were chosen. The lowest temperature and lowest P_{O2} showed the most θ alumina. The conditions for the rosette structure (Ar-H_2 at 1100 °C), was chosen due to the interesting morphology and the mix of both alumina phases. Dry air at 1100 °C was decided to be satisfactory for forming only α alumina.

The XRD measurements gave very disappointing results. Scans were done using the θ – 2θ geometry to determine the substrate peaks. This was followed by a low angle (1°) fixed incidence scan to increase the amount of oxide that the x-rays sample. Unfortunately, the substrate peaks were large in both scans. These peaks overshadowed most of the α alumina peaks and any θ alumina peaks that may have been present. The incident angle was raised to 8° to account for the ridges on the bond coat (assumes 3 μm in height). The result was the same. Increasing the angle further would only reduce the amount of oxide available for diffraction. The same problem occurred with media finished specimens. No further work was done using XRD.

4.2 PRE-DEPOSITION RESULTS

Due to the unexpected additions of media finished samples in the oxidation study, there was not much new information gained from this stage with respect to SEM analysis. One sample from each grouping was observed on the SEM before and after pretreatment. The full size media finish samples showed the same results as the quarters used in the preoxidation study, in that voids were observed.

Hand polished and barreled finish samples were included in this analysis. The polished specimens show virtually no ridges in the outer portions of the sample (Figure 4-14a). As mentioned above, the samples tend to be thinner in the center, and the presence of the ridges in Figure 4-14b confirms this. The oxide on the pretreated samples appear as whiskers (Figure 4-14c). There were some extremely small voids seen in some of the samples. The barrel finish (Figure 4-15) is similar in appearance to the media finish, but looks much more aggressive, almost to the point of a very fine grit blasting. Very little, if any sign of the aluminide ridges remain. Due to the rough appearance of the finish, it is difficult to discern voids in the oxidized sample (Figure 4-15b).

Photoluminescence measurements were also done on the samples prior to TBC deposition. The results returned by UCONN were different than the previous samples. Instead of a ratio that gives a rough estimate of the amount of the metastable alumina, only the location of the peak for θ alumina was given. Due to this, the data can only be used to determine if θ alumina was present or not. There is no way to quantify the amount of θ alumina present. The results are given in Table 2.

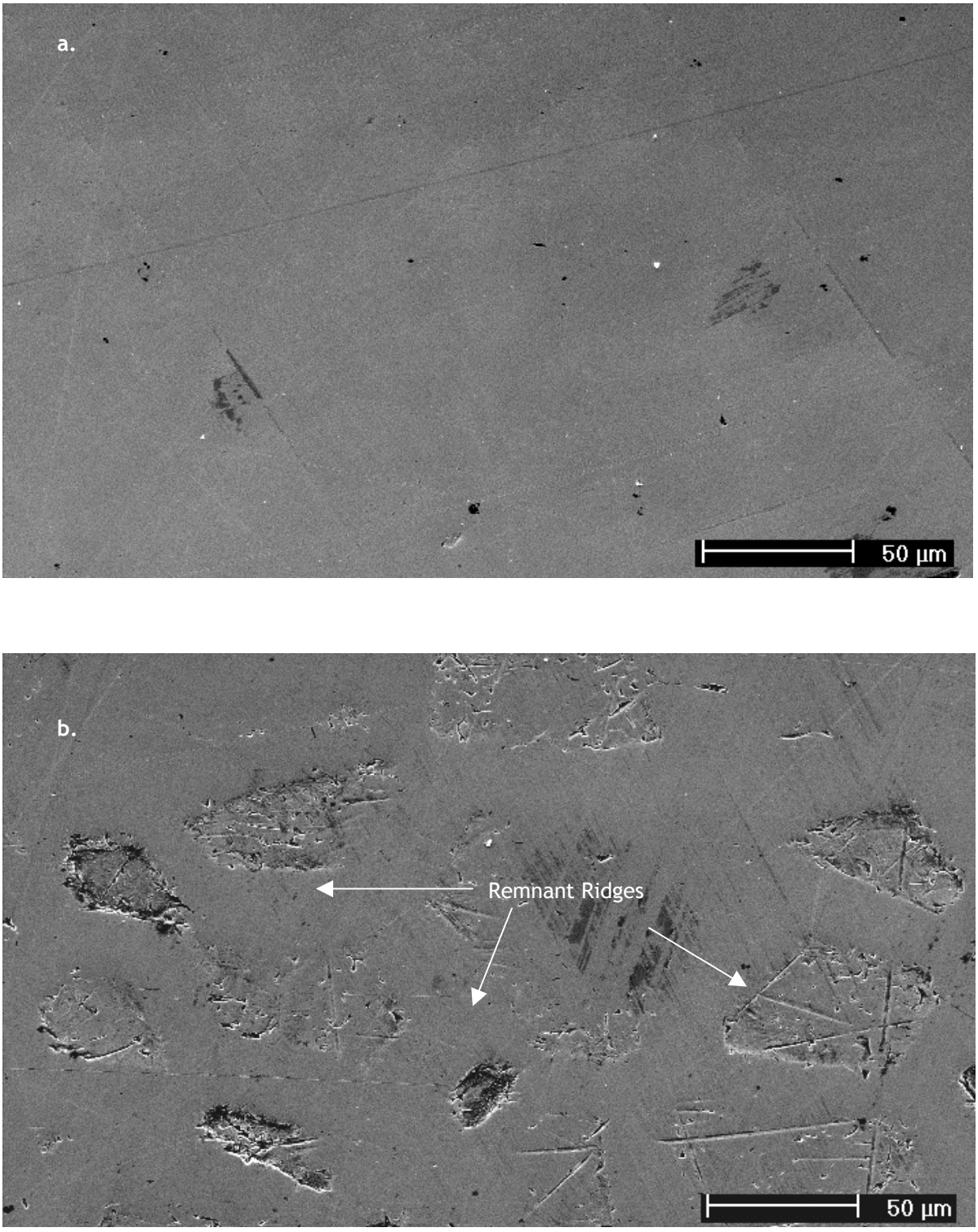

Figure 4-14. Micrographs showing 3 µm polished samples in the as finished and exposed (Ar-H_2 at 1100°C for 2 hrs.) conditions. The polish eliminated the ridges near the edges of the sample (a.), but left remnants in the center (b.). The exposed sample (c.) shows whisker like alumina possibly due to formation of metastable alumina.

Figure 14 (continued)

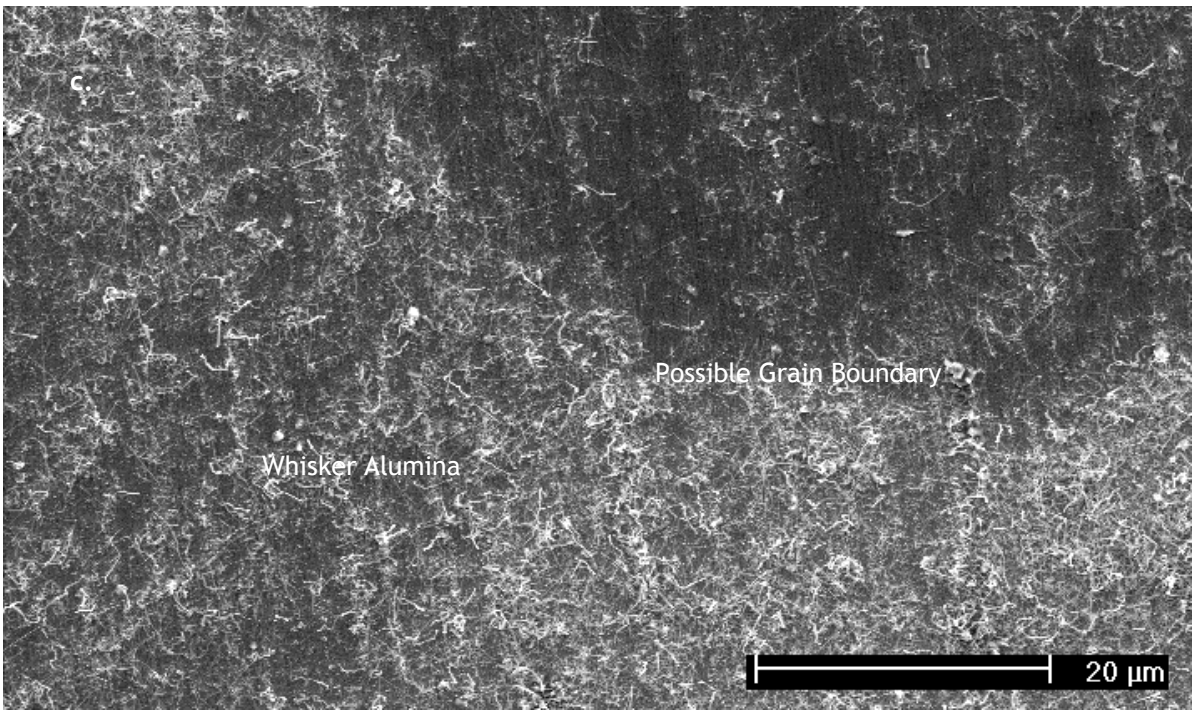

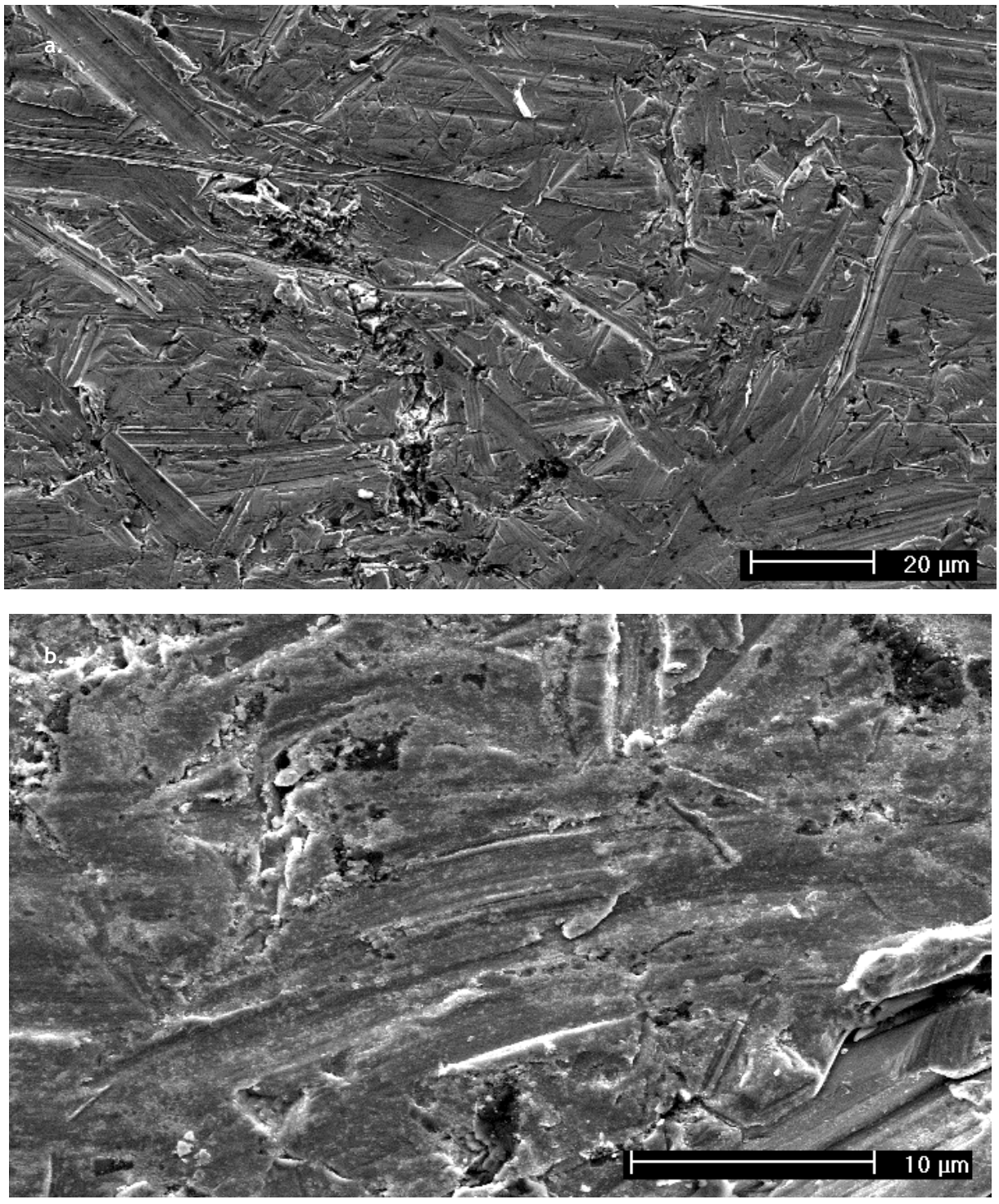

Figure 4-15. Micrograph of the highly deformed as finished (a.) and exposed (b.) barrel finished samples. The exposure was done in Ar-H2 at 1100^{o}C for 2 hrs. No voids were discernable.

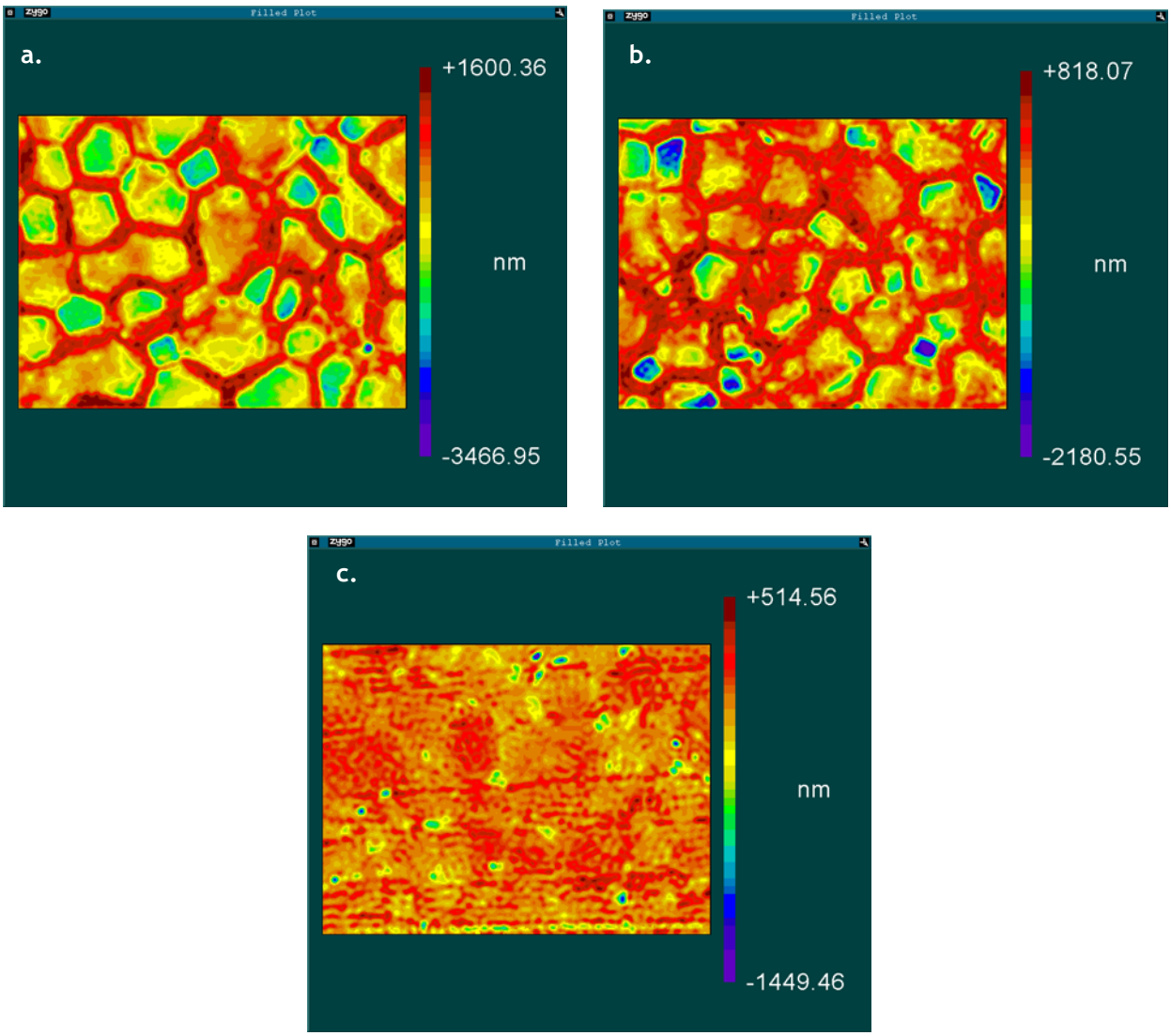

Figure 4-16. Topological plots of the surfaces for 40 min media finished (a.), 120 min media finished (b.), and hand polished (c.) samples. The colors represent the deviations from a zero elevation as given by the scales beside the plot. Note that the scale gets finer and the surface is more uniform (indicated by less green and blue) as the surface gets smoother.

Also found in Table 2 are the surface roughnesses of the samples. Graphical results were also provided by UCONN. Figure 4-16 shows topographical maps of the surface for some of the media finished and hand polished samples that were generated by equipment at UCONN. The difference in the surface roughness between the finishes is readily apparent from these results

4.3 TBC EXPOSURES

The major thrust of this research was to determine if the pretreatments that were decided upon in the previous experiments add any significant benefit to the TBC system. Samples in the as coated (note: refers to TBC, not aluminide coating as before) condition for most of the pretreatments will be discussed first, as well as some samples that were taken out of test prior to failure. Subsequently, the failed samples will be analyzed. These specimens easily fall into three groups that will make the discussion easier. The first group is those samples that failed immediately following the coating process. The other groups are separated by both failure time and the interface that failed.

4.3.1 As Coated Specimens

In all cases, the surface of the bond coat appears much smoother and more uniform (Figure 4-17a-d) as compared to the same surface in a state of the art grit blasted sample (Figure 4-18). This is to be expected, given that the pretreatments result in much lower surface roughnesses. This decrease in surface roughness yields a TBC with much straighter columnar grains. The straighter grains would in theory make the TBC more strain tolerant. There also

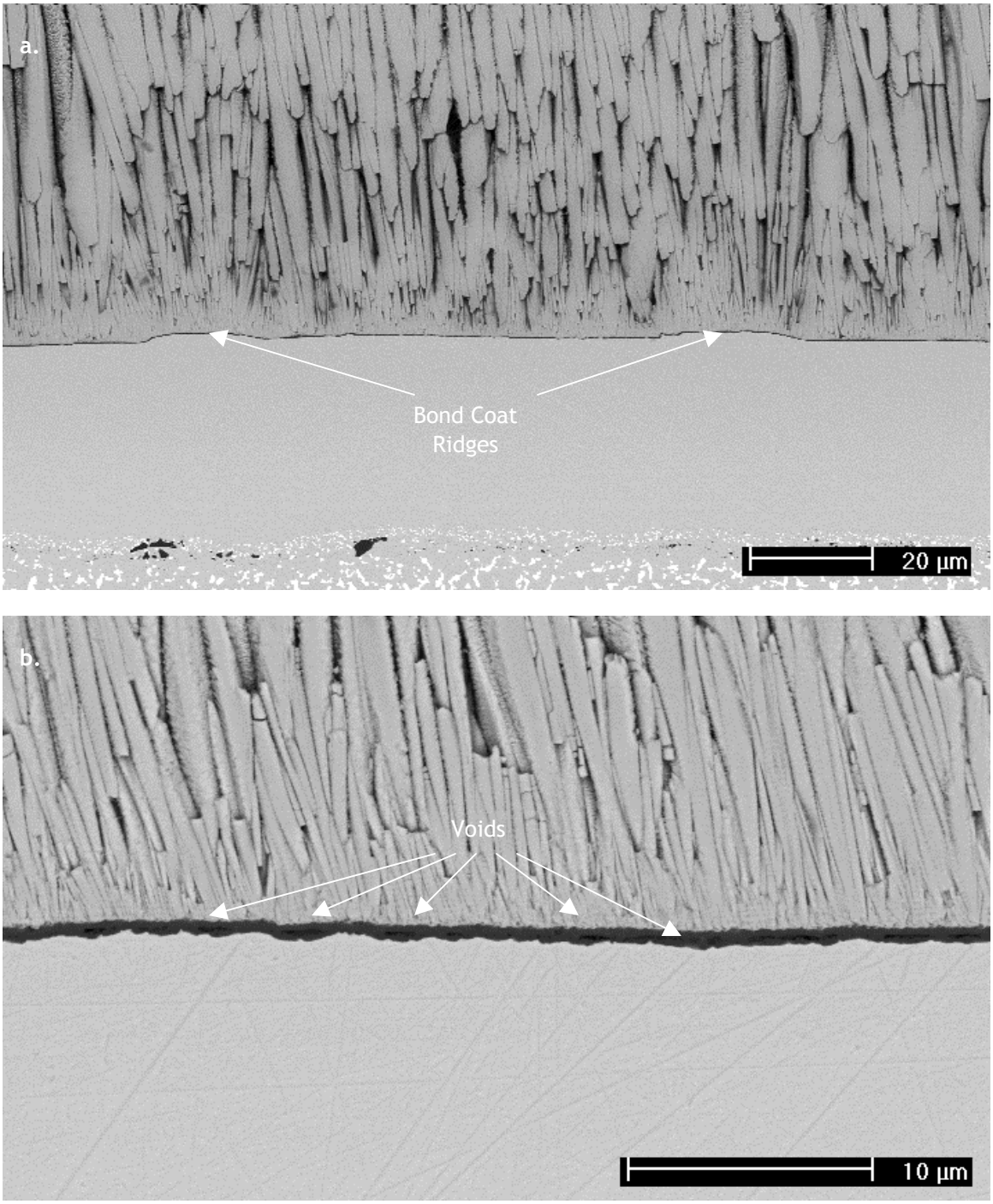

Figure 4-17. Micrographs of as coated TBC specimens LI14 (a. 40 min. media finished, Ar-H_2), LH92 (b. 120 min. media finished, dry air), LG94 (c. polished, Ar-H_2), and LI13 (d. barrel finished, Ar-H_2). Bond coat ridges are visible in LI14. Voids were observed in TGO of LH92.

Figure 4-17 (continued)

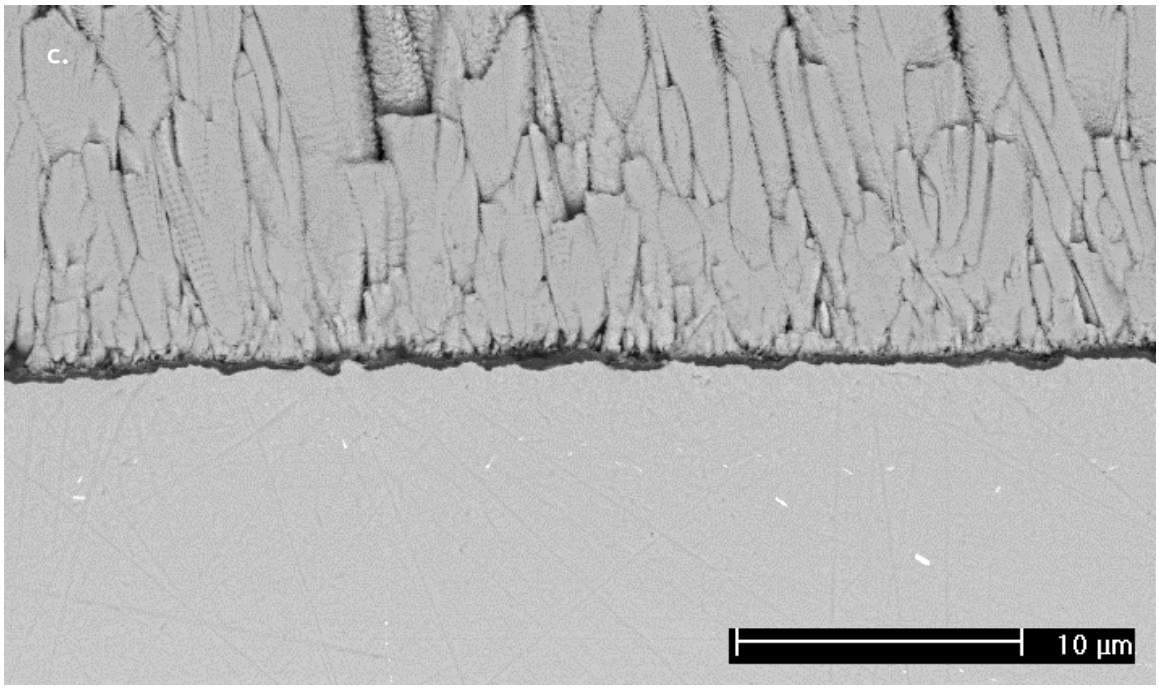

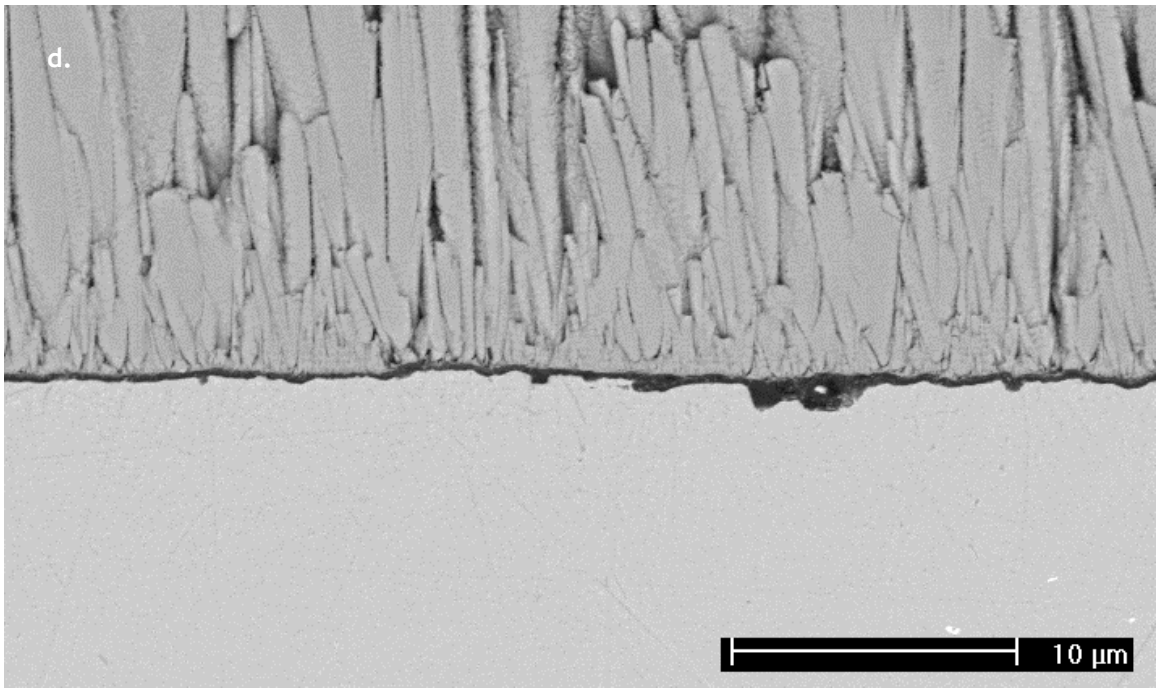

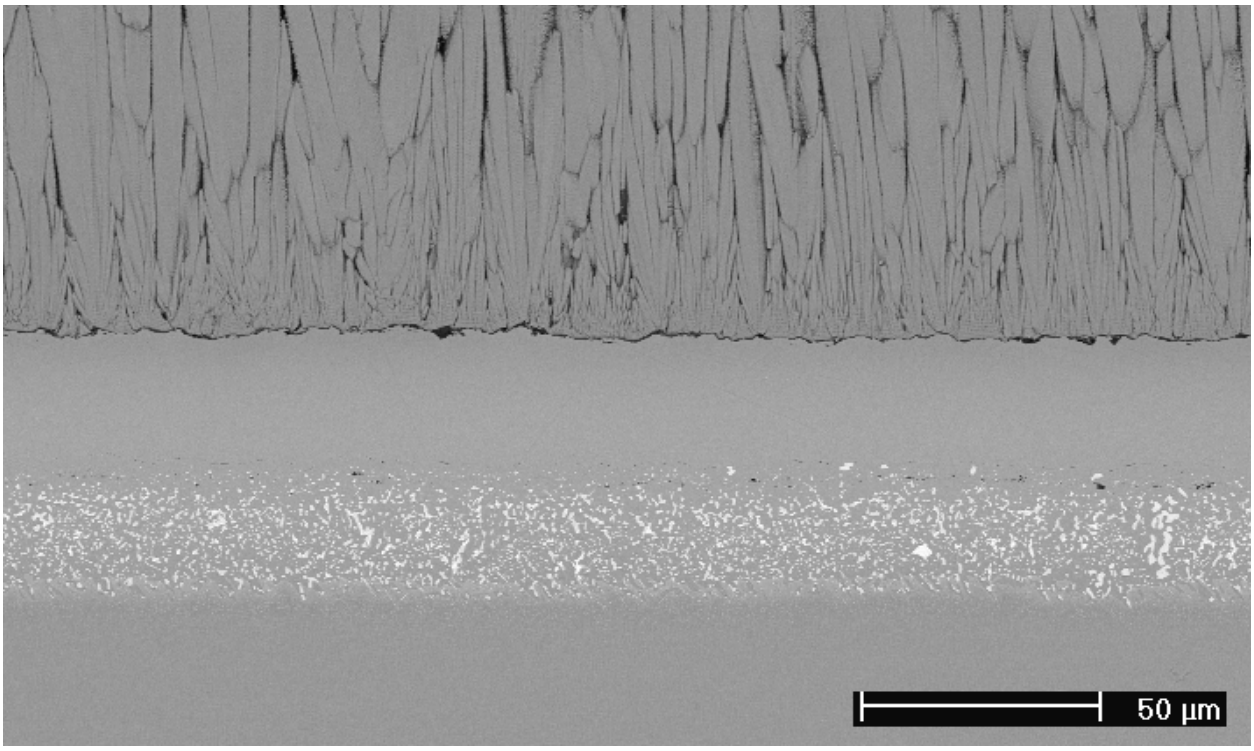

Figure 4-18. Micrograph of a typical grit blasted specimen in the as coated condition.

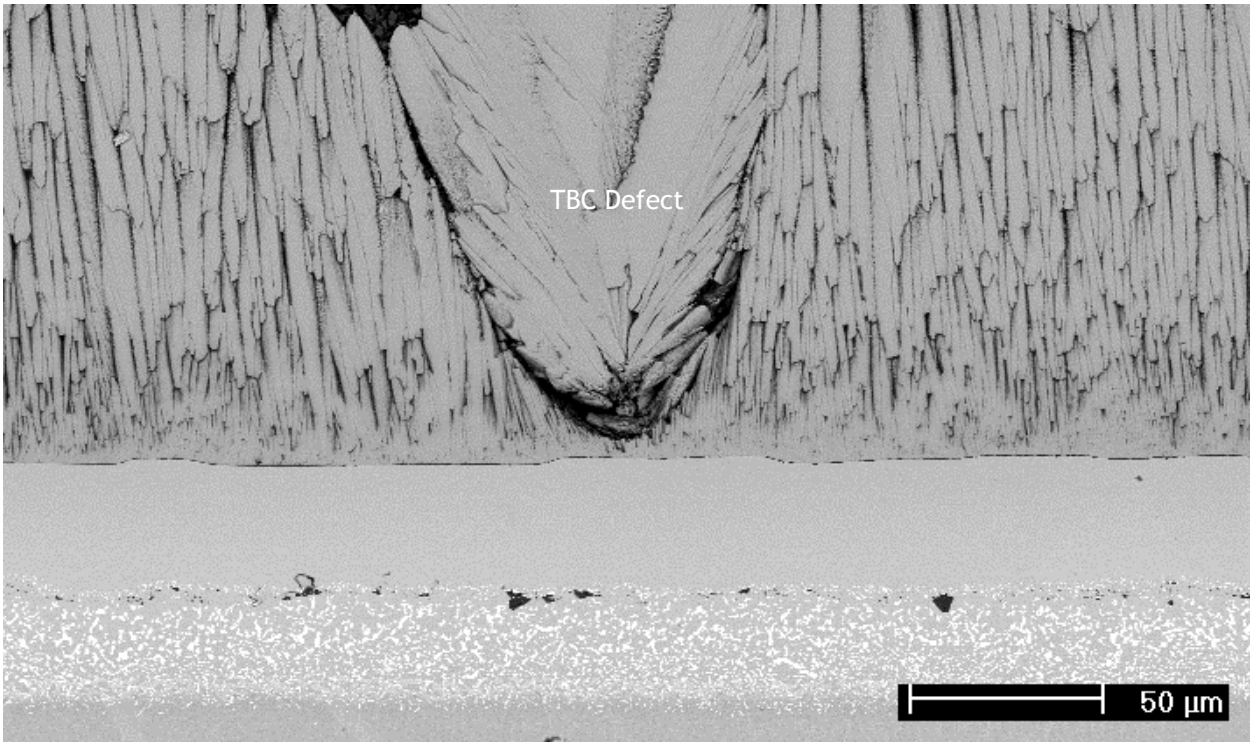

Figure 4-19. Micrograph of a large scale defect found in sample LI14 (40 minute media finished, Ar-H_2 at 1100^{o}C for 2 hrs). There were very few defects of this type found in the samples used in this project.

appears to be a few of the undesirable, large scale defects shown in Figure 4-19 that could reduce the strain tolerance.

Several of the samples contain defects at the interfaces on either side of the TGO or inside the TGO itself. The most common defects were small voids and/or cracks at the TGO – TBC interface. As mentioned, these defects were usually small and probably not really a concern in small and well distributed numbers. Figure 4-17c shows these small voids. Some of these defects will link up with exposure or are large to begin with and will greatly weaken the TBC – TGO interface, leading to shorter lifetimes. Very few defects were present on the TGO – bond coat interface. The most interesting defect is the voids found in the TGO itself (Figure 4-17b). These were possibly formed by the phase change mechanism described above. In the as coated state, only the 120 min media finish with the dry air pretreatment displayed these defects. This is the condition that yielded the longest lifetime. Similar voids were seen in a different sample that had a lifetime ~300 hours longer than the others in the same pretreatment group. This will be discussed later.

4.3.2 Failures at the Coater

A rather alarming result in this project was the number of samples that were unusable after coating. Out of 33 specimens, 12 were not put into cyclic oxidation testing. Samples LI9 and LH97 were essentially destroyed in the coating process. Sample LI11 was never received, and was presumed lost. Due to problems with coating the hand polished NiCoCrAlY bond coats from UCONN, samples LG90 and LG91 were pulled from the coating run. Howmet attempted α - alumina deposition on these samples prior to TBC application. These samples failed, but it was not reported how or when they did so. Finally, seven specimens experienced somewhat more normal failures after the TBC was applied.

Failures immediately after coating are known to occasionally occur, but not with the high frequency that was the case with this work. All of the failures occurred on the TBC – TGO interface, as seen in the surface micrographs (Figure 4-20). Cross sections (Figure 4-21) only show the very thin oxide layer that would be expected for such a short thermal history.

All of the samples that failed at the coater did have a unifying characteristic. The pretreatment in all cases consisted of surface modifications combined with either no preoxidation or the Ar – H_2 environment at 900°C and 1100°C. These conditions are those most likely to form metastable alumina phases. The oxides on these samples were examined using the photoluminescence technique. Only α - alumina was found in all cases. It is likely that the initial scale during deposition was a metastable phase such as θ - alumina. The phase change from this metastable to the stable alumina involves a volume reduction. The stress generated during this process combined with the stress from the CTE (coefficient of thermal expansion) mismatch on cooling could be sufficient to cause the coating failure. This is shown schematically in Figure 4-22. In this case, only the stable phase would be expected on the failure surface. Another idea is that the metastable alumina phase does not provide the same quality of bonding to the YSZ as α - alumina does. It is also not entirely impossible that some sort of contamination may have occurred, but randomization of the samples during coating reduces the legitimacy of this thought. In any case, this part of the study shows that metastable alumina TGOs should be avoided at all costs.

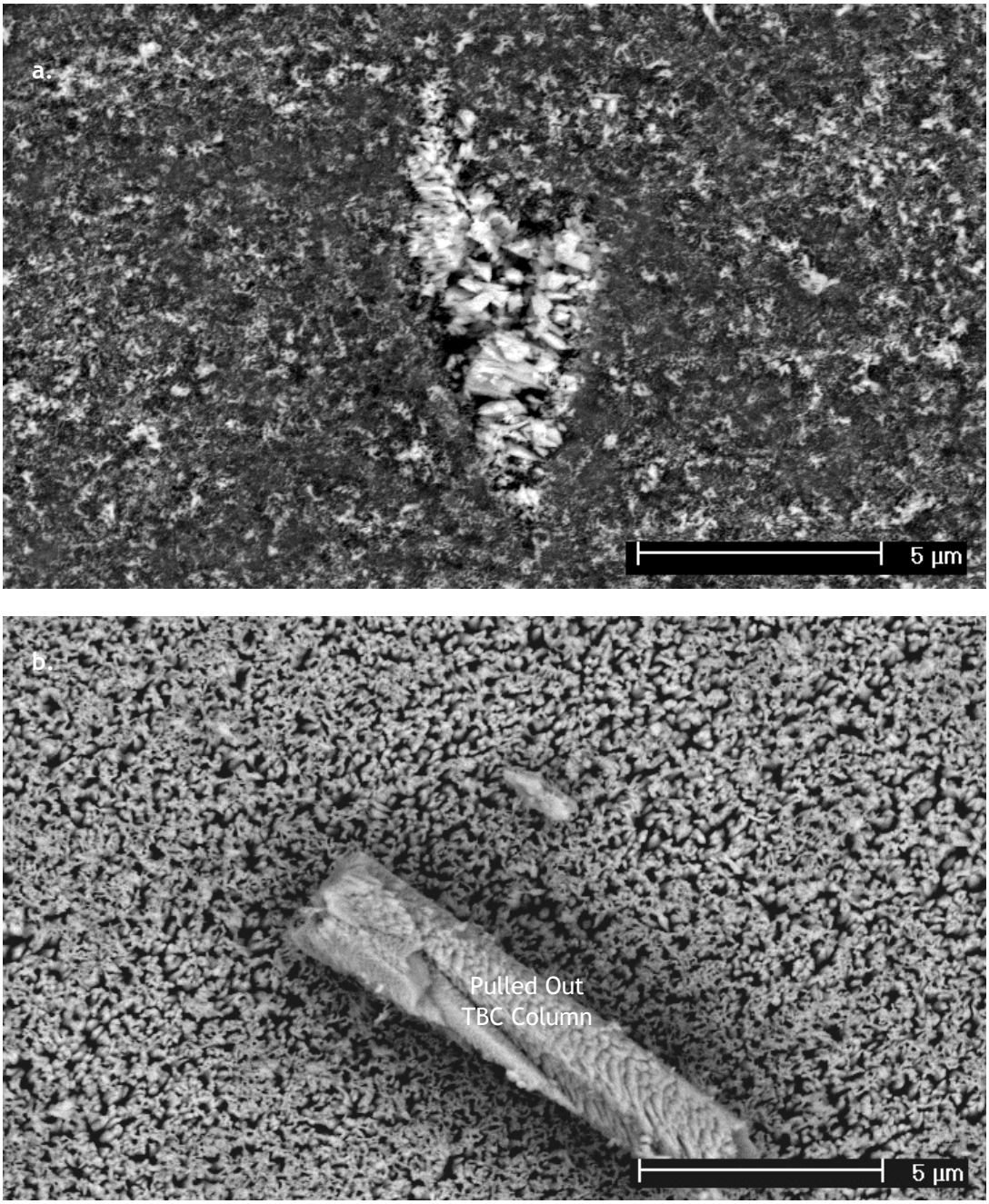

Figure 4-20. Micrographs of sample LG89 (polished, no preoxidation), which represent the typical fracture surfaces for samples that failed at the coater. The TGO (dark grey) appears intact on the bond coat surface (a.) with very little adhered zirconia (white). The lack of TGO on the underside of the TBC (b.) confirms that the failure was along the TBC/TGO interface.

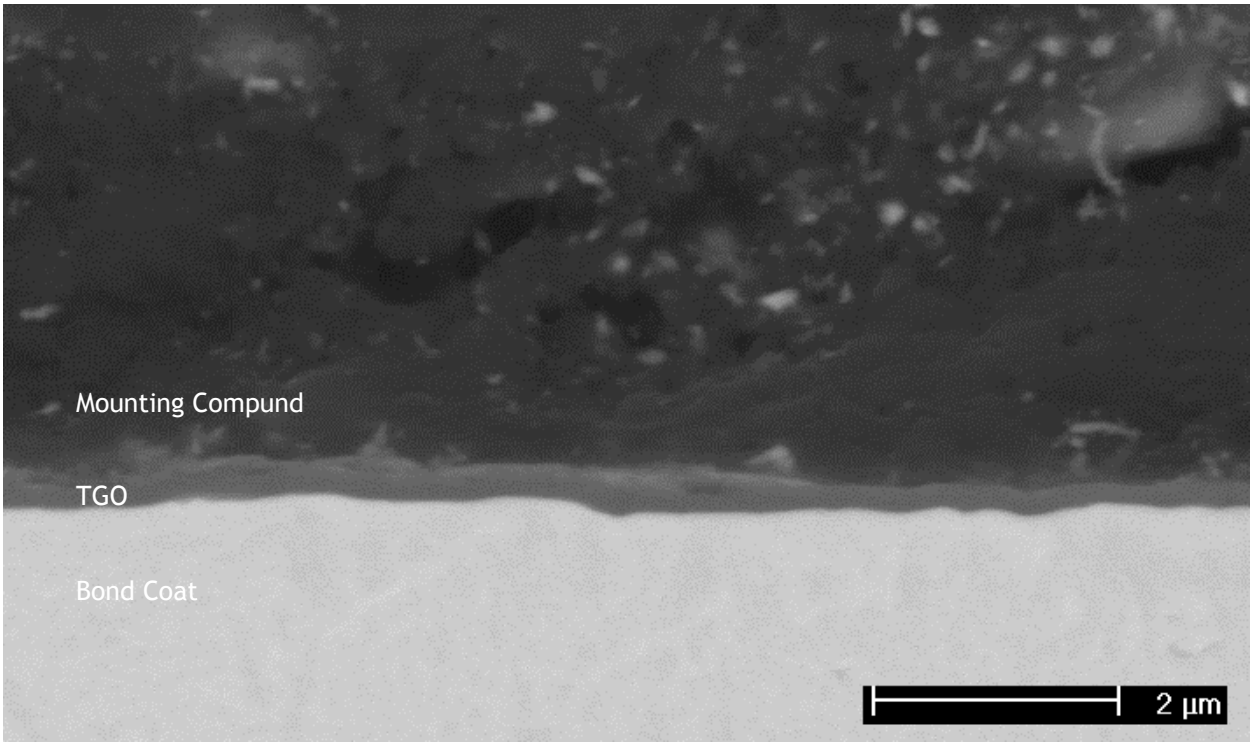

Figure 4-21. Cross sectional micrograph of sample LG89 (polished, no preoxidation) showing a submicron TGO (dark grey) with no adhered TBC (white).

4.3.3 Short Time failures

Of the 21 samples that survived the coating deposition, only 5 had lifetimes over 750 cycles (see Table 2 for lifetime data). The lifetime of roughly 750 cycles is that predicted for grit blasted samples at this temperature using the Arrhenius plot generated by Yanar[25] (Figure 4-23), and this lifetime will be used as a guide for comparison of these results to more conventionally processed TBC's. The vast majority of those shorter failures were less than 300 cycles. The only sample that surpassed 300 cycles had a lifetime of 640 cycles and appeared to have a slightly different microstructure.

In general, all of the specimens in this group demonstrated the same type of failure (Figure 4-24). All of them cracked around the edges of the sample before failure. This is to be expected given the complicated stress state due to having a 90^{o} angle present. This is usually avoided in the design of actual components. Some small areas of separation could be seen in the samples rather early in the exposure. These began to grow and coalesce as the exposure continued. The major failure began as a buckle near, but not usually at the edges. The buckle would grow on subsequent exposure. Once a certain stress level at the interfaces was reached, the TBC would then crack and fall off. This occurred most of the time while the sample was in the desiccator. In this case, the failure was restricted to the area that had buckled. There were occasionally failures that occurred in the furnace. These were usually "catastrophic" failures, meaning the entire TBC failed with little warning (buckling or separations) and was usually broken into small pieces.

As with the failures at the coater, all of the short time failures were primarily along the TBC – TGO interface. Sample LH100 is show in Figure 4-25 as an example of the fracture surface of one of these samples. On the fracture surface, the TGO (dark grey in the micrographs)

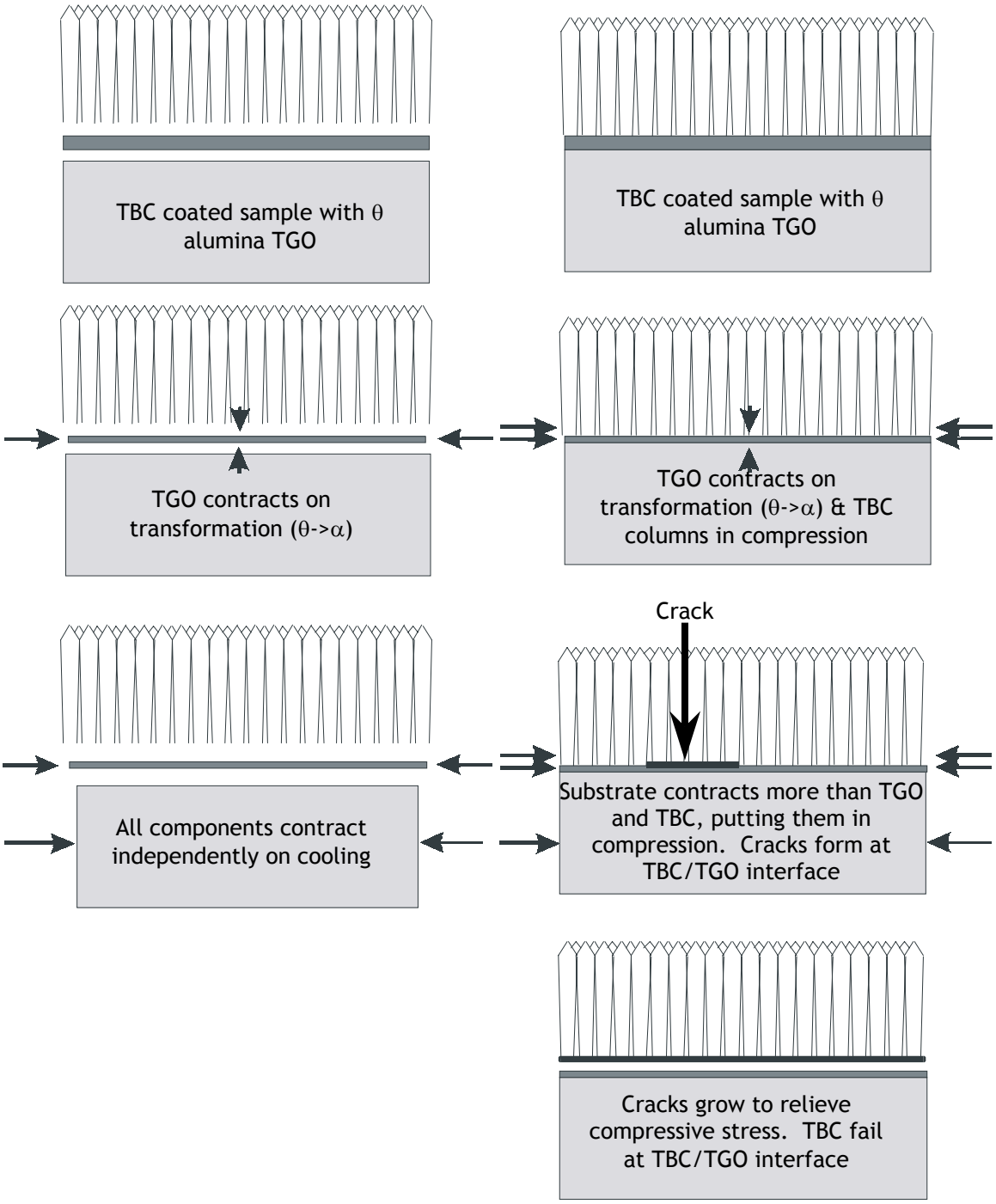

Figure 4-22. Schematic showing a mechanism for TBC failures at the coater. The left side shows the process with the layers acting separately, while the right side shows the layers constrained as they are in the real system.

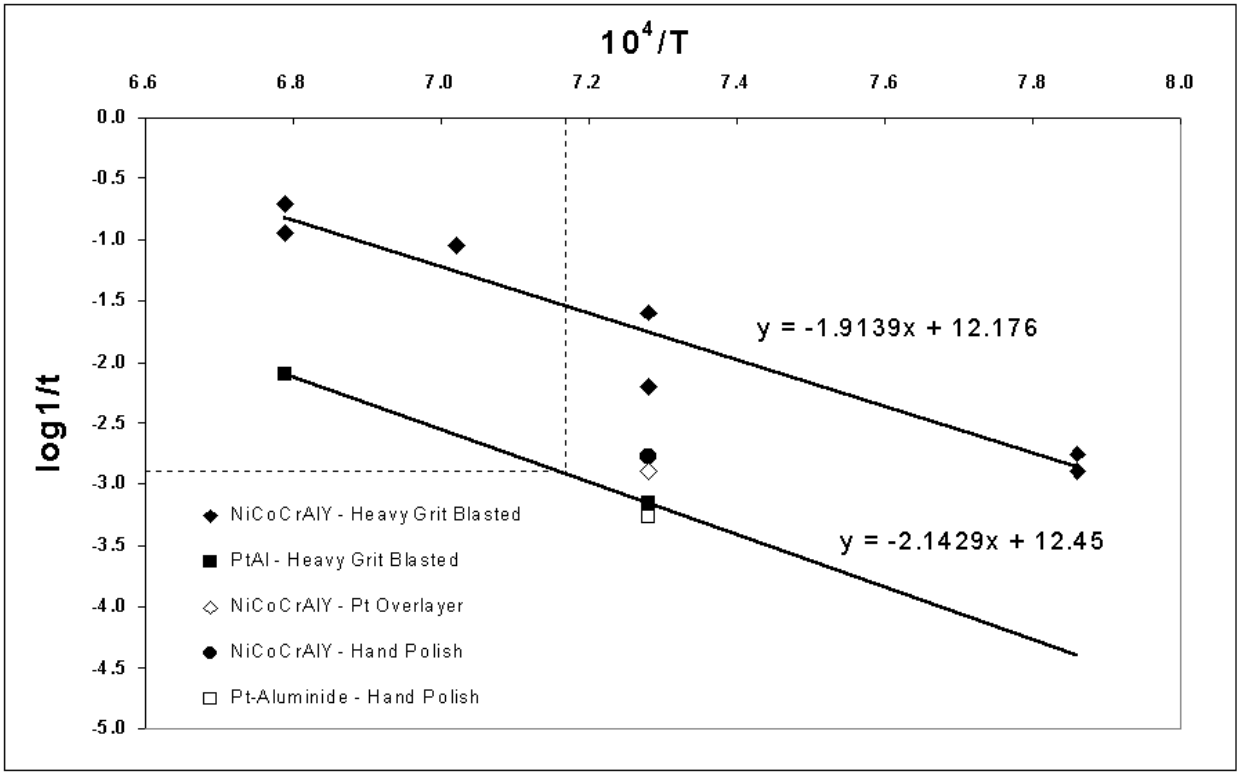

Figure 4-23. Arrhenius plot of temperature vs. sample life time (in terms of 1 hr. cycles) for TBC specimens in various conditions.

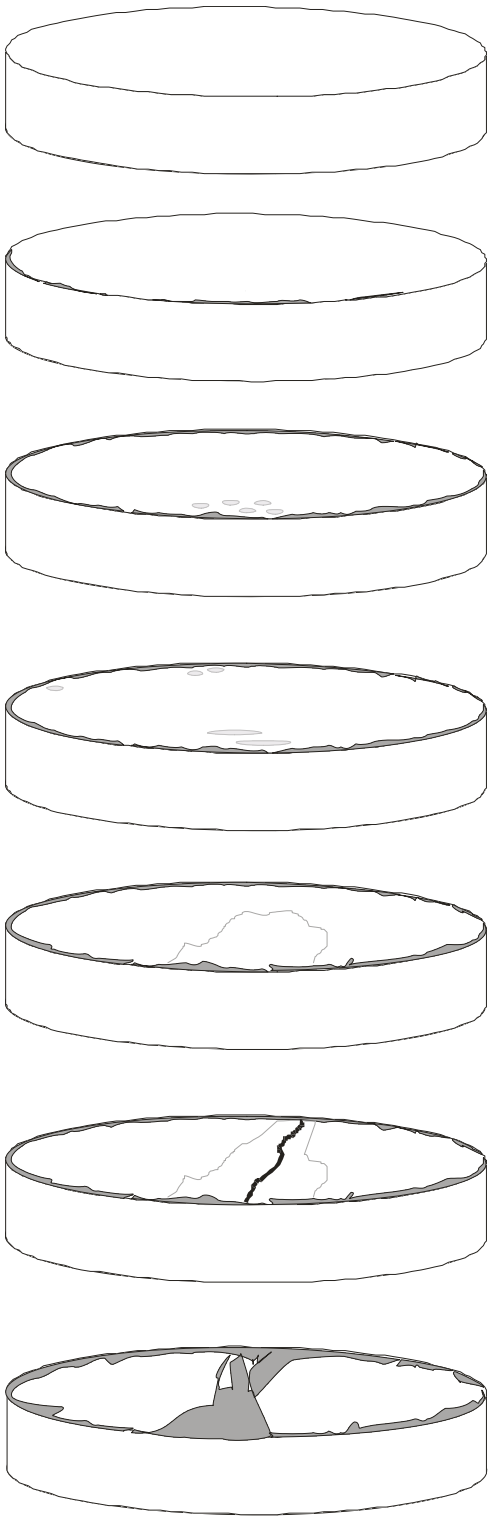

Figure 4-24. Schematic of the typical degradation of a TBC sample with exposure time.

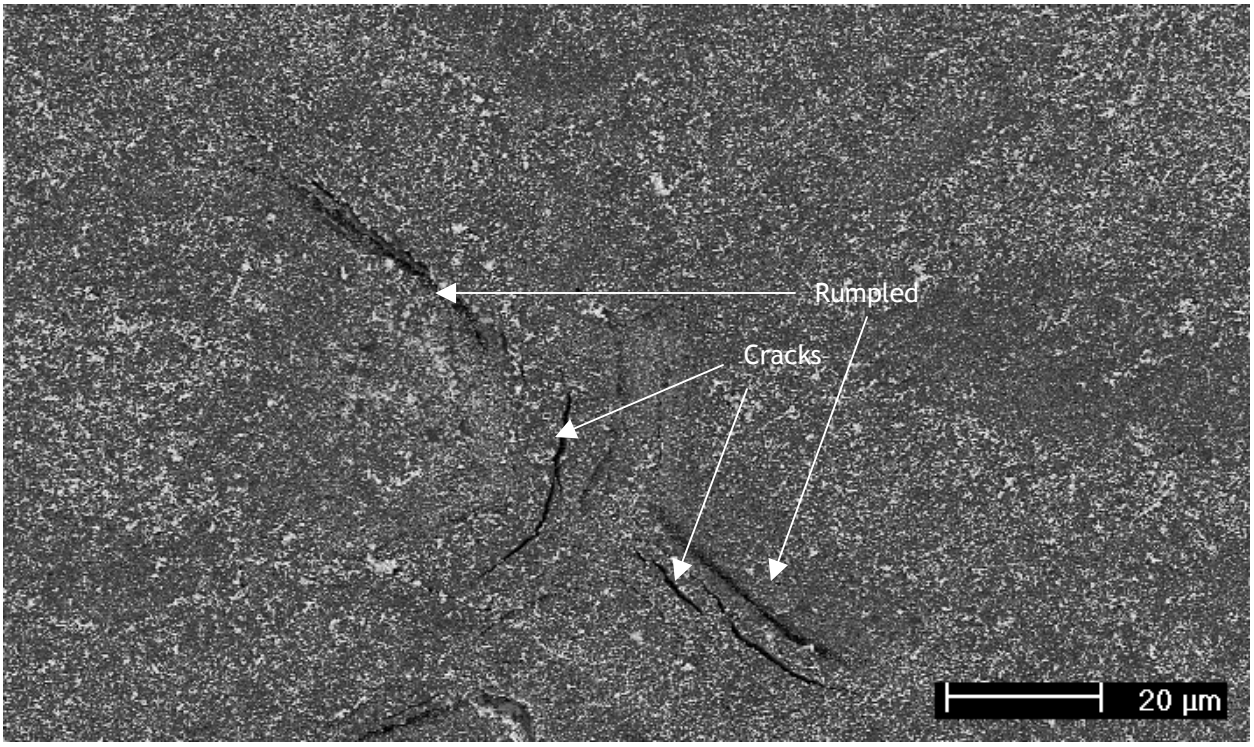

Figure 4-25. Micrograph of the bond coat fracture surface from sample LH100 (120 media finished, Ar-H2 at 1100°C for 2 hrs, 100 cycles) which represents the typical appearance of this surface for the short time group. Similar to the coater failures, there is no significant areas of TBC adherence. The TGO appears to be intact, but does show some rumpling and cracking near what could be remnant bond coat ridges.

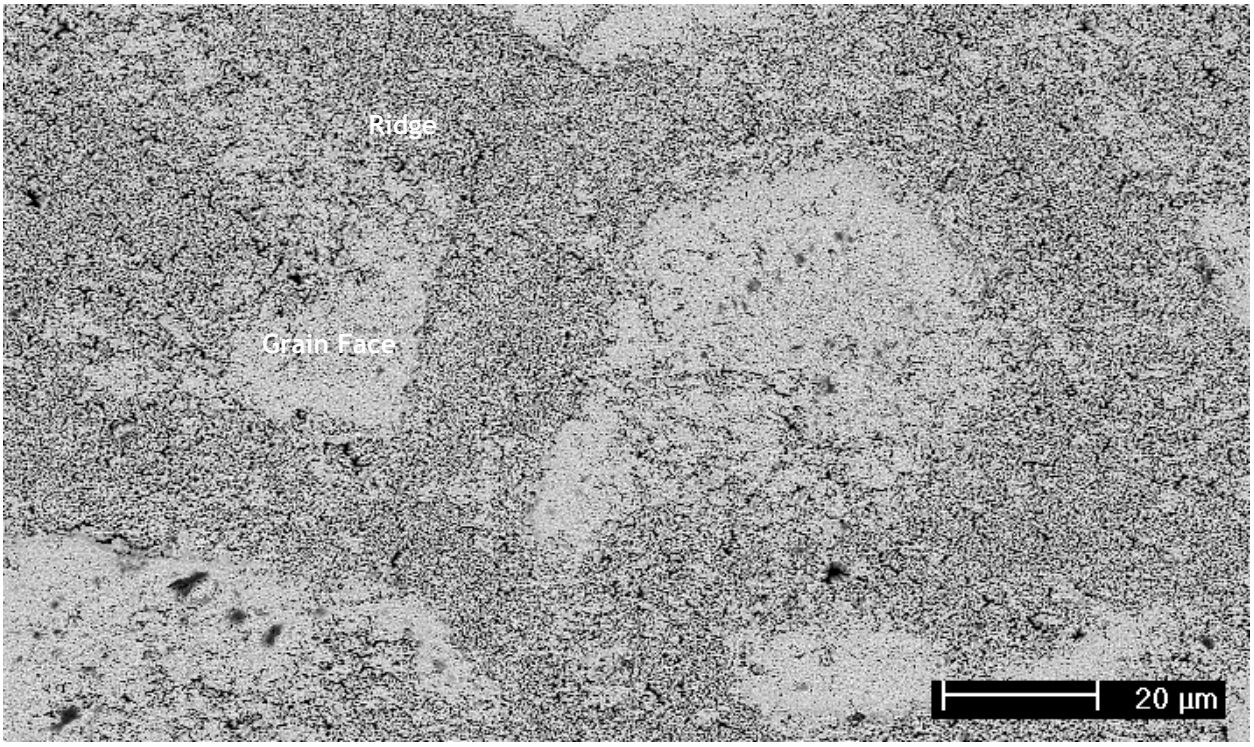

Figure 4-26. Micrograph of the corresponding underside of the TBC from sample LH100 (120 min. media finished, Ar-H2 at 1100°C for 2 hrs, 100 cycles). Once again this is typical for samples in the short time grouping. Very little TGO is adhered to this surface. It is of interest to note that imprints of the remnant bond coat ridges can be seen. The TBC appears to be less dense in these areas.

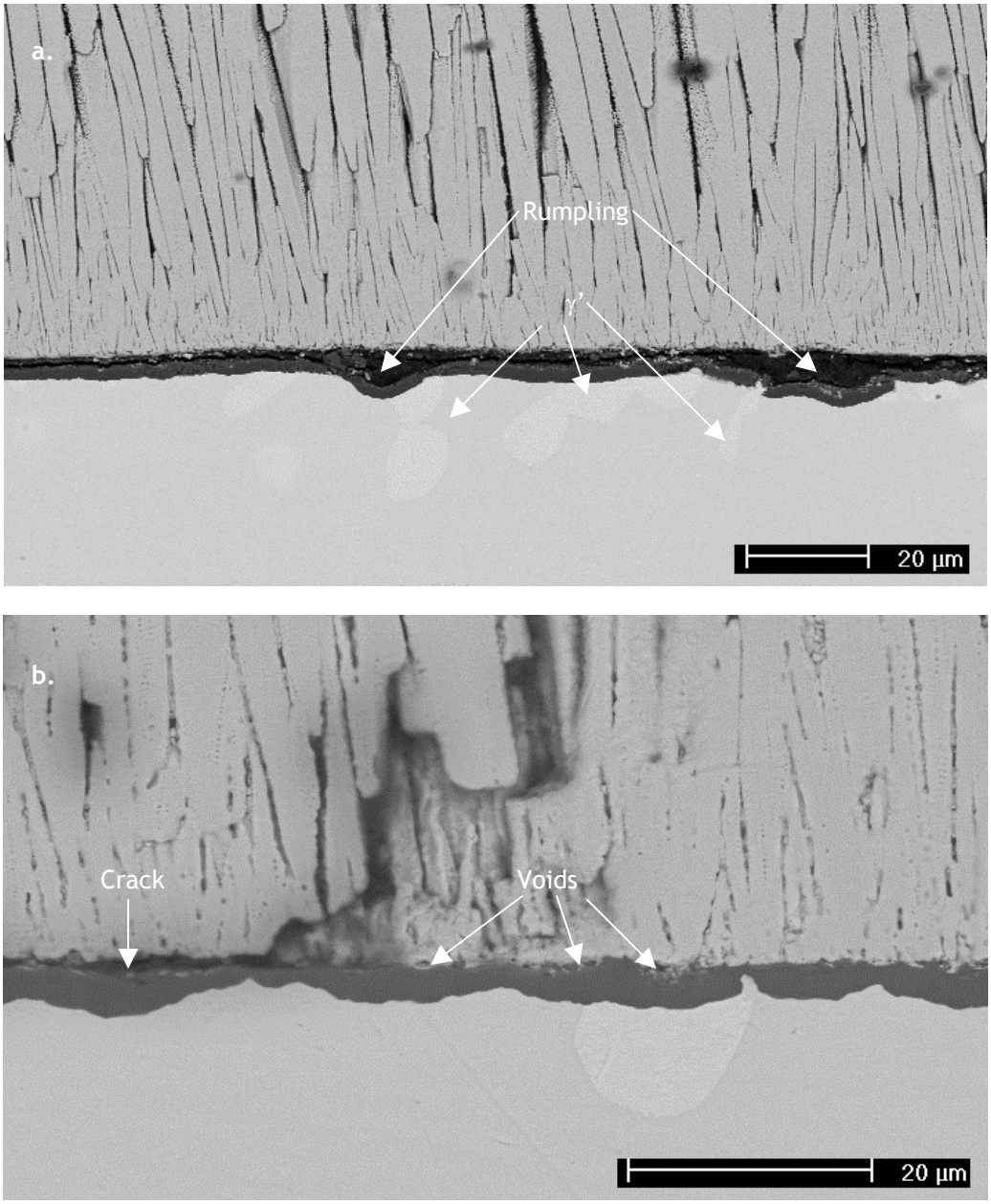

Figure 4-27. Micrographs of cross sections from samples LH100 (a. 120 min. media finished, Ar-H_2 at 1100°C for 2 hrs, 100 cycles) and LH01 (b. polished, Ar-H_2 at 1100°C for 2 hrs., 240 cycles). LH100 shows very little zirconia on the TGO, some rumpling of the bond coat surface, and some areas in the bond coat that have transformed to γ'. The TBC on LH01 appears to still be adherent in this location on the sample, but several small defects can be seen at the TBC/TGO interface.

is intact on the bond coat. Small fragments of the TBC remain on the TGO, and appear white in the backscatter SEM micrographs. There are very few areas where the TGO has spalled and/or remained adherent to the TBC and very few reoxidized areas that would indicate spalling before failure. The underside of the failed TBC (Figure 4-26) is consistent with this, in that it appears as white (YSZ) with very little dark gray (alumina) in backscatter mode. The TBC appears very flat and as if it had never really been adherent to the TGO. In some cases imprints of the bond coat ridges were visible, but never the finer surface morphology created by the surface finishing.

Cross section micrographs (Figure 4-27a) confirm that the TGO is still intact on the bond coat surface. There were several areas where the bond coat had deformed either by yielding from stresses in the TGO, or by phase change. The TGO remained adherent even to these areas, while the TBC was unaffected. It is common in bond coats that have been grit blasted that when this deformation occurs, the TBC will fail locally and remain adherent to the TGO, which in turn remains adhered to the bond coat. This strengthens the idea that the TBC – TGO interface was extremely "weak". Figure 4-27b shows a number of defects along a still adherent region of TBC that could eventually lead to failure.

The results seem to indicate that the presence of the metastable alumina plays a role in the premature failure of these samples. As mentioned above, the phase change to the stable alumina involves a volume reduction. Due to the strong bonding to the TBC and the bond coat, the TGO itself is in tension, while both interfaces are in compression. It is possible that the samples that failed at the coater contained cracks or flaws at the TGO/TBC interface that were larger than the critical size for the given stress state, and quickly failed. The samples that exhibited short lifetimes did not initially contain critical sized flaws. During the expansions and contractions involved with thermal cycling, the stress state in and around the TGO becomes

much more complicated. The flaws in the system can also grow and link up during cyclic exposure. Eventually, the stress state and flaw size achieve the critical conditions for failure at the TGO/TBC interface, resulting in the premature loss of the TBC.

Samples LG99 and LG93 demonstrated the two of longest lifetimes of this grouping, and are of some interest to discuss. The lifetime of LG93 was 300 cycles and the lifetime of LG99 was 640 cycles. Both of these samples were polished and given pre-oxidation treatments.

The micrographs from sample LG93 are shown in Figure 4-28. The underside of the TBC was examined first, and contained large amounts of TGO adhered to it. This behavior was different from the rest of the group. Examination of the bond coat surface also showed nearly complete coverage by the TGO. This is inconsistent with the results from the underside of the TBC. This TGO had areas that did not have any remnant TBC on them as well as a few spalled areas along with reoxidized areas. This gives the impression that failure occurred, for the most part, along the TBC/TGO interface paired with cracking in the TGO and occasional excursions to the bond coat interface. This was confirmed by extremely long cracks in the TGO observed in the cross sections.

Sample LG99 showed similar behavior (Figure 4-29). The underside of the TBC only had a few patches of alumina. The bond coat surface showed vast areas of failure along the TBC/TGO interface. There were also some areas of bare bond coat and reoxidized areas. In these reoxidized areas, the TGO appeared to have multiple layers. The TGO in cross section did show multiple layers in some areas. There was also substantial cracking in the TGO. It is believed that the cracking in the TGO alleviated the stressing in the TBC by allowing the TGO to act as two loosely attached layers. This resulted in what could be an artificially long life for this sample.

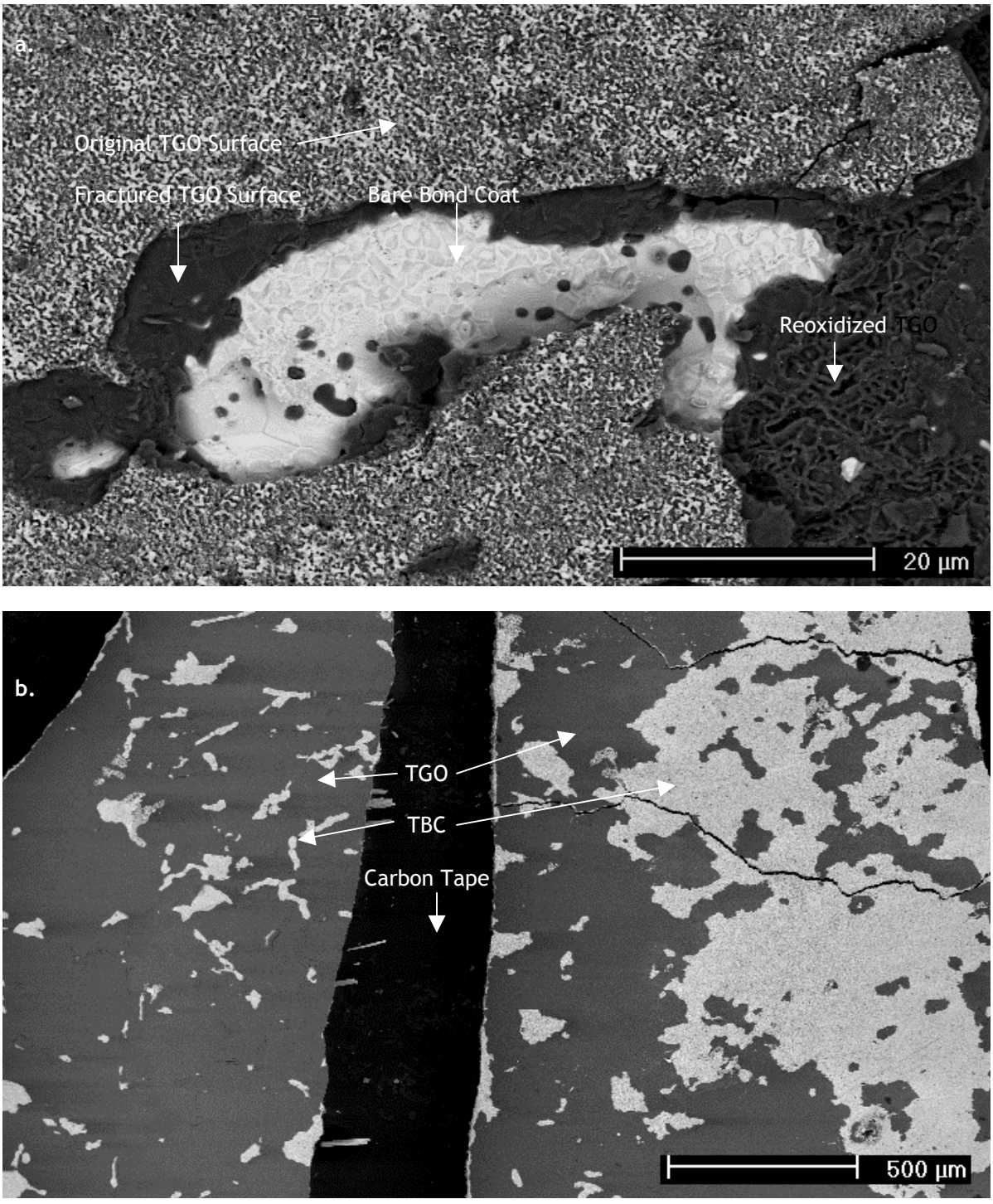

Figure 4-28. Micrographs from sample LG93 (polished, dry air 1000°C for 2 hrs, 300 cycles) showing the bond coat (a.) and TBC (b.) fracture surfaces, as well as the corresponding cross section (c.). The failure appears to have been within the TGO as evidenced by the large amount of TGO on both fracture surfaces and the large cracks seen the cross section. Al depletion is apparent at both bond coat interfaces.

Figure 4-28 (continued)

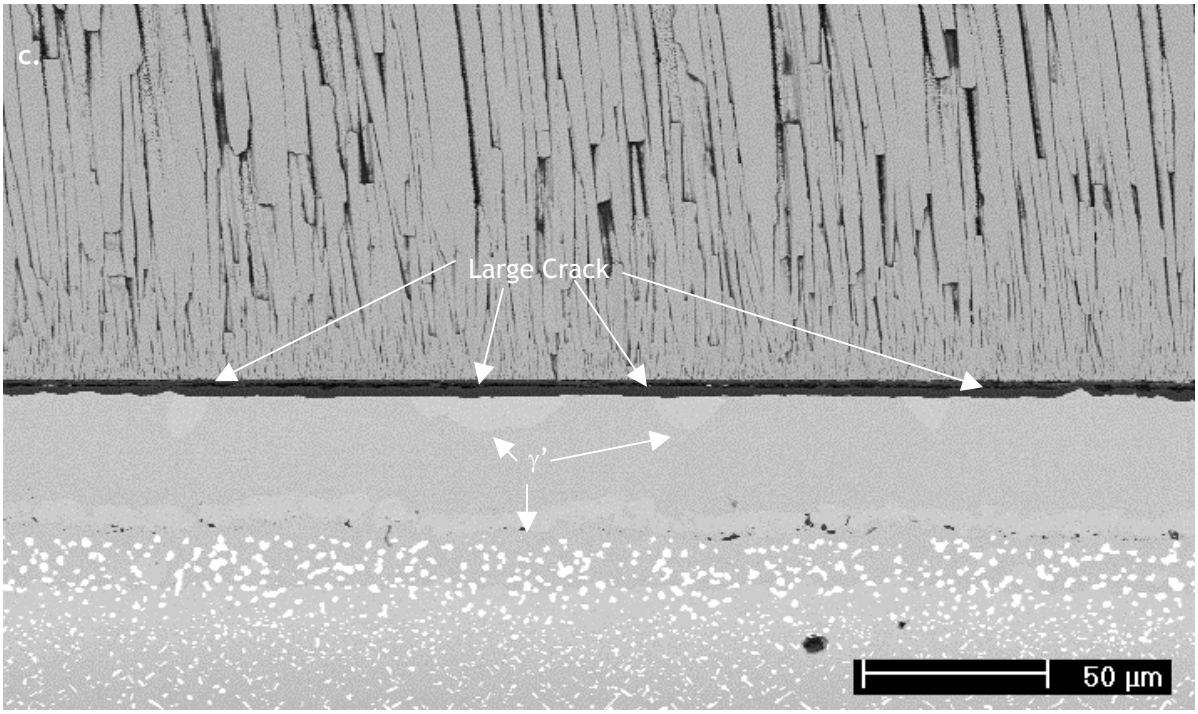

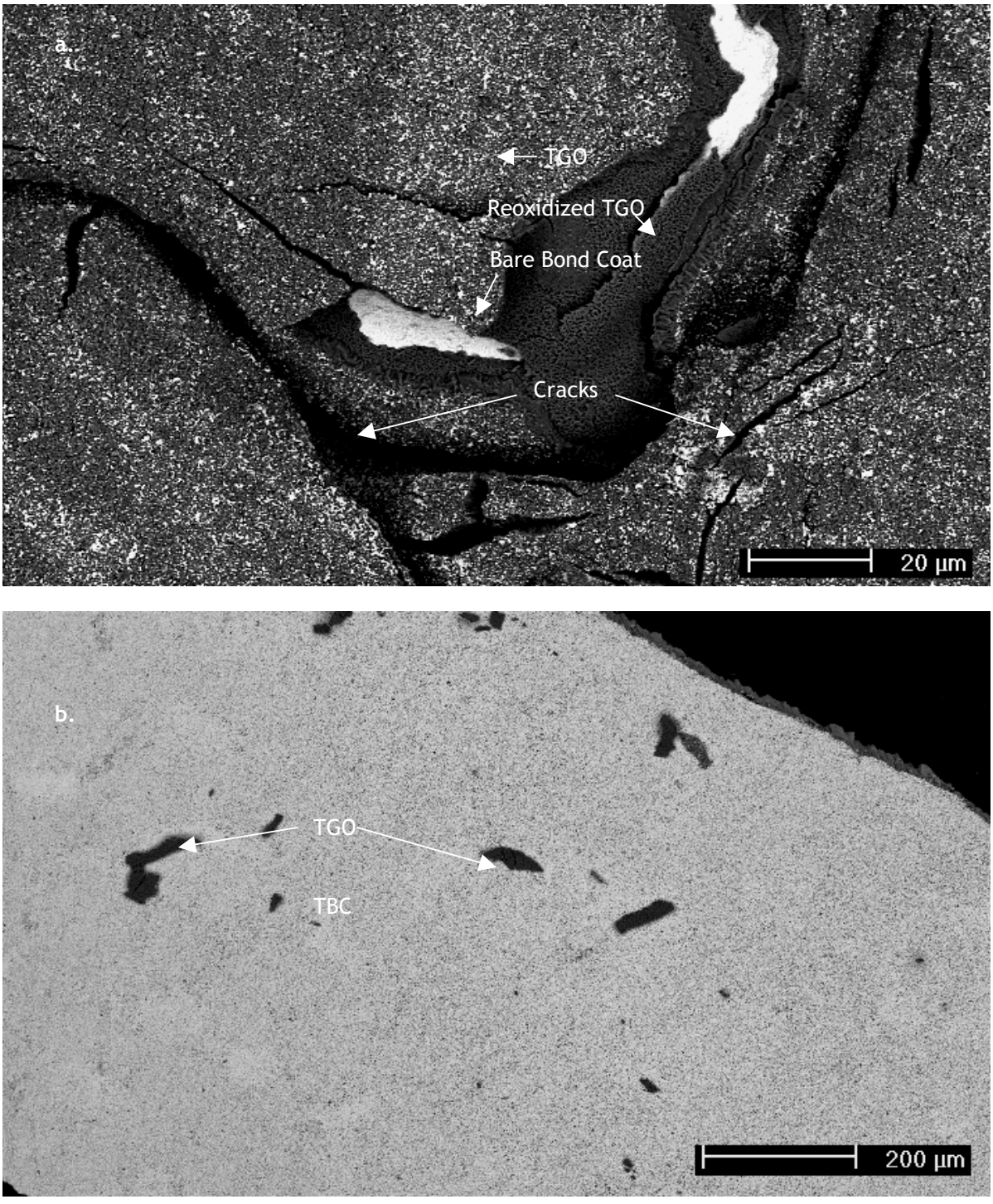

Figure 4-29. Micrographs from sample LG99 (polished, Ar-H_2 at 1100°C for 2 hrs, 640 cycles) showing the bond coat (a.) and TBC (b.) fracture surfaces, as well as the corresponding cross section (c.). The failure appears to be mostly along the TBC/TGO interface. Large scale cracking in the TGO as seen in a. and c. may have caused the TGO to act as two independent layers and lead to an artificially long life.

Figure 4-29 (continued)

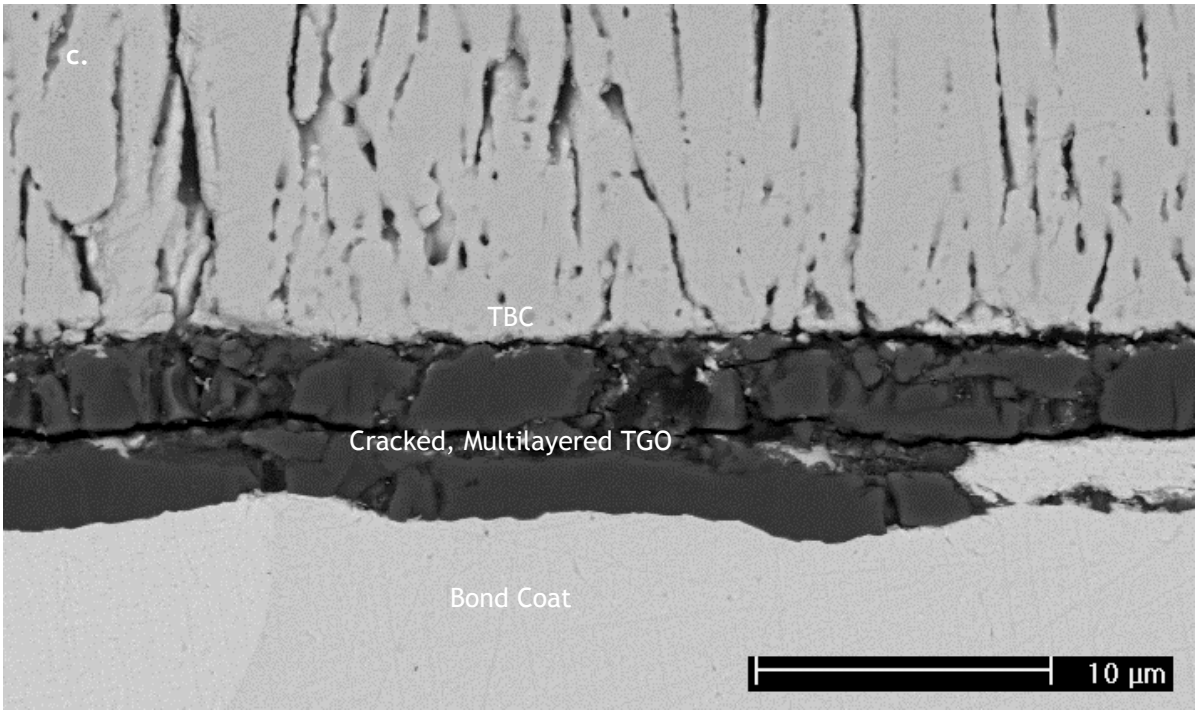

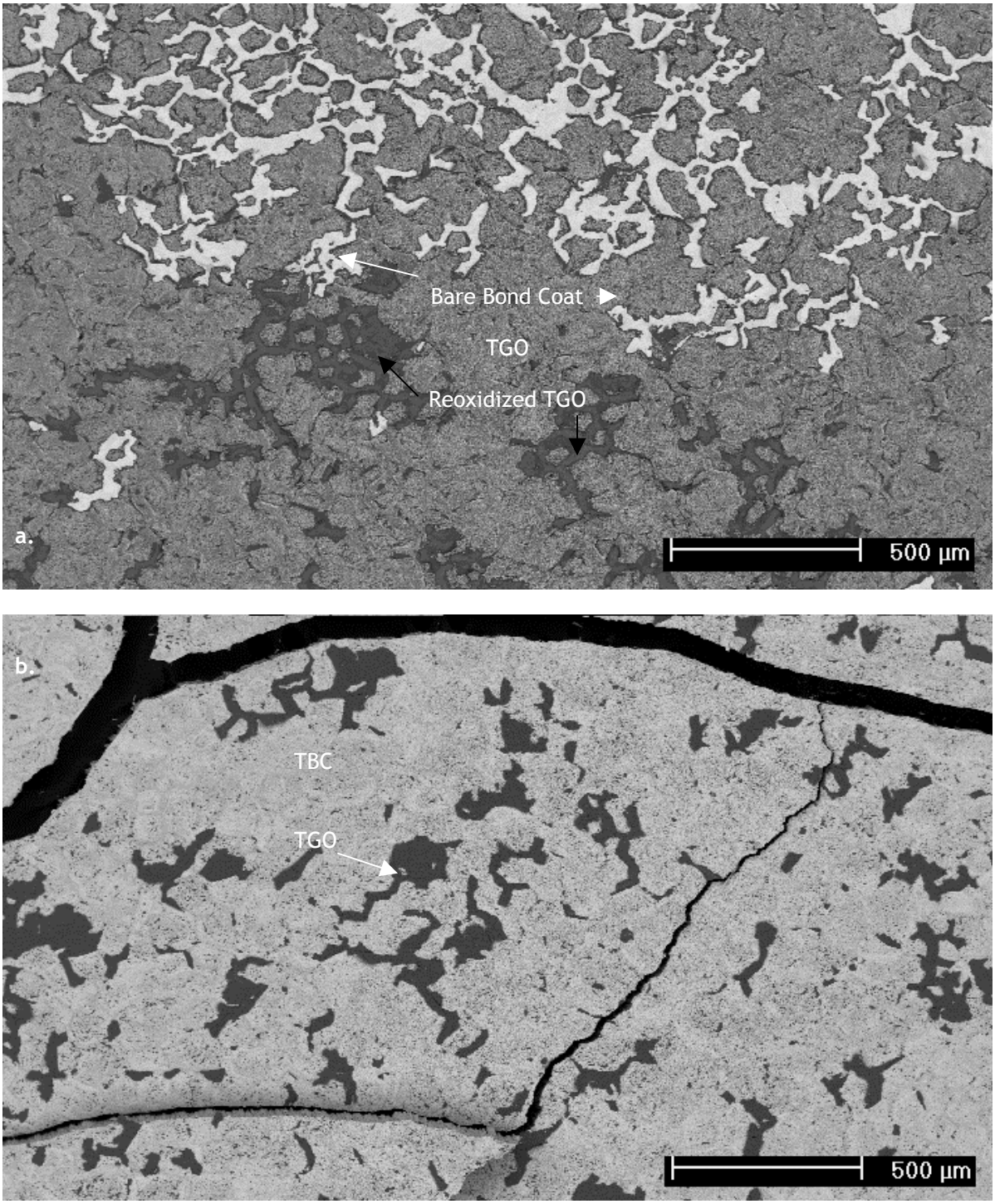

Figure 4-30. Micrographs of typical bond coat (a.), underside of the TBC (b.) and cross section (c.) appearance for 40 minute media finished samples in the long time group. The bond coat surface shows spallation and reoxidation at the bond coat ridges. Failure was still predominately along the TBC/TGO interface. The underside of the TBC also shows the pattern of the bond coat ridges. The cross section shows the TGO has loss adhesion at both interfaces.

Figure 4-30 (continued)

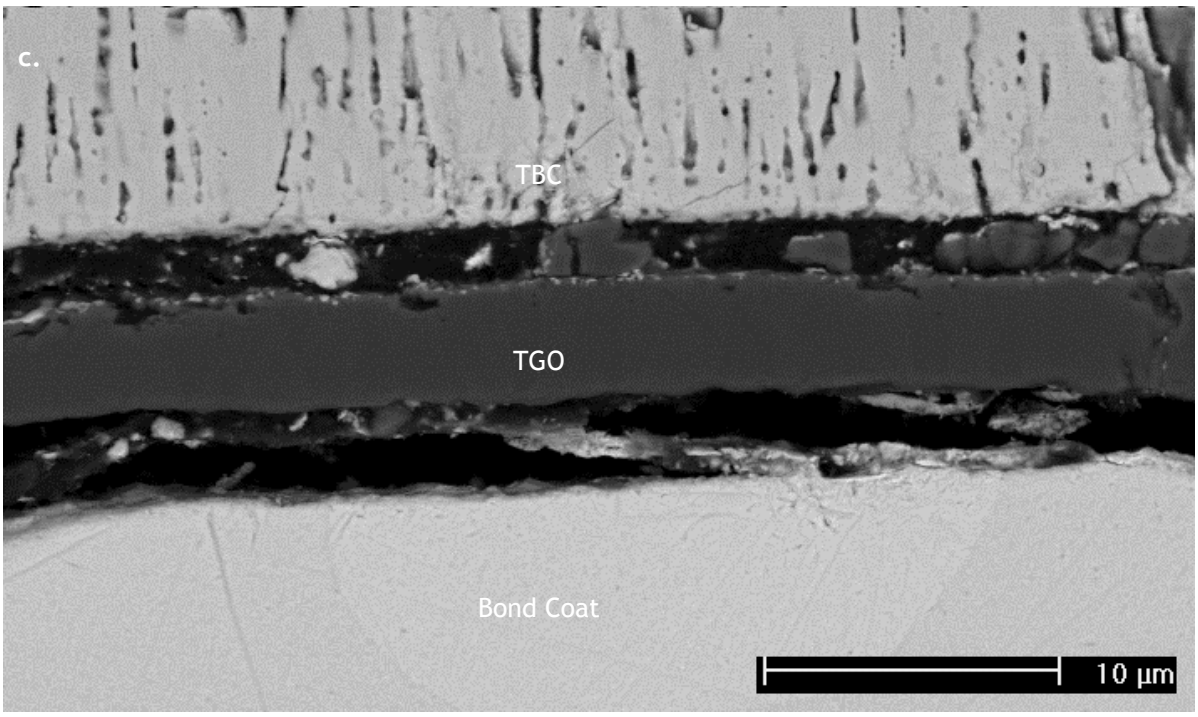

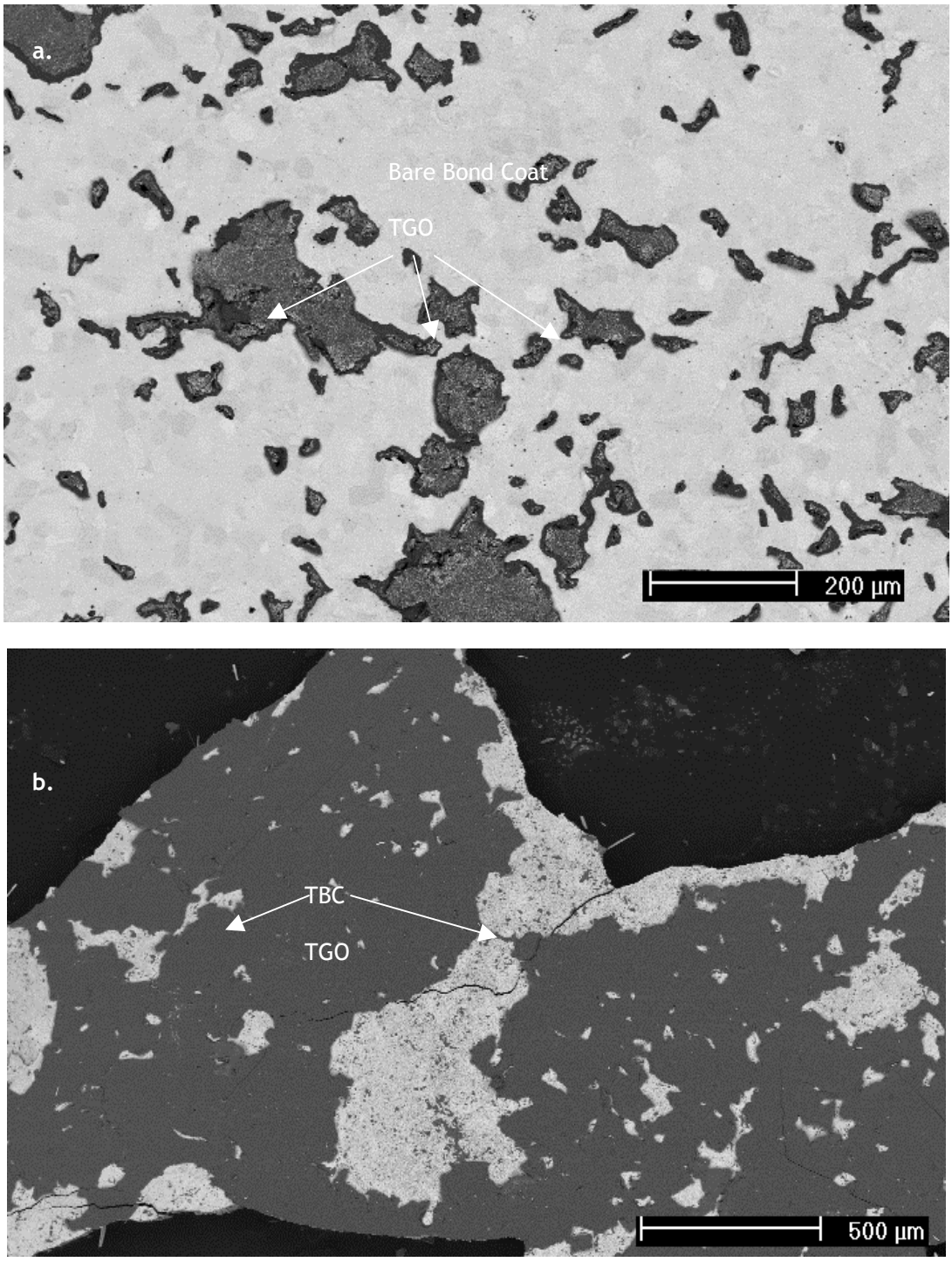

Figure 4-31. Micrographs of sample LH96 (120 min. media finished, dry air at 1100°C for 2 hrs.1040 cycles) showing the bond coat (a.) and TBC (b.) fracture surfaces, as well as the corresponding cross section (c.). Vast areas of bare bond coat are visible on the bond coat fracture surface. As can be seen from the TBC fracture surface and the cross section, the TGO is adherent to the TBC.

Figure 4-31 (continued)

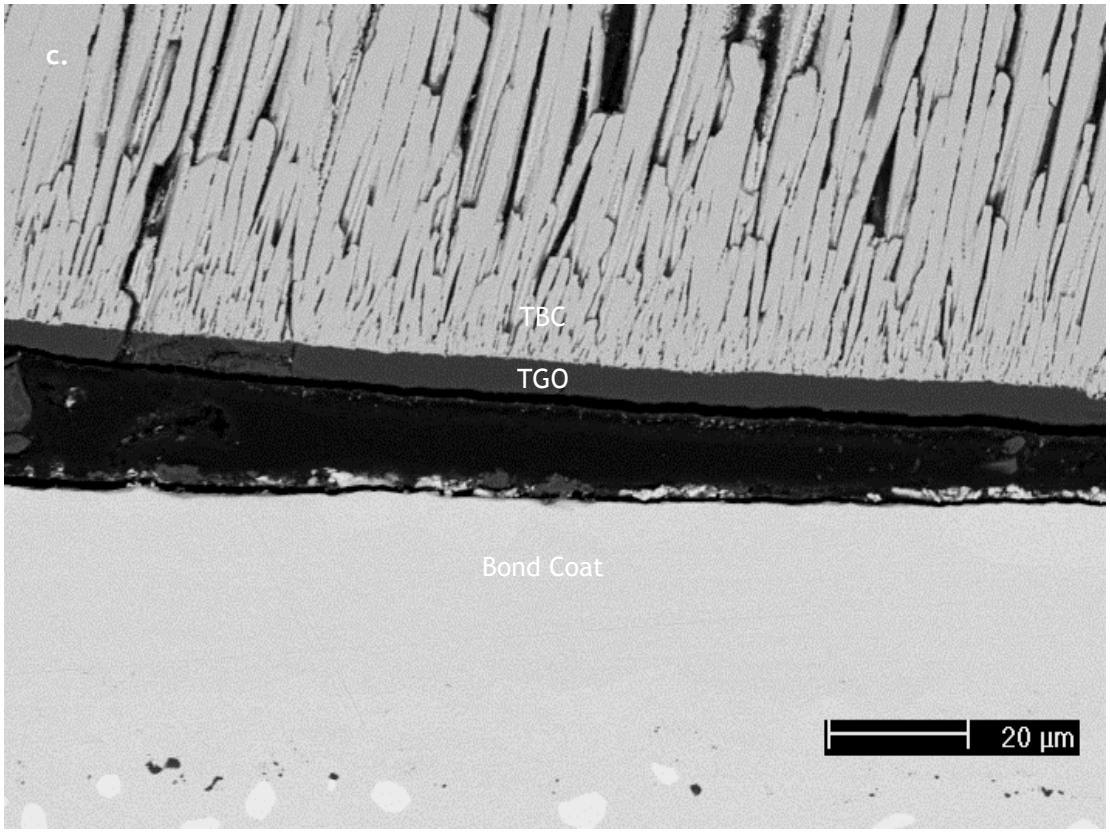

4.3.4 Long Time Failures

It was mentioned above that four samples did succeed in remaining intact longer than the 750 cycles that was predicted for grit blasted TBC's[25]. Once again, these can be grouped by failure circumstances for easier discussion.

The first group consists of samples LI10 and LI12. These samples had lifetimes of 900 and 1020 cycles respectively. Both were given the 40 minute media finish and pretreated in dry air at 1100^{o}C. As can be seen from Figure 4-30, these samples failed in the same manner as all the previous specimens. There was more failure along the TGO/bond coat interface, particularly at the remnants of the bond coat ridges. The only major difference between these and the rest are that they were preoxidized in dry air and should therefore have mostly, if not all, α alumina on the surface early during the TBC deposition. There are no notable differences in the micrographs to explain why these samples displayed the lifetime that they did. Excluding the special case of sample LG99, these samples ran nearly 600 cycles longer than others that failed in the same manner.

The second group consists of samples LH95, LH94, and LH96. These three displayed some of the longest lifetimes, 960, 1020 and 1040 cycles respectively. Figure 4-31 shows that the failure in these samples was predominant along the TGO – bond coat interface. This differs from all of the previous samples. Failure along the TGO – bond coat interface is the more typical failure location of the state of the art TBC samples. At this point, the alumina is at or near the threshold thickness at which it begins to naturally lose adherence to the bond coat due to stress build up. This indicates that these samples display nearly the maximum possible lifetime for the given TBC and bond coat surface. With respect to the lifetimes of the other samples examined, the combination of the 120 minute media finish and preoxidation to form α alumina

provide the optimum processing path. The average lifetime of this group (~1000 cycles) is about 40 cycles longer than the average for the 40 minute media finished group (~960 cycles) and several hundred cycles longer than the other groups. It also demonstrated an average lifetime over 200 cycles longer than what would be expected for state of the art grit blasted bond coat specimens.

5.0 CONCLUSIONS

The goal of this project was to determine if surface preparations can improve the exposure life of the TBC system. While five samples did "beat" what can be considered the standard, it is difficult to think of this as a hugely successful venture. Figure 5-1 is a graphical representation of the lifetime data in Table 2. This graph clearly shows that most of the pretreatments fall well short of the expected lifetime for the "state of the art" TBC. Most of the results can be used as a guide of what conditions to avoid to improve the lifetime.

The preoxidation study yielded some interesting and occasionally disturbing results. Platinum modified aluminide bond coats can form small faceted voids very early during exposure. These voids appear to grow and link up. The voids cause a loss of contact between the bond coat and the TGO. If the TGO were to crack in the vicinity of one of these voids, the TGO and the TBC on top of it could spall off. This could have a devastating effect on the part if this were to happen. Some speculations as to possible mechanisms for forming the voids were made above, but this should be studied further to gain insight to more exact causes, possible prevention, and the long term effects of the voids.

Another area that should be studied further is the short-term development of the TGO. The reason for many of the exposure conditions was to form scales containing metastable alumina. The exposure matrix was created as a trial and error method for finding the best conditions for accomplishing this. More work with tighter control of conditions should be done to determine how to form a given alumina phase and what effect this has on further oxidation or lifetime of the sample.

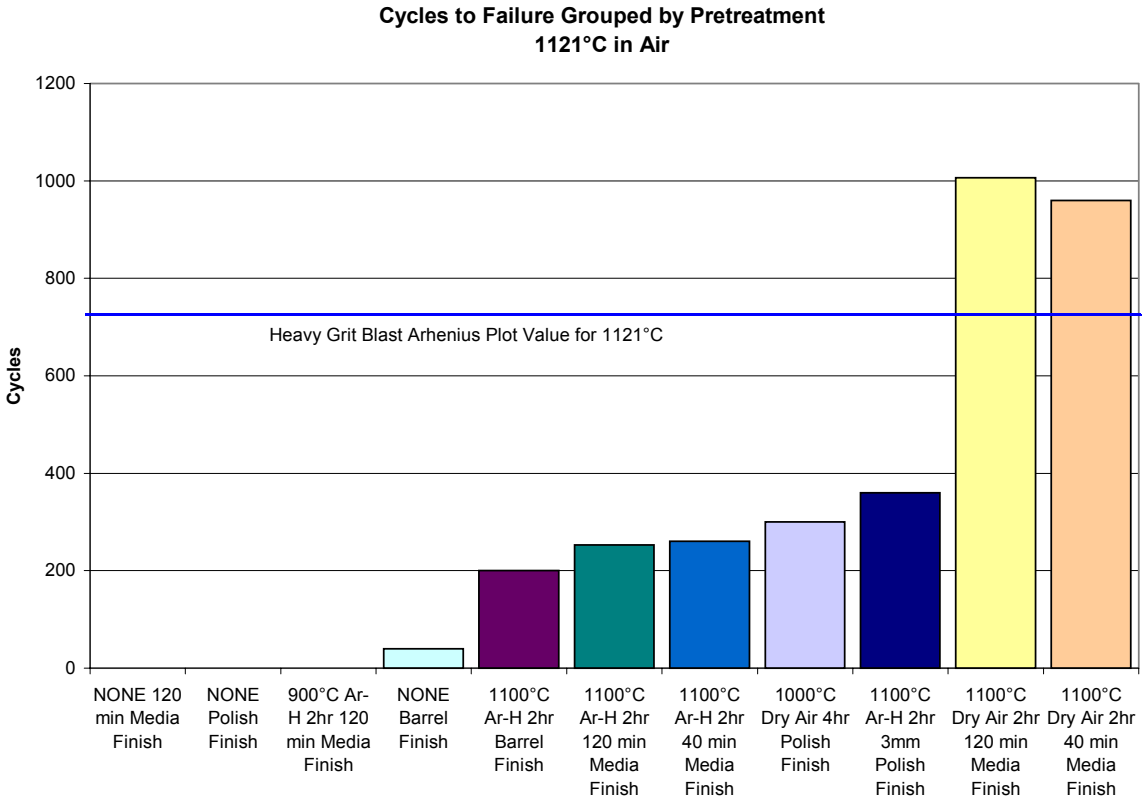

Figure 5-1 Graphical representation of the average TBC lifetimes for the various pretreatments

Practically all of the samples that contained large amounts of metastable alumina prior to or during TBC deposition failed out of the coater or very soon after. It appears that the volume change from θ to α alumina should be avoided. This strengthens the previous point of needing better knowledge of the transition between the two phases. Dry air or other "higher" P_{O2} containing gases will form α alumina, but the question is which one provides the best combination of time and cost.

There was a very large percentage of failures at the coater and after very short exposures. While this appears to be a result of the TGO phase, other things must be considered. UCONN and UCF also had significant numbers of early failures. There is the question of quality control during the coating process, especially given the five samples that were destroyed or not returned. It is possible that some of these early failures are also related to the coating process. Processing problems cannot be ruled out due to the common problems with such a wide variety of coating types and surface preparations.

Forming α alumina appears to be the most effective way to improve the lifetime. The dry air pretreatment formed the most α alumina on the samples. There were no unexplainable failures at the coater for samples preoxidized in dry air. The five samples that were given the dry air pretreatment combined with the 120 minute and 40 minute media finishes demonstrated the five longest lives, with the smoother 120 minute finish showing the longest. This does suggest that smoother surfaces and preoxidation are the correct routes to improving lives. It would have been interesting to have enough samples to include polished (smoothest surface) and barrel finished (similar to media finish, but cheaper) groups with the dry air pretreatment, since sample LG93 performed as it did with obvious defects in the TGO and the possibility that the remnant ridges in the center also played a role in shortening the life.

Howmet and some of its competitors are beginning to utilize surface finishes similar to the media finish. While the results show that this is the right direction to move in with respect to lifetime, no consideration was taken with respect to cost. Grit blasting is an inexpensive and rapid process compared to what is known of the media finishes. Since the finishing methods are proprietary, there is no way to know if the addition of 200 cycles to the lifetime by adding a 2 hr (120 minutes) surface finishing step can satisfactorily justify any increase in cost or decrease in productivity incurred. Whether results like the ones found here are used or not by industry may ultimately be determined by financial issues.

REFERENCES

1. Schwab, G., *Gods and Heroes of Ancient Greece*. Pantheon Books, 2001, pp 82

2. Reed-Hill, R.E., Abbaschian, R., *Physical Metallurgy Principles, 3rd ed*., 1994, PWS Publishing Co: Boston.

3. Birks, N., Meier, G.H., *Introduction to High Temperature Oxidation of Metals*, 1983, Edward Arnold: London.

4. Kofstad, P. *High Temperaure Corrosion*, 1988, Elsevier Applied Science LTD.

5. Sharke, P. "Lost and Foundary." Mechanical Engineering Sept 2000

6. Smialek, J.L., Metallurgical Transactions A, 1978, **9A**, p. 309-320.

7. Birks, N., Meier, G.H., Pettit, F.S., *Introduction to High Temperature Oxidation of Metals, 2nd ed.*, Unpublished Manuscript.

8. Tolpygo, V. and Clarke, D., Acta Materialia, 2000, **48**, p. 3283-3293.

9. Smith, J.S., Boone, D.H., *ASME Paper No. 90-GT-319*, ASME, New York, NY, 1990.

10. Laney, S. J., "The Effect of Platinum on the Growth and Adherence of Alumina Films", Undergraduate Thesis, University of Pittsburgh, 2001.

11. Zhang, Y., et al, Metallurgical and Materials Transactions A, 1999, **30A**, p. 2679-2687.

12. Zhang, Y., et al, Metallurgical and Materials Transactions A, 2001, **32A**, p. 1727-1741.

13. Pettit, F. S., private communication.

14. Basta, W.C., et al; U.S. Patent 5,658,614, 1997.

15. Taylor, T.A. and Taylor, R.E., Testing of Stability and Thermal Properties of Thermal Barrier Coatings, *ASM Handbook, Surface Engineering*. 1994, ASM: Materials Park, OH.

16. Meier, S. M., Gupta, D. K., and Sheffler, K.D., Journal of Materials, 1991, p. 50-53.

17. Wood, J.H. and Goldman, E.H., *Superalloys 2*. 1987: John Wiley and Sons.

18. Teer, D.G., Coatings for High Temperature Applications. 1983. Netherlands: Applied Science.

19. Strangman, T.E., Thin Solid Films, 1985, **127**, p.93-105.

20. Mattox, D.M., Growth and Growth Related Properties of Films Formed by Physical Vapor Deposition, *ASM Handbook, Surface Engineering*. 1994, ASM: Materials Park, OH.

21. Pettit, F.S., private communication.

22. Grabke, H.J., Intermetallics, 1999, **7**, 1153-1158.

23. Levin, I., Brandon, D., Journal of the American Ceramic Society, 1995, **81**, 1995-2012.

24. Schaffer, J.C., TBC Workshop. 1997. NASA Lewis Research Center, Materials Division, 21000 Brookpark Rd., Cleveland, OH, 44135.

25. Clarke, D.R., et al, Elevated Temperature Coatings: Science and Technology III. Proceedings of Symposium, 1999, p. 67-78.

26. Hiromichi, A., Masoto, M., Applied Catalysis A: General, 1996, **138**, 161-176.

27. Roux, J.P., Grabke, H.J., Applied Surface Science, 1993, **49**, 68.

28. Schaffer, J.C., private communication.

29. Yanar, N.M., "The Failure of Thermal Barrier Coatings at Elevated Temperatures", PhD Thesis, University of Pittsburgh, 2004.

30. Gell, M., et al, Metallurgical and Materials Transactions A, 1999. **30A**, p. 427-435.

31. Stiger, M., unpublished research.

32. Gell, M., et al, "Thermal Barrier Coatings and Metallic Coatings With Improved Durability", Final Report for DOE Contracts 01-01-SR091, 02-1-SR092 and DOE Cooperative Agreements DE-FC21-92MC29061, DE-EC26-02NT41431.

33. Oquab, D. and Monceau, D., Scripta Materialia, 2001, **44**, p. 2741-2746.

34. Haynes, J.A., Scripta Materialia, 2001, **44**, p. 1147-1152.

35. Tolpygo, V., in presentation given at Gordon Research Conference: High Temperature Corrosion, 2003.

36. Smialek, J.L., private communication.

37. Tolpygo, V.K., Clarke, D.R., Materials at High Temperatures, 2000.**17, p. 59-70.**